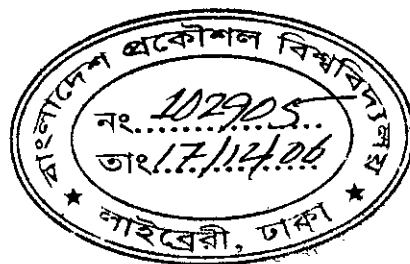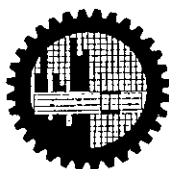# Influence of Protonation Level on the Specific Surface Area of Polyaniline and Its Application to Surface Processes

BY

FARHANA SULTANA SALEH

SUBMITTED IN PARTIAL FULFILMENT OF THE REQUIREMENT FOR THE DEGREE OF M.PHIL IN CHEMISTRY

DEPARTMENT OF CHEMISTRY

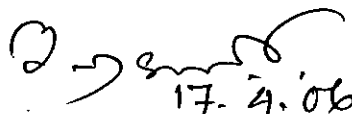**BANGLADESH UNIVERSITY OF ENGINEERING AND TECHNOLOGY (BUET) DHAKA-1000, BANGLADESH**

APRIL 2006

DECLARATION

This thesis work has been done by the candidate herself and does not contain any material extracted from elsewhere or from a work published by anybody else. The work for this thesis has not been presented elsewhere by the author for any degree or diploma.

Saleh 17.4.06
Farhana Sultana Saleh
(Candidate)
M. Phil Student
Roll No. 040303213 P
*Department of Chemistry*
BUET, Dhaka
Bangladesh

CERTIFICATE

This is to certify that the research work embodying in this thesis has been carried out under my supervision. The work presented herein is original. This thesis has not been submitted elsewhere for the award of any other degree or diploma in any University or institution.

17. 4. '06

Dr. Al-Nakib Chowdhury
(Supervisor)
Professor
Department of Chemistry
BUET, Dhaka
Bangladesh

Bangladesh University of Engineering and Technology, Dhaka
Department of Chemistry
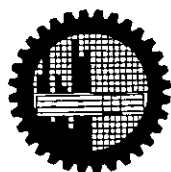
Certification of Thesis

A thesis on
"Influence of Protonation Level on the Specific Surface Area of Polyaniline and Its Application to Surface Processes"
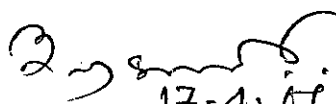
By

Farhana Sultana Saleh

has been accepted as satisfactory in partial fulfillment of the requirements for the degree of Master of Philosophy (M.Phil) in Chemistry and certify that the student has demonstrated a satisfactory knowledge of the field covered by this thesis in an oral examination held on April 17, 2006.
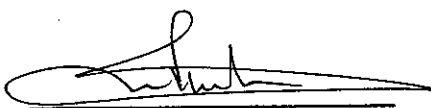
Board of Examiners

1. **Dr. Al-Nakib Chowdhury**
   Professor
   Department of Chemistry
   BUET, Dhaka

   17-4-06
   Supervisor & Chairman
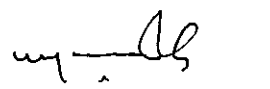
2. **Dr. Nazrul Islam**
   Head
   Department of Chemistry
   BUET, Dhaka.

   Member (Ex-officio)

3. **Dr. Md. Rafique Ullah**
   Professor
   Department of Chemistry
   BUET, Dhaka

   Member

4. **Dr. M. Yousuf Ali Mollah**
   Professor
   Department of Chemistry
   Dhaka University, Dhaka.

   Member (External)

DEDICATED
TO
MY BELOVED
FAMILY

Acknowledgement

Let me end by paying unqualified tribute to my creator Whose guidance and blessings had been with me through out the completion of this work as in all matters of my life and so praise be to Allah, the beneficent and the merciful.

FARHANA SULTANA SALEH
Author

Contents

EXPERIMENTAL   **29-111**

LIST OF TABLES

LIST OF FIGURES

ABSTRACT

The variation in the specific surface areas of polyaniline (PANI) and polyaniline/silica (PANI/SiO$_2$) substrates was monitored at different protonation levels of the system.

Aniline was polymerized chemically from an acidic solution using an oxidant, ammonium peroxydisulfate. Polyaniline thus obtained was treated with double distilled water (pH = 6.95), aqueous hydrochloric acid (pH = 1.09) and aqueous ammonia (pH = 10.15) solutions in order to make the PANI matrix neutral and charged, respectively. Preparation of PANI/SiO$_2$ was performed by the chemical polymerization of aniline in the presence of fine colloidal silica particles in aqueous media. A stable PANI/SiO$_2$ composite was found to be formed in the reaction mixture under experimental conditions.

These substrates were characterized by a wide range of experimental techniques including Infrared (IR) spectroscopy, X-ray diffraction and scanning electron microscopy (SEM) measurements. The treated PANI and PANI/SiO$_2$ matrices were found to be correlated with the idealized forms of PANI protonated states proposed by A. G. MacDiarmid. The acid treated matrix seemed to be positively charged while the other two matrices seemed to be either neutral or negatively charged.

Infrared spectroscopy studies yielded qualitative information on the treated PANI and PANI/SiO$_2$ substrates. From the spectra, the band characteristics confirmed differences between treated PANI matrices. Also, the spectra exhibited absorption bands attributable to both polymer and silica components.

The diffused X-ray scattering patterns of the treated PANI and PANI/SiO$_2$ indicated the amorphous nature of the substrates. The scattering pattern of the PANI and that of PANI/SiO$_2$ seemed to be indifferent. This finding suggested that incorporation of silica particles did not have any influence on the structure of the substrates.

Surface morphology obtained by SEM provided very interesting results. The acid treated PANI is consisted of agglomerates and stacked over the surface to make a big deposit. On the other hand, double distilled water treated matrices showed granular morphology in which grain

aggregated to a stone like body. The base treated PANI matrices also showed granular morphology but the grains were collected to a body like coral with sharp edges. For the PANI/SiO$_2$ substrate the morphology was found different compared to PANI. In this case most of the portions were powdery and other portions were granular with a shape like small stone.

The specific surface areas of PANI and PANI/SiO$_2$ substrates were determined from an aqueous solution of methylene blue (MB) dyestuff by allowing the dye to adsorb onto the surface of the substrates. This adsorption phenomenon produced the monolayer coverage on the surface of the adsorbent. The PANI and PANI/SiO$_2$ substrates were used as adsorbents and found to be adsorbed the dyestuff, MB from its aqueous solutions at various pH. The adsorption was monitored spectroscopically by measuring the change of absorbance at λ_{max} 664 nm. The cationic dye, MB showed a significant adsorption on the base treated PANI (negatively charged) and PANI/SiO$_2$. The adsorption isotherms were found to follow Langmuir isotherm. The specific surface area was calculated using the value of monolayer capacity, which was estimated from the plot of amount of MB, adsorbed against equilibrium concentration of the MB solution. For two different molecular cross-sectional areas of MB (130 Å^2, BET with N$_2$ and 78 Å^2, BET with Ar) the specific surface area of acidic PANI were found as 15 and 9 m^2 g^{-1}, for neutral PANI they were 11 and 7 m^2 g^{-1}, for basic PANI 29 and 17 m^2 g^{-1}, for PANI/SiO$_2$ in acidic condition 21and 13 m^2 g^{-1}, PANI/SiO$_2$ in neutral condition 18 and 11m^2 g^{-1}, and PANI/SiO$_2$ in basic condition 33 and 20 m^2 g^{-1}, respectively. The surface area measurements showed higher area for basic PANI than the acidic and neutral PANI substrates and PANI/SiO$_2$ composite showed more surface area than that of PANI. The incorporation of fine silica particles to the polymer might lead to this increased surface area.

INTRODUCTION
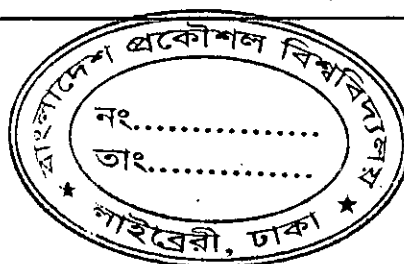
1.1 Conductive Polymers

Conductive polymers are conjugated polymers, namely organic compounds that have the extended p-orbital system, through which electrons can move from one end of the polymer to the other. The most common are polyaniline (PANI) and polypyrrole (PPY). The discovery in 1973 that poly sulfur nitride $(SN)_x$ was intrinsically conducting provided a proof that polymers could be conducting and thus greatly stimulated the search for other conducting polymers[1]. During the last two decades, a new class of organic polymers has been devised with the remarkable ability to conduct electrical current. These materials constituted a class called conducting polymers[2].

One of the earliest approaches to make the polymers conductive is to prepare a composite of polymers and conductive filler, such as, metal powder, graphite powder, flake or wire etc. Conductive fillers remain embedded more or less evenly dispersed in the polymer matrix and conduct electric current. But these composites cannot be regarded as conducting polymers because the polymers present in such composites are non-conducting[3-6].

In 1964, W. A. Little[7] synthesized a superconductor at room temperature with polymeric backbone and large polarizable side groups, which led the discovery of new organic compounds with high electrical conductivity.

In the early 1980s, excitement ran high when several prototype devices based on conductive polymers, such as rechargeable batteries and current rectifying *p-n* junction diodes[8] were announced. Among the many polymers known to be conductive, polyacetylene (PAT), PANI, PPY and polythiophene (PT) have been studied most intensively[9-15]. However, the conductive polymer that actually launched this new field of research was PAT.

Research has been expanded into the studies of heteroatomic conductive polymers because of their better chemical stability and the interest in the polaron and bipolaron conduction

mechanism[16,17]. Among the heteroatomic polymers PPY, PT and PANI have been studied extensively.

During the 1980s, PANI was subjected to intense structural, physical, and electrical characterization, using modern experimental techniques. A brief survey, out of numerous features and studies made on PANI is presented in the section 1.7.1.

1.2 Composites

Since 1965 a distinct discipline and technology of composite materials begun to emerge. That is 80% of all research and development on composites has been done since 1965 when the Air Force launched its-all out development program to make high performance fiber composites a practical reality. There are two major reasons for the revived interest in composite materials. One is that the increasing demands for higher performance in many product areas specially in the aerospace, nuclear energy and aircraft fields is taxing to the limit our conventional monolithic materials. The second reason, the most important for the long run is that the composites concept provides scientists and engineers with a premising approach in designing rather than selecting materials to meet the specific requirements of an application.

The term 'composite' refers to something made up of various parts or elements. In definition of composite depends on the structural level of the composite we are thinking about. At the submicroscopic level that of simple molecules and crystal cells all materials composed of two or more different atoms or elements would be regarded as composites. This would include compounds, alloys plastics and ceramics. Only the pure elements would be excluded. At the microscopic level (or microstructural level) that of crystals, polymers, and phases of composite would be a material composed of two or more different crystals, molecular structures or phases. By this definition most of our traditional materials, which have always been considered monolithic, would be classified as composites. At the macro structural level which is most useful for composites, the definitions of composites is that they are a mixture of macro constituent phase composed of materials which are in a divided state and which generally differ in form and/or chemical composition. Note that, contrary to a widely held assumption, this

definition does not require that a composite be composed of chemically different materials, although this usually the case. The more important distinguishing characteristics of a composite are its geometrical features and the fact that its performance is the collective behavior of the constituents of which it is composed. A composite material can vary in composition, structure, and properties from one point to the next inside the material.

The major constituents used in structuring composites are fibers, particles, laminas, flakes, filters, and matrix. The matrix that can be thought of as the body constituent gives the composite its bulk form. The other four can be referred to as structural constituents determine the character of the composites internal structure. A special type of composite, fiberglass embedded in a polymer matrix is a relatively recent invention but has in a few decades, become a commonplace material. Characteristic of good composites, fiberglass, provides the 'best of both worlds', it carries along the superior properties of each component, producing a product that is superior to either of the components separately. The high strength of the small diameter glass fibers is combined with the ductility of the polymer matrix to produce a strong material capable of with standing the normal loading required of a structural material.

1.3. Surface Process: Adsorption Phenomena

Adsorption is a surface phenomenon. It may be defined as a process in which the concentration of a chemical species is greater on the surface than in the bulk resulting from inelastic collision suffered by molecules on the surface. The species that is adsorbed is called adsorbate and the material of the surface on which adsorption takes place is called adsorbent. Adsorption strictly refers to accumulation of adsorbates on the surface only due to residual field of force.

The adsorption surface is generally a solid or liquid. Surface of solid or liquids have certain properties and characteristic that makes them different from the bulk of matter. Although there is no chemical distinction between the molecules or atoms on the surface and the molecules or atoms in the bulk, energy considerations lead to quite dissimilar properties.

When two immiscible and chemically non-reactive phases are brought into contact with each other, adsorption is a common observation, which means that the concentration of one phase is

greater at the interface than the bulk. This occurs due to unsaturation of the surface atoms. Most studies of adsorption from solution have been concerned with equilibrium conditions and predominantly with the adsorption isotherm. Generally two types of adsorption have been distinguished: (a) Physical adsorption (Physisorption) and (b) Chemical adsorption (Chemisorption). Physical adsorption results purely from physical forces like van der Waals forces and chemical adsorption is due to formation of chemical bonds.

1.3.1 Adsorption isotherms

There are three adsorption isotherms known which are used most frequently:

i) Langmuir adsorption isotherm: Langmuir derived a relation between gas pressure and amount of gas adsorbed at a constant temperature. The Langmuir equation can be written as

$$X = \frac{X_m bp}{(1+bp)} \tag{1}$$

or, $$\frac{1}{X} = \frac{1}{X_m bp} + \frac{1}{X_m} \tag{2}$$

where X = amount adsorbed at a definite concentration, $X_m = k_1/k_2$; k_1 and k_2 are the rate constant for adsorption and desorption, respectively, b = constant and p = pressure.

ii) Freundlich adsorption isotherm: The variation of adsorption with concentration of the substance in solution is usually represented by Freundlich isotherm as follows:

$$y = kC^{\frac{1}{n}} \tag{3}$$

or, $$\log y = \log k + \frac{1}{n} \log C \tag{4}$$

Where, y = mass of substance per unit mass of adsorbent, C = equilibrium concentration of solid in solution, k and n are the empirical constants.

iii) BET adsorption isotherm: The theory of Brunauer, Emmett and Teller (BET) is an extension of the Langmuir treatment to allow for multilayer adsorption on non-porous solid surface. The BET equation is usually written as:

$$\frac{P}{X(P_o - P)} = \frac{1}{X_m C} + \frac{C-1}{X_m C} \cdot \frac{P}{P_o} \tag{5}$$

where, P_o = saturation vapor pressure, X_m = the monolayer capacity and

$C = \exp [(\Delta H_L - \Delta H_l) / RT]$.

1.3.2 Factors affecting adsorption

i) Temperature: The level of adsorption at any particular concentration decreases with the increase in temperature; that is the overall process is exothermic. At higher temperature the adsorbed molecules have greater vibrational energies and therefore, more likely to desorb from the surface.

ii) Nature of the solvent: The solvent has an important effect, since it competes with the surface of the adsorbent in attracting the solute. There are three different ways to describe the influence of solvent on adsorption behavior of the solvent (a) its interaction with the solute in solution, (b) its interaction with the adsorbed layer, and (c) its interaction with the solute in the adsorbed layer. However, when the solvent is water, it is worthless to consider the solvent effect.

iii) Particle and pore size: The adsorption efficiency increases as mean diameter of the particle decreases. Large surface area is available for adsorption with the small particles. Another reason is the reduced diffusive path length of the interior of small adsorbent particles and the adsorbate particles require less energy of jump from one active site to another, resulting in higher uptake by the adsorbent.

iv) pH of the solution: The effect of pH is extremely important when the adsorbing species is capable of ionizing in response to prevailing pH. It is well known that substances adsorb poorly when they are ionized. When the pH is such that an adsorb able compound exists in ionic form, adjacent molecules of the adsorbed species on the adsorbent surface will repel each other to a significant degree, because they carry the same electrical charges. Thus the adsorbing species cannot be packed together very densely on the surface. This is the common observation that

non-ionized forms of acidic and basic compounds adsorb much better than their ionized counterparts. The acidic species thus adsorb better at low pH and basic species adsorb better at high pH.

1.3.3 Adsorption from solution

Adsorption from solution is much simpler than that of gas adsorption. A known mass of adsorbent is kept in touch with a known volume of solution at a given temperature until there is no further change in the concentration of the supernatant solution. This concentration can be determined by a variety of methods involving chemical or radiochemical analysis such as colorimetry, refraction index, *etc.* The experimental data are usually expressed in terms of an apparent absorption isotherm in which the amount of solute adsorbed at a given temperature per unit mass of adsorbents calculated from the decreases of solution concentration is plotted against the equilibrium concentration. By analogy with gas adsorption, one might hope to calculate the monolayer capacity, the application of an equation of the individual isotherm has a pattern of a sharp knee followed by a clear plateau; the monolayer capacity is then given by the height of the plateau.

1.4 Specific surface area of the adsorbent

The specific surface area refers to the area per unit weight of the material, usually expressed as m^2g^{-1}. This area depends on particle size, shape and on type of material present. Relative methods for measuring specific surface area are based on retention of a polar organic molecule such as ethylene glycol; these have been related to absolute values derived from statistical calculations of surface area. Another method for the estimation of surface area from adsorption measurements viz. those based on adsorption from solution, on heat of immersion, chemisorptions, and on the application of Gibbs adsorption equation to gaseous adsorption. Amongst them adsorption from solution method is used in this purpose. This is particularly true of those solids that contain very fine pores and give rise to Langmuir-type isotherms.

The principle on which the determination of area is based required knowledge of the number of molecules in the unimolecular layer per gram of adsorbent and the average cross-sectional area of the molecule.

1.5 Monolayer Capacity

The monolayer capacity is defined as the quantity of the adsorbate, which can be accumulated in a completely filled, single layer of molecules (a monolayer) on the surface of the solid. The specific surface area, S (m^2g^{-1}) is directly proportional to the monolayer capacity. The relationship between the two is given by the following equation.

$$S = (\chi_m/M) \times N \times A_m \times 10^{-20} \tag{6}$$

Here, χ_m = The monolayer capacity in grams adsorbate per gram of solid

M = Molecular mass of adsorbate

N = Avogadro's number

A_m = The area in $Å^2$ occupied per molecule of adsorbate in the completed

Monolayer

S = The specific surface area of adsorbent in m^2g^{-1}.

To find the value of χ_m from the isotherm, it is necessary to interpret the isotherm in quantitative terms. In the calculation of χ_m, Langmuir-type isotherm is considered.

1.6 Solution pH: The Protonation Level

The pH concept was originated in 1909 by the Danish biochemist S. P. L. Sorensen while he was working on the control of acidity during the brewing of beer. The p in pH stands for

puissance (in French), potenz (in German), or power in English; the H stands for hydrogen ion. L. Sorensen introduced the hydrogen ion exponent pH defined by the relation:

$$pH = \log_{10} 1/[H^+] \qquad (8)$$

$$\text{or} \quad [H^+] = 10^{-pH} \qquad (9)$$

The quantity pH is thus the logarithm (to the base 10) of the reciprocal of the hydrogen ion concentration, or is equal to the logarithm of the hydrogen ion concentration with negative sign. This method has the advantage that all states of acidity and alkalinity between those of solutions containing, on the one hand, 1 mol L^{-1} of hydrogen ions, and on the other hand, 1 mol L^{-1} of hydroxide ions, can be expressed by a series of positive numbers between 0 and 14. Thus, a neutral solution with $[H+] = 10^{-7}$ has a pH of 7; a solution with a hydrogen ion concentration of 1 mol L^{-1} has a pH of 0 ($[H^+] = 10^0$); and a solution with a hydroxide-ion concentration of 1 mol L-1 has $[H^+] = K_w/ [OH^-] = 10^{-14}/ 10^0 = 10^{-14}$, and possesses a pH of 14. A neutral solution is therefore one in which pH= 7, an acid solution one is which pH < 7, and an alkaline solution one is which pH > 7. An alternative definition for a neutral solution, applicable to all temperatures, is one in which the hydrogen ion and hydroxide ion concentrations are equal. In an acid solution the hydrogen ion concentration exceeds the hydroxide ion concentration, whilst in an alkaline or basic solution, the hydroxide ion concentration is greater. Thus, pH refers to the protonation level of a solution. The extend of protonation, therefore can be controlled by controlling the pH of the solution.

There are several methods for determining the pH of a solution. One of the most familiar techniques for measuring pH is the litmus paper test. An acidic solution turns blue litmus red, and basic solution turns red litmus blue. However, the very elementary and inaccurate measurement determines only whether the pH is greater or less than 7. Other pH-indicating papers enable one to estimate pH to about ± 0.5 to 1 unit. Mixture of indicators, which are often colored plant extracts, change color with pH, and can be used to determine pH calorimetrically. Several instrumental colorimetric methods and electrical methods are also available. In one electrical method, a voltage proportional to the pH develops when appropriate electrodes are dipped into a solution, and the pH is displayed on a pH meter. For solution of fairly high

concentration, the most accurate technique for determining the acid or base concentration is titration.

1.7 The Adsorbent

1.7.1 Polyaniline

i) Structural features: Organic conducting polymer, PANI, is being studied more and more, and up to the recent years has been the centre of considerable scientific interest. However, PANI is not really a new material and its existence has been known for the past 150 years or over, since it had already been made by Runge in 1834.

PANI has been described in many papers[18] usually as ill-defined forms such as 'aniline black' emeraldine, nigraniline, *etc.* synthesized by the chemical or electrochemical oxidation of aniline. Figure1.1 shows the idealized oxidation state of PANI: leucoemeraldine, emeraldine, pernigraniline and emeraldine salt. Different structures result in different electrical behaviours of the material.
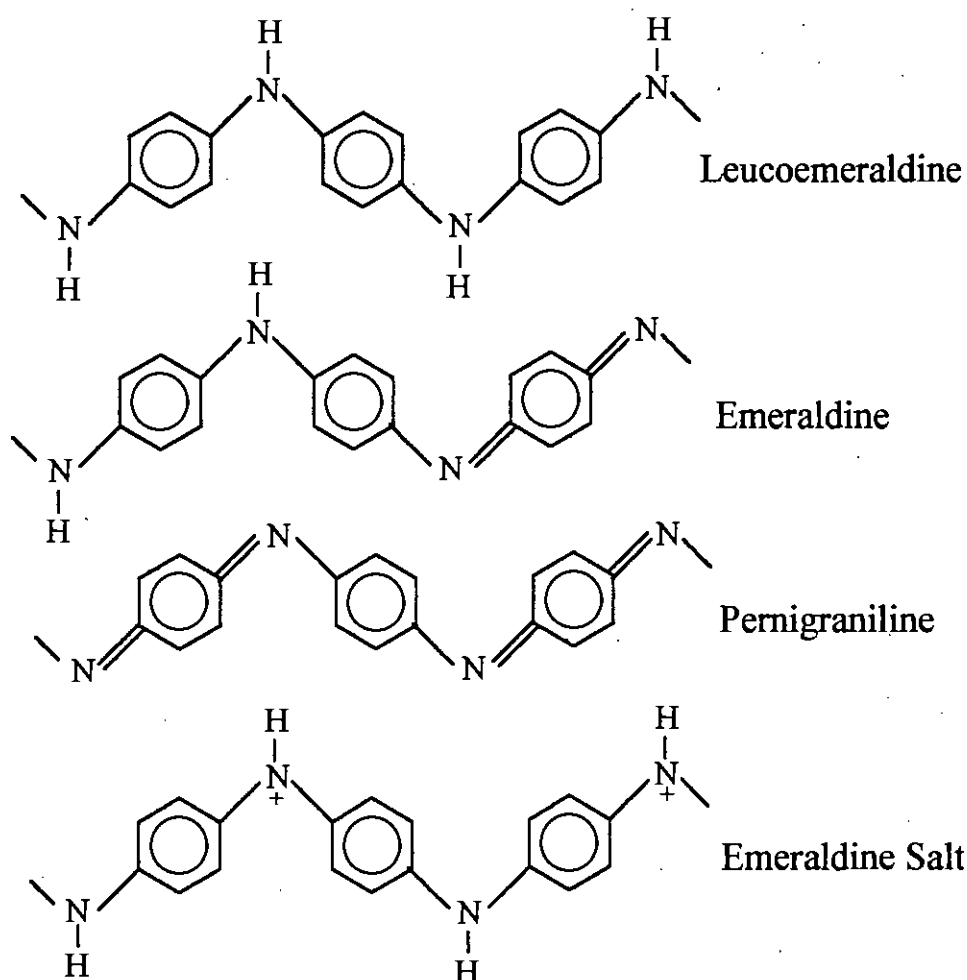
Fig. 1.1: Representation of idealized oxidation states of PANI.

Emeraldine salt is a partially oxidized compound, protonated, with electrical conducting characteristics. Leucoemeraldine is a fully reduced compound with electrical insulating characteristics. There are no double bonds between the aromatic rings and the N-H groups. Emeraldine base is an insulating compound, partially oxidized with few N-H groups in the main chain. Emeraldine changes from insulator to conductor when it is protonated with proton donor acids, such as, hydrochloric acid. This change is one of the most interesting properties of PANI. The structure of emeraldine PANI can be changed to emeraldine salt by removing an electron from the N-H group. Pernigraniline is a fully oxidized compound without conducting characteristics. There are no N-H groups in the structure. The level of protonation in the

structure causes dramatic changes in the conductivity. The base form of the polymer in the emeraldine oxidation state (y = 0.5)
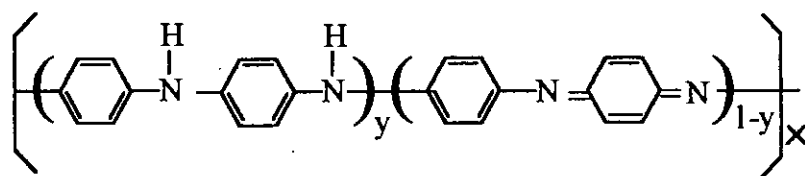
which contains equal number of alternating reduced,

  and oxidized
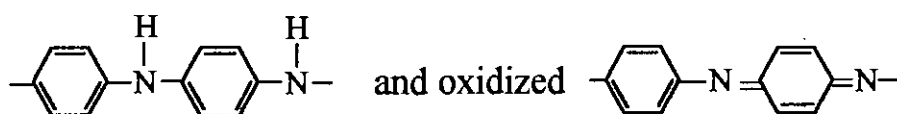
repeat units can be protonated by dilute aqueous acid to produce the corresponding salt (A=anion)
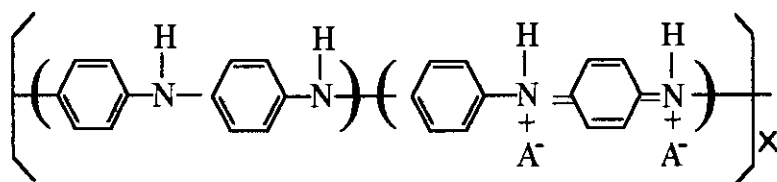
which is believed to exist as polysemiquinone radical cation[19-21].
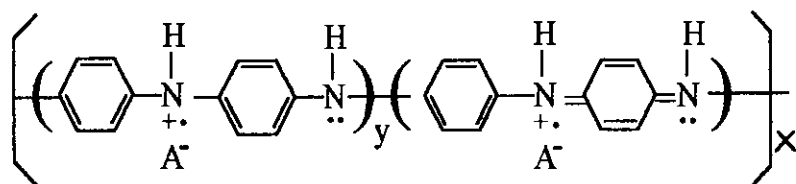
The polymer exhibits conductivities of ~ 1-5 S cm^{-1} when approximately half of its nitrogen atoms are protonated as shown above.

ii) Methods of preparation

PANI is generally prepared by direct oxidation of aniline using an appropriate chemical oxidant or by electrochemical oxidation on different electrode materials.

Various chemical oxidizing agents have been used by different authors: potassium bichromate[22,23], ammonium persulfate or peroxydisulfate[24], hydrogen peroxide, ceric nitrate and ceric sulfate[25,26]. The reaction is mainly carried out in acid medium, in particular sulfuric acid, at a pH between 0 and 2. However, MacDiarmid *et al.* used hydrochloric acid at pH 1. Genies *et al.*[27] used a eutectic mixture of hydrofluoric acid and ammonia, the general formula of which is NH_4F: 2.3 HF, for which the pH is probably less than 0.

When aniline is mixed with the chemical oxidant in a reaction vessel and left for a certain period of time (the duration of which depends on the temperature and the concentration of active species), the solution gradually becomes colored and a black precipitate appears[28]. The coloration of the solvent is possibly due to the formation of soluble oligomers.

Anodic oxidation of aniline on an inert metallic electrode is the most current method for the electrochemical synthesis of PANI. This method offers the possibility of coupling with physical spectroscopic technique such as visible, IR, Raman, ellipsometry and conductimetry, for *in situ* characterization.

The anodic oxidation of aniline is generally affected on an inert electrode material, which is usually Pt[29,30]. However, several studies have been carried out with other electrode materials: iron[31], copper[32], zinc[33], chrome-gold[34], lead[33], palladium[35] and different types of carbon vitreous, pyrolic or graphite[36] or on semiconductor[37,38]. When the polymerization is carried out at constant current, a maximum current density of 10 mA cm^{-2} is rarely exceeded.

iii) Reaction mechanism for polymerization of aniline

The efficient polymerization of aniline is achieved only in an acidic medium. The mechanism of this reaction is shown in Fig 1.2. The first five steps involve the establishment of the anilinium radicals and the possible reactions between the anilinium radicals themselves or with each other, and finally the oxidation of ADPA by the peroxide to form PBQI. Step 6 is the most important one, because it shows that the catalytic action of the acidic reaction medium accelerates the coupling of aniline (or, more precisely anilinium radical 2) with existing

dimmers and higher oligomers (step 6b). Moreover step 6b also supplies a reasonable explanation for the different oxidation states in PANI powders prepared under similar conditions.

Step 1: Formation of the aniliniumradicalcation 1
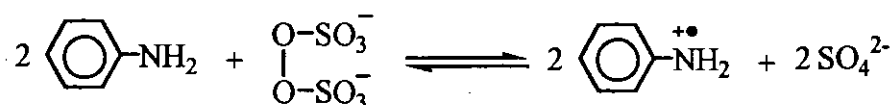
Step 2: Formation of the aniliniumradical 1
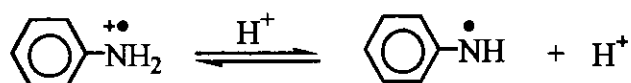
Step 3: Formation of the aniliniumradical 2
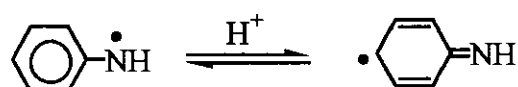
Step 4: Coupling of the aniliniumradicals 1 and 2 (Generation of *p*-aminodiphenylamine)
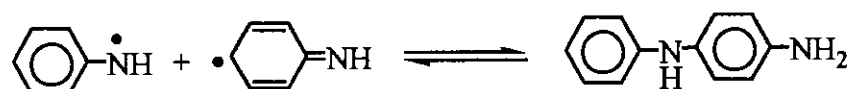
Step 5: Generation of N-phenyl-1,4-benzoquinone diimine from *p*-aminodiphenylamine

Step 6: Growth of aniline oligomers and polymers

(a) Growth via *p*-aminodiphenylamine and aniliniumradical 2
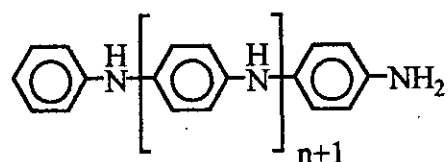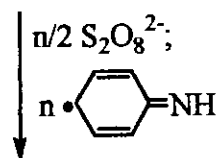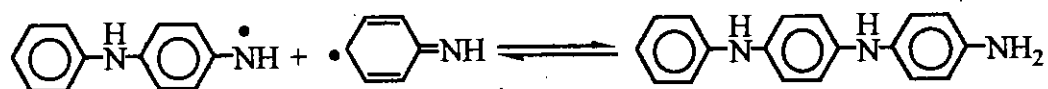
(b) Growth via N-phenyl-1,4-benzoquinone diimine and aniliniumradical 2, catalyzed by the acid HX
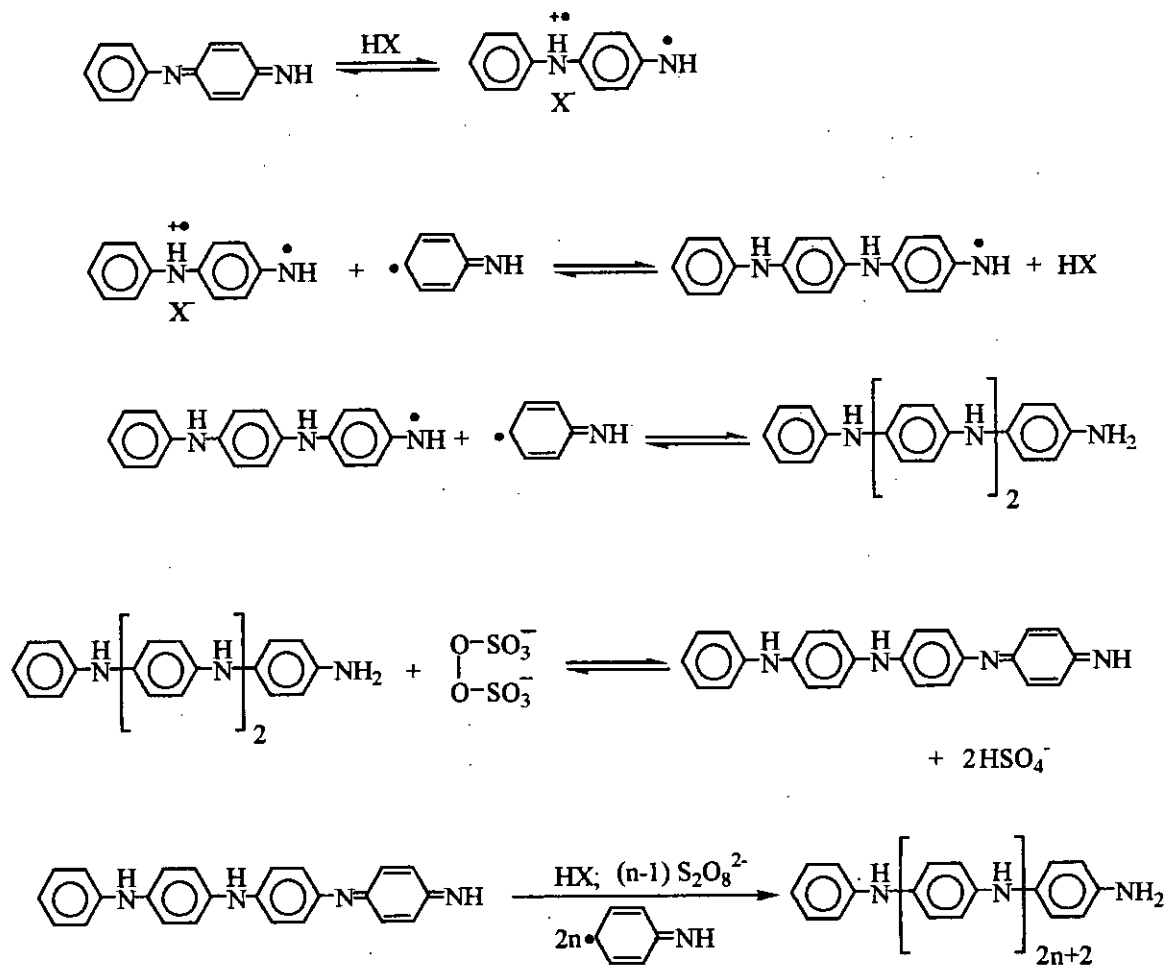
Fig. 1.2: Mechanism for the polymerization of aniline

iv) Morphology and structure

The adherence and the homogeneity of a PANI film on an electrode vary according to the method of synthesis employed. Diaz[39] has observed weak adherence for a polymer prepared by electrochemical oxidation at constant potential, whereas good adherence results when potential cycling is employed. Kitani *et al.*[40] have reported that, using the same method, a thin homogenous film is initially deposited on the electrode, followed by the formation of an amorphous powder, which eventually becomes detached, from the electrode surface.

Electrochemical investigations on the polymer growth by Thyssen *et al.*[41] yielded evidence for cross-linking reactions leading to the formation of hemispheres.

There is, therefore, a myriad of possible chemical structures for the polymeric backbone of PANI. Elucidation of the precise molecular arrangement is complicated by the fact that these structures are affected by both electronic excitation and reduction and by concomitant protonation and deprotonation of the nitrogen atoms in the polymer.

v) Applications

PANI has attracted considerable attention as a polymer due to its simple synthesis, good environmental stability, and adequate level of electrical conductivity.

PANI can be used as material for modified electrodes[36,39], as corrosion inhibitors for semiconductors in photoelectro-chemical assemblies[42], in microelectronics[43] and as electrochromic material[44]. The application, which has inspired most interest, is in the area of electrochemical batteries. The possible use of PANI as active anodic material is in rechargeable batteries[45].

PANI is unique in that its electrical properties can be reversibly controlled both by charge-transfer doping and by protonation.

The wide range of associated electromechanical and optical properties, coupled with good stability, make PANI potentially attractive for application as an electronic material.

One of the most important applications of PANI is as electrodes in the rechargeable batteries. In such applications, use is made for the electromechanical reversibility of the polymers acting as electrodes. It can be used as material for modified electrodes and as an electrode for direct electrolytic metallization of copper. Because of its solubility, the polymer is deposited directly onto a PCB by a dip-coating process.

Another use of polymer structure is for gas sensors. The integrated structure includes a sensitive layer (PANI) and a conductive bridge consisting of poly (3,4-ethylenedioxidethiophene) (PEDOT). Good sensitivity, stability, and response of the multiplayer material to gaseous HCl indicate a possible application of PANI polymer to provide a binding of sensitive elements in sensors.

A large number of gas sensors use PANI because they offer great design flexibility. The change of conductance on exposure to a gas is the sensing mechanism in a chemiresistor. These sensors can also be used to measure concentrations of acids and bases in aqueous solutions. Likely applications could include measuring concentrations of HF, HCl, HBr, an HI near incinerators in which halogenated hydrocarbons are burned; measuring concentrations of HF in and near semiconductor processing plants; and measuring concentrations of HCl from rocket-engine exhausts. In a chemiresistor, the film is made of a PANI, the resistivity of which decreases upon exposure to acids in both vapor and aqueous phases. In addition, the color of a PANI varies with the acidity of its environment; thus, in principle, a PANI can be deposited on the end of an optical fiber and be monitored the concentration of acidic gas by measuring the optical absorption spectrum from the opposite end of the fiber.

PANI can be used for device fabrication such as photovoltaic and photocells. Suitable energy gaps are required and optical energy gaps decreases due to the increase of the degree of disorder.

PANI is used for most biosensors applications because it is a poor conductor in neutral solutions. PANI is a promising material for shielding electromagnetic radiation and reducing or elimination of electromagnetic interference (EMI) because of its relatively high conductivity and dielectric constant and ease of control of these properties through chemical processing.

PANI polymer offers a new alternative for ESD protection. The conductivity of such polymer can be tuned, can easily meet the high end of the dissipative range, and is stable.

1.7.2 PANI-SiO$_2$ Composite

The most important ceramic compound is silica or silicon dioxide (SiO$_2$). Silicon dioxide is an acidic oxide. It is very inert. It has very high surface area and for this property, recently it is used for the preparation of colloidal nanocomposites with Polyaniline. In recent years, the synthesis and characterization of various polymer-inorganic oxide composite materials were reported in the literature. Of these polyaniline-silica (PANI-SiO$_2$) and polypyrrol-silica (PPY-SiO$_2$) composites[46] are worth mentioning. They show very interesting physical properties. The silica composites have been mostly prepared by polymerizing the organic monomers in the presence of colloidal silica solutions[47-49]. The silica particles are embedded in the polymer matrix. The uniformity in the size of the silica particles is obviously a key factor in determining the quality of the polymer-silica composite.

Silica sol   Polyaniline-silica composite

Fig. 1.3: Schematic representation of the formation of PANI-SiO$_2$ particles.

1.8 The Adsorbate: Methyene Blue

The use of dyestuffs for the determination of specific surface area is quite common. The dyestuff, which is often recommended for the estimation of surface area, is methylene blue. By far, the most widely method of determining the amount of dye adsorbed by a substrate is spectroscopy in the visible region. The following types of forces either singly or combined are

attribute for the adsorption affinity of dyes for solid adsorbents: ionic and ion-dipole, hydrogen bond, van der Waals, hydrophobic and covalent bond. Because of the intense color of dyes, it is very easy to monitor the adsorption by observing its color change at various intervals of adsorption process.

1.9 Theoretical Aspects of Experimental Techniques

1.9.1 Ultraviolet-visible (UV-Vis) spectroscopy

Electromagnetic radiation of suitable frequency can be passed through a sample so that photons are absorbed by the samples and changes in the electronic energies of the molecules can be brought about. So it is possible to effect the changes in a particular type of molecular energy using appropriate frequency of the incident radiation. When a beam of photons passes through a system of absorbing species, then we can write

$$-\frac{dI}{dx} = \alpha I \tag{10}$$

where, $I \rightarrow$ intensity of photon beam

$dI \rightarrow$ reduction of intensity

$dx \rightarrow$ rate of photon absorption with distance (x) traversed

$\alpha \rightarrow$ absorption co-efficient of the material

Now if I_0 is the initial intensity at thickness $1 = 0$ and I is the transmitted radiation at $x = 1$, then by integration, we can write

$$ln \frac{I_0}{I} = \alpha l \tag{11}$$

For polymers and polymeric composites, UV-Vis spectrum is taken to measure the impurity level, band gap energy etc. The electrode spectra of the prepared compounds were recorded on a UV-Vis recording spectrophotometer in the wavelength range 300-800 nm. A schematic diagram of UV-Vis spectrophotometer is shown in Fig. 1.4.
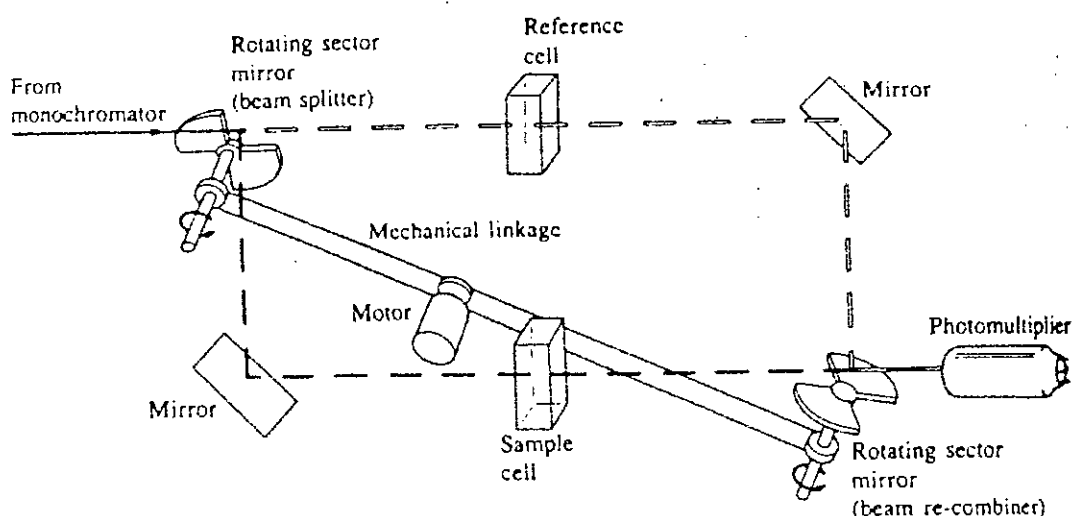
Fig. 1.4: A block diagram of an UV-Vis spectrophotometer.

1.9.2 Infra-red (IR) spectroscopy

Emission or absorption spectra arise when molecules undergo transition between quantum states corresponding to two different internal energies. The energy difference ΔE between the states is related to the frequency of the radiation emitted or absorption by the quantum relation

$$\Delta E = h v \hspace{4cm} (12)$$

where $h \rightarrow$ Planck's constant $v \rightarrow$ frequency. Infrared frequencies have the wave length range from 1 μm to 50 μm are associated with molecular vibration and vibration-rotation spectra. Detection of chemical groups and bonding are done by the typical spectra.

In polymer, the IR absorption spectrum is often surprisingly simple, if one considers the number of atoms involved. This simplicity results first from the fact that many of the normal vibrations have almost the same frequency and therefore appear in the spectrum as one absorption band and second, from the strict selection rules that prevent many of the vibrations from causing absorptions. In our experiment, we tried to observe the change in frequency of

different samples and detection of SiO_2 by following the Si-O or O-Si-O frequencies. IR spectrums of all the compounds were recorded on IR spectrophotometer in the region of 4000-400 cm^{-1}. Samples were introduced as KBr pellets. A block diagram of an IR spectrophotometer is shown in Fig. 1.5.
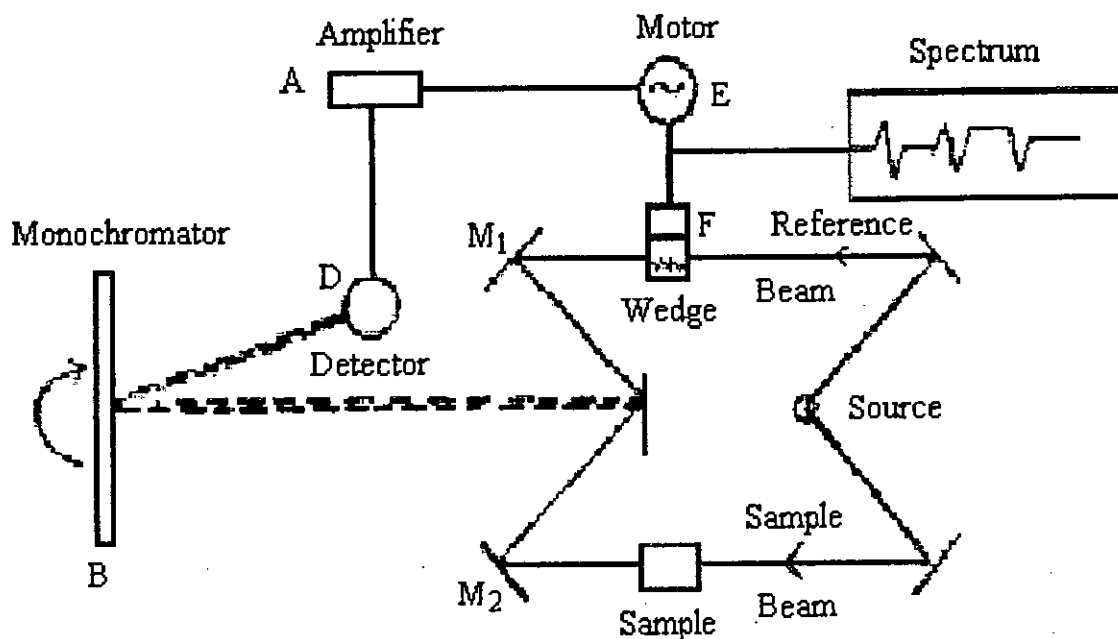
Fig.1.5: A block diagram of an IR spectrophotometer.

1.9.3 X-ray diffraction

The X-ray diffraction (XRD) provides substantial information on the crystal structure. This method is applied for the investigation of orderly arrangements of atoms or molecules through the interaction of electromagnetic radiation to give interface effects with structures comparable in size to the wavelength of the radiation. Studies on the crystal structures developed based on methods using single crystals after the discovery of X-ray diffraction by crystals made by the Von Laue[50]. Now a days XRD is used not only for the determination of crystal structure but

also chemical analysis, such as chain conformations and packing for polymers, for stress measurements and for the measurement of phase equilibria and the measurement of particle size, for the determination of the orientation of the crystal and the ensemble of orientations in a polycrystalline material.

X-rays are the electromagnetic radiation whose wavelength is in the neighborhood of 1° A. The wave length of an X-ray is thus of the same order of magnitude as the lattice constant of crystals, and it is this which makes X-rays so useful in structures analysis of crystals whenever X-ray are incident on a crystal surface they are reflected. The reflection abides by the celebrated Bragg's law as given below:

$$2d\,Sin\theta = n\lambda \tag{13}$$

where d is distance between crystal planes, θ is the incident angle, λ is the wave length of X-ray and n is a positive integer. The diffracted X-ray may be detected by their action on photographic films or plates or by means of a radiation counter or electronic equipment feeding data to a computer[51].

The main purpose of using this technique for the analysis of the studied polymeric samples is to observe, from the X-ray diffraction pattern, the change in crystallinity in the series upon same condition.

1.9.4 SEM technique

The scanning electron microscope (SEM) uses a finely focused beam of electrons to scan over the area of interest. The beam-specimen interaction is a complex phenomenon. The electrons actually penetrate into the sample surface, ionizing the sample and cause the release of electrons from the sample. These electrons are detected and amplified into a SEM image that consists of Back Scattered Electrons and Secondary Electrons. Since the electron beam has a specific energy and the sample a specific atomic structure, different image will be collected from different samples, even if they have the same geometric appearance.

The specimen stage allows movement of the specimen along 5 axis as indicated in Fig.1.6. The basic stage is controlled manually by micrometers and screw-type adjusters on the stage door. The motorized stage has motors driving the X, Y, Z and rotation controls, all with manual override.

The stage can be tilted over 90°. The tilt axis always intersects the electron optical axis of the column at the same height (10 mm). When the specimen positioned at this height, the specimen can be tilted in the eucentric plane. This means that during tilt, almost no image displacement occurs. The tilting mechanism can be locked for more stability at high magnification.

Rotation in the
tilted plane

Y ± 75 mm in the plane
of tilt, perpendicular to
the tilt axis

X ± 75 mm along the
tilt axis

Z 37 mm

Tilt range –30° to +60°
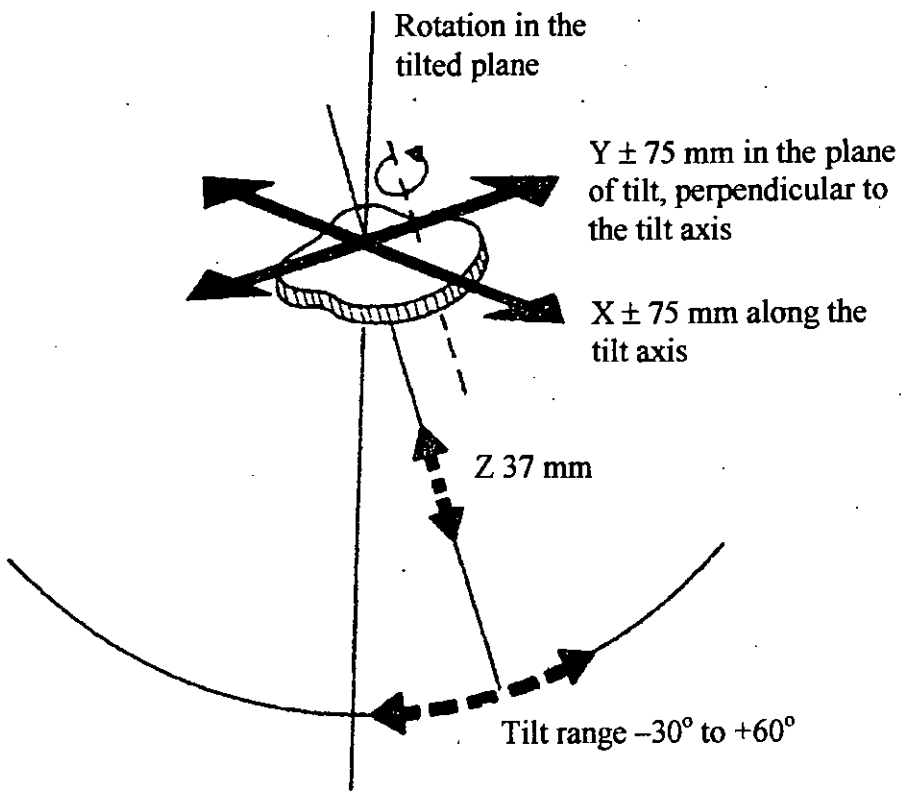
Fig. 1.6a: Illustration of specimen stage movement
in SEM arrangements.
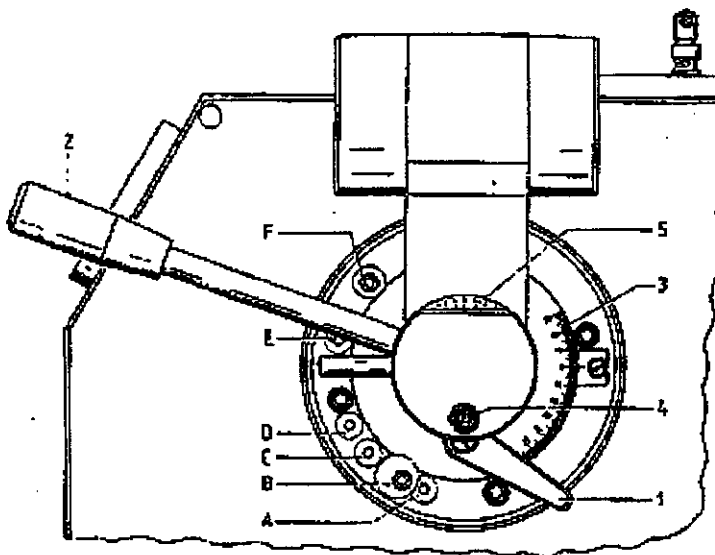
Fig. 1.6b: Mechanical controls and tilt stops on the stage
door of SEM.

1.9 Literature Reviews and Proposed Plan of the Work

A number of conducting polymers has been extensively studied in the last decades, in particular because of the great possibilities of application they offer such as electronic and optical devices, and batteries[52,53]. PANI is by far the most investigated conducting polymer; it has attracted considerable attention as a polymer due to its simple synthesis, good environmental stability, and adequate level of electrical conductivity.

In recent years, the synthesis and characterization of various polymer-inorganic oxide composite materials were reported in the literature. Of these PANI/SiO$_2$ composite[54] is worth mentioning. They show very interesting physical properties. The silica composites have been mostly prepared by polymerizing the organic monomers in the presence of colloidal silica solutions[55]. The silica particles are embedded in the polymer matrix. The uniformity in the size of the silica particles is obviously a key factor in determining the quality of the polymer-silica composite.

There are two major reasons for the revived interest in composite materials. One is that the increasing demand for better performance in many product areas, especially in the aerospace, nuclear energy and aircraft fields is taxing to the limit of our conventional monolithic materials. The second reason- the most important for the long run is that the concept of composites provides scientists with a promising approach to designing, rather than selecting, materials to meet specific requirements of an application.

Although PANI and PANI/SiO$_2$ are expected to exhibit excellent surface properties, to our knowledge, only few reports have appeared to the surface phenomena of these substrates. Detailed characterization of their adsorption behaviors, surface area measurements etc. have not been made in those reports.

In the present work, it is aimed not only to focus on the adsorption characteristics but also to investigate the variation in the specific surface areas of PANI and PANI/SiO$_2$ depending on the different protonation level of the MB solution that will be used as adsorbate in the adsorption

process. Moreover, to characterize these substrates by physical means *viz.* IR spectroscopy, XRD and SEM.

E XPERIMENTAL

2.1 Materials and Probes

2.1.1 Chemicals

The chemicals and reagents used in this work are listed below. These are analytical grade and used as received except for the aniline, which was distilled twice prior to use. Doubly distilled water was used as solvent to prepare most of the solutions of this work.

i) Aniline [E. Merck, Germany]

ii) Hydrochloric acid (32%) [E. Merck, Germany]

iii) Ammonium peroxydisulfate [E. Merck, Germany]

iv) Ammonium hydroxide (25%) [E. Merck, India]

v) Methylene blue [Fluka, England]

2.1.2 Instruments

The instruments and probes employed in this work are mentioned below:

i) Infra red spectrophotometer [IR-470, Shimadzu, Japan]

ii) UV-visible spectrophotometer [UV-1601PC, Shimadzu, Japan]

iii) Automatic X-ray diffractometer [JDX – 8P, JEOL Ltd., Japan]

iv) Scanning electron microscope [Philips XL 30, Holland]

v) pH meter [HM –16s, TOA, Japan]

vi) Centrifuge machine [Universal 16A, Hettich. Germany]

vii) 100 mesh sieve [Endecotls test sieves limited, England]

viii) Digital balance [FR –200, Japan]

2.2 Preparation of Adsorbents

2.2.1 Polyaniline substrates

PANI was prepared by a chemical method at room temperature, 30°C (± 2°) following the procedure described elsewhere[56-58]. In brief, the procedure is as follows: 2.5 mL of aniline, 5 mL of hydrochloric acid (HCl) and 3.0g of ammonium peroxydisulfate ((NH_4)$_2S_2O_8$) were

added to double distilled water maintaining the total volume of the mixture 400 mL. The reaction mixture was turned into deep blue polymeric sediment instantaneously. However, the content was left over night for the completion of polymerization. The deep blue sediment was then filtered and treated separately with aqueous solutions having pH of 1.09, 6.95 and 10.15 in order to get three different PANI substrates – described below:

i) The polymeric sediment as obtained was washed with double distilled water (pH = 6.95) until the pH of the supernatant reaches 6.95. The mass was then kept in contact with the double distilled water for over night and then filtered. The PANI thus treated is called neutral PANI (*n*-PANI) in this work.

ii) In other case, the sediment was washed with aqueous 0.1M HCl (pH = 1.09) solution and continued washing as before until the supernatant shows a pH value 1.09. The content was then left over night in the acid solution. PANI treated in this way is called acidic PANI (*a*-PANI).

iii) And in another case, the sediment was washed with 0.1M aqueous ammonium hydroxide (NH$_4$OH) solution (pH = 10.15) until the supernatant attains the pH value 10.15. The sediment was then kept over night in the ammonia hydroxide solution. The PANI thus treated is called basic PANI (*b*-PANI) throughout the work.

The PANI substrates thus treated were then dried initially in air followed by vacuum drying. The dried mass was grounded and then sieved using 100 mesh sieves and stored in a vacuum desicator.

2.2.2 Polyaniline-SiO$_2$ composite substrates

Synthetic procedure was followed as described in detail elsewhere for the preparation of PANI/SiO$_2$ composites. Preparation procedure is as follows: Aqueous colloidal suspension of silica was prepared by adding 2.0 g of silica particles to double distilled water followed by beating the mixture for two hours. The resulted dispersion was then allowed to settle for two hours. During this span of time relatively bigger silica particles were sedimented at the bottom

of the container. The smaller particles remain in the system and dispersed colloidally. The colloidal solution was then decanted and used for PANI/SiO$_2$ composite preparation.

2.5 mL of aniline, 5 mL of hydrochloric acid (HCl) and 3.0g of ammonium peroxydisulfate ((NH$_4$)$_2$S$_2$O$_8$) were added to the 400 mL of the prepared aqueous suspension of colloidal silica at room temperature. The polymerization was allowed to proceed for over night. The reaction mixture was then centrifuged for 30 minutes and the resulting deep blue sediment was redispersed in double distilled water. The centrifugation-redispersion cycle was repeated thrice in order to remove completely the excess small silica particles from the PANI/silica composite.

2.3 Spectral Analysis

2.3.1 IR spectra

IR spectra of all the dried samples were recorded on an IR spectrometer in the region of 4000 - 400 cm^{-1}. IR spectra of the solid samples were frequently obtained by mixing and grinding a small amount of materials with dry and pure KBr crystals. Thorough mixing and grinding were done in a mortar by a pestle. The powdered mixture was then compressed in a metal holder under a pressure of 8-10 tons to make a pellet. The pellet was then placed in the path of IR beam for measurements.

2.3.2 X-ray diffraction

PANI and PANI/SiO$_2$ substrates thus treated were analyzed for their x-ray diffraction pattern in the powder state. For this purpose, the samples were prepared as the procedure described in section 2.2. The powder samples were pressed in a square aluminum sample holder (40 mm × 40 mm) with a 1 mm deep rectangular hole (20 mm × 15 mm) and pressed against an optical smooth glass plate. The upper surface of the sample was labeled in the plane with its sample holder. The sample holder was then placed in the difractometer.

X-ray diffraction pattern were recorded on an automatic X-ray diffractometer using Mo(Zr) radiation of wave length 1.54 A°. The diffractometer was operated at 30 KV and 20 mA with a scan speed of $1°$ min^{-1}.

2.3.3 UV-vis spectra

The UV-vis spectral analysis of the sample solutions employed a double beam spectrophotometer. UV-vis spectroscopic analysis for the adsorption studies involved the aqueous solution of different pH. The references in these cases were the corresponding aqueous solutions that used for preparing the adsorbate solutions. The determination of the amount of dye adsorbed by a substrate was done by spectroscopy in the visible region.

2.4 Surface Morphology

PANI matrices thus prepared and treated following the methods described in section 2.3 were examined for their surface morphology. For this purpose, scanning electron microscopy technique was adopted. The dried powder PANI and PANI/SiO_2 samples were dispersed on a conducting carbon glued strip. The sample-loaded strip was then mounted to a chamber that evacuated to ~ 10^{-3} to 10^{-4} torr and then a very thin gold layer (~ few nanometers thick) were sputtered on the sample to ensure the conductivity of the sample surface. The sample was then placed in the main SEM chamber to view its surface. The system was computer interfaced and thus provides recording of the surface images in the computer file for its use as hard copy.

2.5 Adsorption Study for the Determination of Specific Surface Area

For adsorption studies, polymeric matrices, *viz.*, acidic-PANI, neutral-PANI, basic-PANI, and PANI-SiO_2 were used as adsorbents. Their preparation and post-synthesis treatments with aqueous solution of various pH values are described in section 2.2. On the other hand, organic dye MB was used as adsorbate. The chemical structure of MB is shown in Fig. 2.1.

Adsorption of MB on acidic-PANI, neutral-PANI and basic-PANI and PANI-SiO$_2$ matrices were studied spectroscopically from their aqueous solution of pH 1.09, 6.95 and 10.15, respectively. The double distilled water used in this work has the pH = 6.95. On the other hand, when 2 mL of concentrated NH$_4$OH (25%) was diluted to 500 mL by adding the distilled water, it gives an aqueous solution of pH = 10.15. An aqueous solution of pH =1.09 was made by adding 2 mL of concentrated HCl (32%) to distilled water and making the total volume 500 mL.
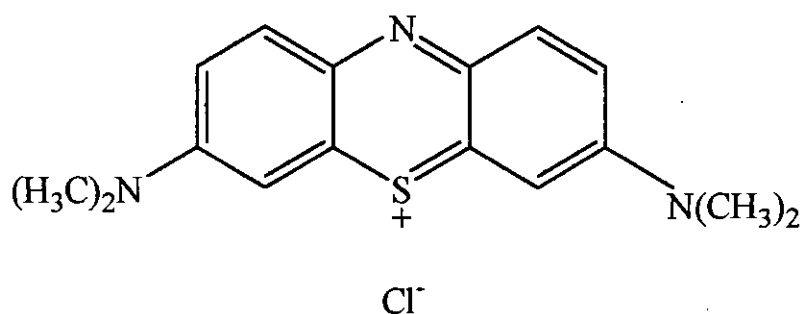
Fig. 2.1: Chemical structure of MB.

2.6 Preparation of Methylene Blue Solution

2.6.1 Stock methylene blue solution

It was prepared by dissolving 0.036g solid methylene blue to 500 mL double distilled water. In this way, 2.02 × 10^{-4} M MB solution was prepared which was used as stock methylene blue solution.

2.6.2 Intermediate methylene blue solution

1×10^{-5} M, 2×10^{-5} M, 3×10^{-5} M, 4×10^{-5} M, 5×10^{-5} M, and 6×10^{-5} M methylene blue solutions were prepared by diluting 5mL, 10 mL, 15 mL, 20 mL, 25 mL and 30 mL respectively of stock solution to 100 mL with double distilled water.

2.7 Procedure of Adsorption of Adsorbate

The method of adsorption of MB (adsorbate) with the substrates (adsorbent) is given below:

A fixed amount, 0.133 g of sample was taken to each of the five reaction vessels. Each vessel was charged with 100 mL methylene blue solution of desired concentration. Immediately after the addition of methylene blue solution to the container, the shaking device was allowed to function. The bottles were put down from the shaker by turn after 15 min, 30 min, 60 min, 90 min, and 120 min respectively. After shaking the solutions were filtered with cotton and pipette until clear solution was appeared. Finally, the absorbance of the remaining unadsorbed clear solution was taken by the UV-visible spectrophotometer.

In this way, the methylene blue solute was allowed to adsorb from its solution on the surface of required substrate for the estimation of specific surface area. To a series of methylene blue solutions of 2×10^{-5} M, 3×10^{-5} M, 4×10^{-5} M, 5×10^{-5} M, and 6×10^{-5} M, the same procedure was adopted for a particular sample. The specific surface areas of others were studied under an identical set of experimental conditions mentioned above.

2.8 Recording the Absorbance Data of Methylene Blue Solution

After the treatment of the samples with the different methylene blue solutions, the remaining unadsorbed solutions were ready to take the absorbance with the spectrophotometer. The remaining solutions were analyzed through the reference standard methylene blue solution of different concentrations with the spectrophotometer at λ_{max} 664 nm.

The absorbance was taken for example at different shaking intervals of five vessels for 1×10^{-5} M methylene blue solution. The absorbance of the rest of methylene blue solutions were also taken one after another for the calculation of adsorption (mg g^{-1}), which refers the monolayer coverage by using the curve, plotted absorbance vs time for one substrate. This monolayer capacity was required for the calculation of the surface area of that compound. In the determination of the specific surface area of all the samples played the same role with those six methylene blue solutions.

2.9 Calculation of Surface area from Adsorption

The amount adsorbed of methylene blue solute from the original solution was found from the absorbance of the remaining solution. In all the case, equilibrium time of adsorption was seen to be reached within ~2h. The equilibrium amount adsorbed (mg g^{-1}) from different concentrations of methylene blue dyestuff was calculated from the original concentration (M) of methylene blue solution and the corresponding concentration for the observed absorbance of the remaining solution. The equilibrium concentration was obtained from the absorbance at equilibrium time with the help of a calibration curve. Calibration curve represents absorbance of stock solution at its different concentrations. Figures 2.2-2.4 show the calibration curves of MB solution prepared in aqueous HCl (pH = 1.09), distilled water (pH = 6.95) and aqueous NH$_4$OH (pH = 10.15) solutions, respectively. In fine, a plot of adsorption (mg g^{-1}) vs equilibrium concentration (M) was used to find out the monolayer capacity (mg g^{-1}) from the steady point of the curve. This value of monolayer capacity was put in the equation. In the equation the values of other parameters like molecular mass, M, of MB (i.e. C$_{16}$H$_{18}$ClN$_3$S. 2H$_2$O = 355.89 g mol^{-1}); Avogadro constant, N, and the cross-sectional surface area of MB, A$_m$, were put and the specific surface area, S (m^2 g^{-1}) of the six different samples were calculated.
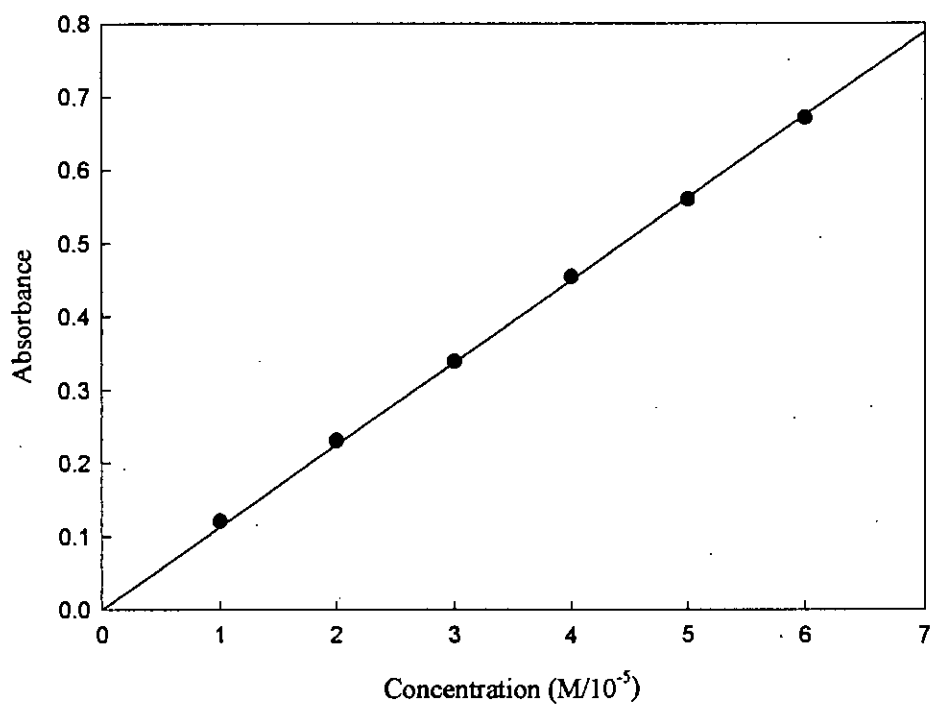
Fig. 2.2: Calibration curve of MB in aqueous HCl solution (pH = 1.09).
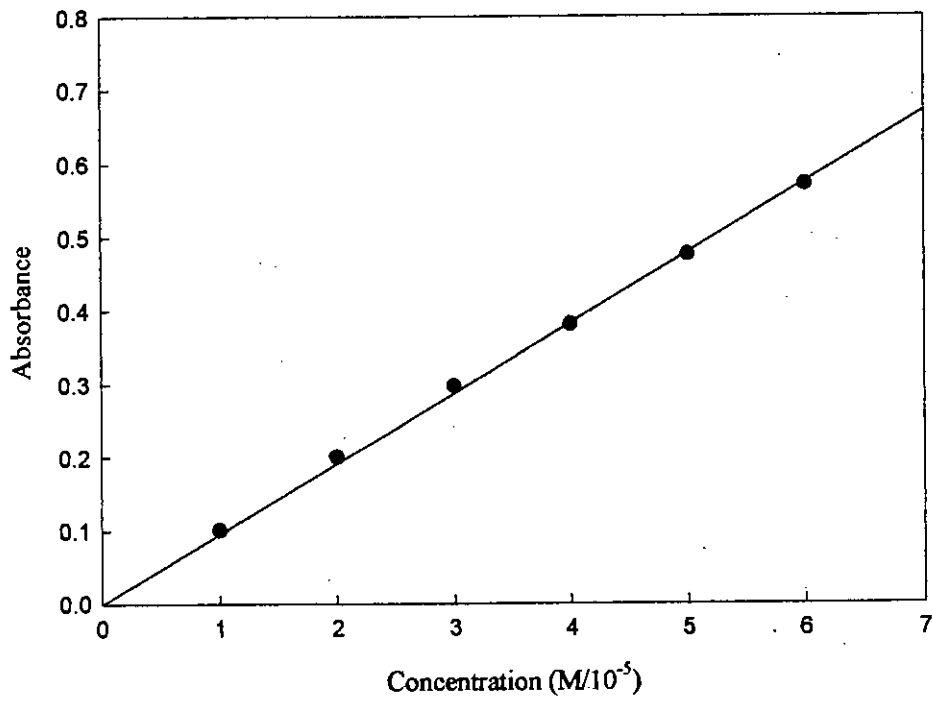
Fig. 2.3: Calibration curve of MB in double distilled water (pH = 6.95).
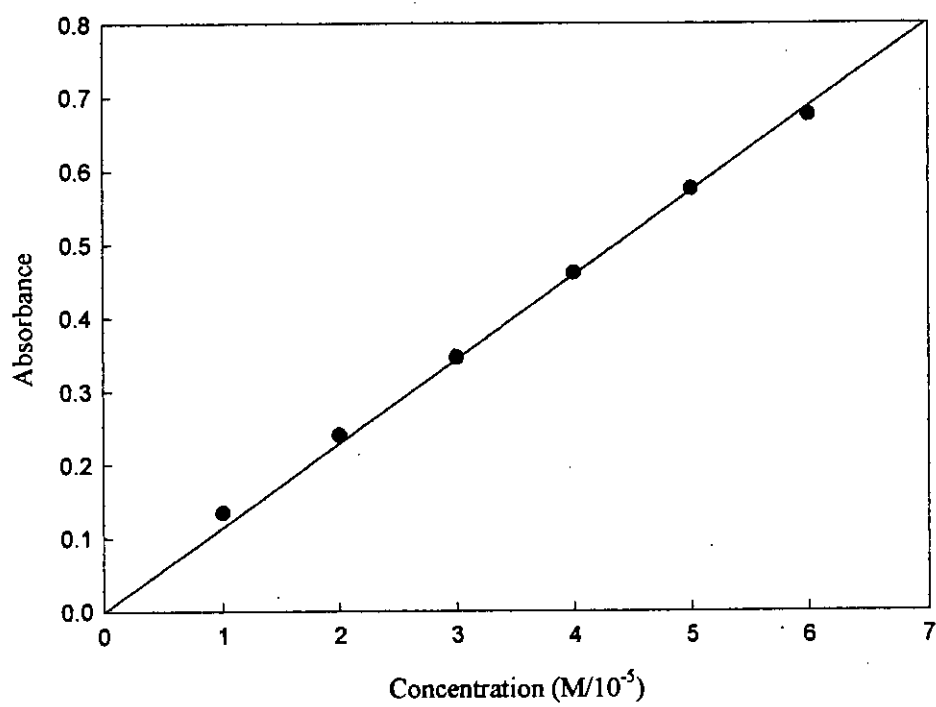
Fig. 2.4: Calibration curve of MB in aqueous NH_3 (pH = 10.15).

2.10 Data in the Determination of Specific Surface Area

In the determination of specific surface area of various samples by adsorption method using methylene blue dyestuff, which follow the above procedure, is given in the following pages one after another.

The determination of specific surface area of acidic PANI by adsorption method using MB dyestuff

MB solution: 1×10^{-5} M

Table 2.1: Absorbance data for 1×10^{-5} M MB solution at different shaking time

Initial conc. of MB (M)	Amount of sample taken in 100 mL solution to each vessel (g)	Time of shaking (min.)	Corresponding absorbance	Original absorbance
1×10^{-5}	0.133	15	0.101	0.121
		30	0.084	
		60	0.062	
		90	0.043	
		120	0.043	

Fig.2.5: Effect of shaking time on the absorbance of 1×10^{-5} M MB solution

Table 2.2: Amount of MB adsorbed by per gram of sample from original concentration of 1×10^{-5} M

Time of shaking (min.)	Absorbance of remaining MB solution at the corresponding time	Difference of absorbance (Original absorbance of 1×10^{-5} M MB solution) - (Absorbance of remaining MB solution at the corresponding time)	Amount of solute adsorbed by the sample at the corresponding time (mg g^{-1})
15	0.101	0.020	0.48
30	0.084	0.037	0.94
60	0.062	0.059	1.47
90	0.043	0.078	1.80
120	0.043	0.078	1.80

Fig. 2.6: Effect of shaking time on the amount of solute (MB) adsorbed from its 1×10^{-5}M solution

MB solution: 2×10^{-5} M

Table 2.3: Absorbance data for 2×10^{-5} M MB solution at different shaking time

Initial conc. of MB (M)	Amount of sample taken in 100 mL solution to each vessel (g)	Time of shaking (min.)	Corresponding absorbance	Original absorbance
2×10^{-5}	0.133	15	0.203	0.231
		30	0.164	
		60	0.124	
		90	0.103	
		120	0.103	

Fig. 2.7: Effect of shaking time on the absorbance of 2×10^{-5} M MB solution

Table 2.4: Amount of MB adsorbed by per gram of sample from original concentration of 2×10^{-5} M

Time of shaking (min.)	Absorbance of remaining MB solution at the corresponding time	Difference of absorbance (Original absorbance of 2×10^{-5} M MB solution) - (Absorbance of remaining MB solution at the corresponding time)	Amount of solute adsorbed by the sample at the corresponding time (mg g^{-1})
15	0.203	0.028	0.72
30	0.164	0.067	1.61
60	0.124	0.107	2.60
90	0.103	0.128	3.21
120	0.103	0.128	3.21

Fig. 2.8: Effect of shaking time on the amount of solute (MB) adsorbed from its 2×10^{-5}M solution

MB solution: 3×10^{-5} M

Table 2.5: Absorbance data for 3×10^{-5} M MB solution at different shaking time

Initial conc. of MB (M)	Amount of sample taken in 100 mL solution to each vessel (g)	Time of shaking (min.)	Corresponding absorbance	Original absorbance
3×10^{-5}	0.133	15	0.254	0.339
		30	0.198	
		60	0.165	
		90	0.160	
		120	0.160	

Fig. 2.9: Effect of shaking time on the absorbance of 3×10^{-5} M MB solution

Table 2.6: Amount of MB adsorbed by per gram of sample from original concentration of 3×10^{-5} M

Time of shaking (min.)	Absorbance of remaining MB solution at the corresponding time	Difference of absorbance (Original absorbance of 3×10^{-5} M MB solution) - (Absorbance of remaining MB solution at the corresponding time)	Amount of solute adsorbed by the sample at the corresponding time (mg g^{-1})
15	0.254	0.085	2.14
30	0.198	0.141	3.53
60	0.165	0.174	4.36
90	0.160	0.179	4.51
120	0.160	0.179	4.51

Fig. 2.10: Effect of shaking time on the amount of solute (MB) adsorbed from its 3×10^{-5}M solution

MB solution: 4×10^{-5} M

Table 2.7: Absorbance data for 4×10^{-5} M MB solution at different shaking time

Initial conc. of MB (M)	Amount of sample taken in 100 mL solution to each vessel (g)	Time of shaking (min.)	Corresponding absorbance	Original absorbance
4×10^{-5}	0.133	15	0.312	0.455
		30	0.253	
		60	0.238	
		90	0.232	
		120	0.232	

Fig. 2.11: Effect of shaking time on the absorbance of 4×10^{-5} M MB solution

Table 2.8: Amount of MB adsorbed by per gram of sample from original concentration of 4×10^{-5} M

Time of shaking (min.)	Absorbance of remaining MB solution at the corresponding time	Difference of absorbance (Original absorbance of 4×10^{-5} M MB solution) - (Absorbance of remaining MB solution at the corresponding time)	Amount of solute adsorbed by the sample at the corresponding time ($mg\ g^{-1}$)
15	0.312	0.143	3.61
30	0.253	0.202	4.74
60	0.238	0.217	5.43
90	0.232	0.223	5.75
120	0.232	0.223	5.75
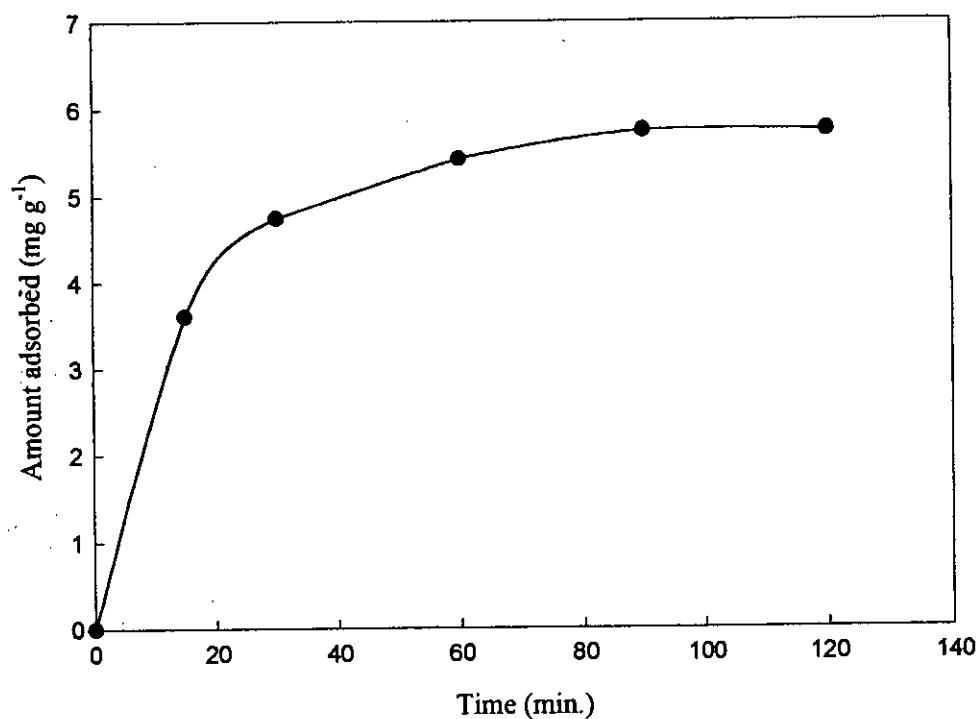
Fig. 2.12: Effect of shaking time on the amount of solute (MB) adsorbed from its 4×10^{-5}M solution

MB solution: 5×10^{-5} M

Table 2.9: Absorbance data for 5×10^{-5} M MB solution at different shaking time

Initial conc. of MB (M)	Amount of sample taken in 100 mL solution to each vessel (g)	Time of shaking (min.)	Corresponding absorbance	Original absorbance
5×10^{-5}	0.133	15	0.341	0.560
		30	0.298	
		60	0.291	
		90	0.290	
		120	0.290	

Fig. 2.13: Effect of shaking time on the absorbance of 5×10^{-5} M MB solution

Table 2.10: Amount of MB adsorbed by per gram of sample from original concentration of 5×10^{-5} M

Time of shaking (min.)	Absorbance of remaining MB solution at the corresponding time	Difference of absorbance (Original absorbance of 5×10^{-5} M MB solution) - (Absorbance of remaining MB solution at the corresponding time)	Amount of solute adsorbed by the sample at the corresponding time (mg g^{-1})
15	0.341	0.219	5.35
30	0.298	0.262	6.39
60	0.291	0.269	6.64
90	0.290	0.270	6.68
120	0.290	0.270	6.68

Fig. 2.14: Effect of shaking time on the amount of solute (MB) adsorbed from its 5×10^{-5}M solution

MB solution: 6×10^{-5} M

Table 2.11: Absorbance data for 6×10^{-5} M MB solution at different shaking time

Initial conc. of MB (M)	Amount of sample taken in 100 mL solution to each vessel (g)	Time of shaking (min.)	Corresponding absorbance	Original absorbance
6×10^{-5}	0.133	15	0.461	0.671
		30	0.392	
		60	0.385	
		90	0.381	
		120	0.381	

Fig. 2.15: Effect of shaking time on the absorbance of 6×10^{-5} M MB solution

Table 2.12: Amount of MB adsorbed by per gram of sample from original concentration of 6×10^{-5} M

Time of shaking (min.)	Absorbance of remaining MB solution at the corresponding time	Difference of absorbance (Original absorbance of 6×10^{-5} M MB solution) - (Absorbance of remaining MB solution at the corresponding time)	Amount of solute adsorbed by the sample at the corresponding time (mg g^{-1})
15	0.461	0.210	5.08
30	0.392	0.279	6.69
60	0.385	0.286	6.82
90	0.381	0.290	6.95
120	0.381	0.290	6.95

Fig. 2.16: Effect of shaking time on the amount of solute (MB) adsorbed from its 6×10^{-5} M solution

The determination of specific surface area of neutral PANI by adsorption method using MB dyestuff

MB solution: 1×10^{-5} M

Table 2.13: Absorbance data for 1×10^{-5} M MB solution at different shaking time

Initial conc. of MB (M)	Amount of sample taken in 100 mL solution to each vessel (g)	Time of shaking (min.)	Corresponding absorbance	Original absorbance
1×10^{-5}	0.133	15	0.082	0.101
		30	0.066	
		60	0.052	
		90	0.041	
		120	0.041	
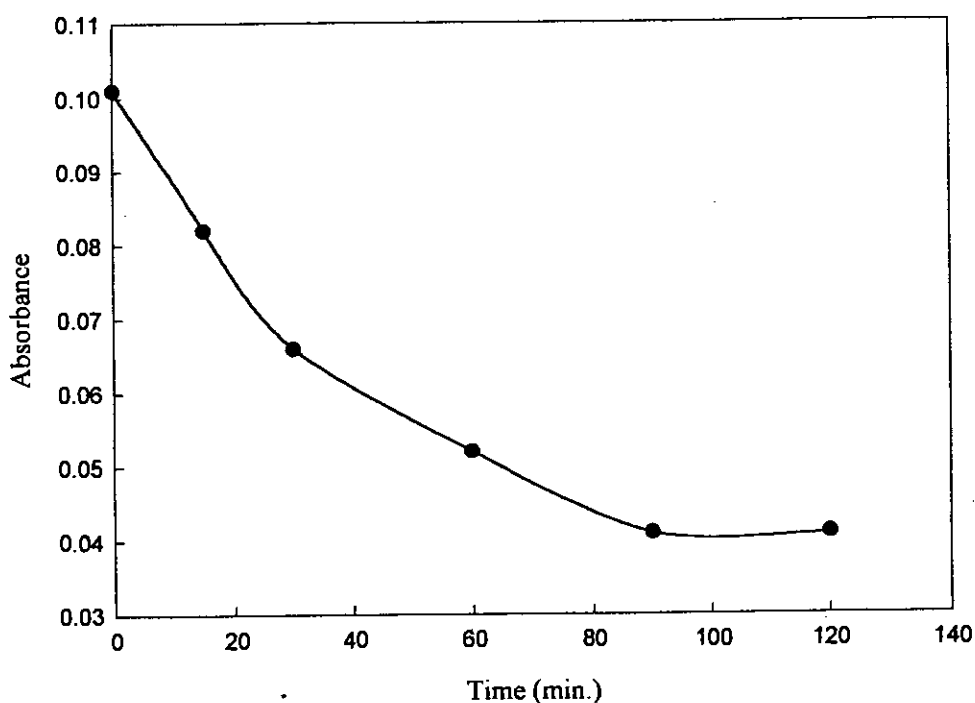
Fig. 2.17: Effect of shaking time on the absorbance of 1×10^{-5} M MB solution

MB solution: 2×10^{-5} M

Table 2.15: Absorbance data for 2×10^{-5} M MB solution at different shaking time

Initial conc. of MB (M)	Amount of sample taken in 100 mL solution to each vessel (g)	Time of shaking (min.)	Corresponding absorbance	Original absorbance
2×10^{-5}	0.133	15	0.167	0.201
		30	0.132	
		60	0.116	
		90	0.113	
		120	0.113	

Fig. 2.19: Effect of shaking time on the absorbance of 2×10^{-5} M MB solution

Table 2.16: Amount of MB adsorbed by per gram of sample from original concentration of 2×10^{-5} M

Time of shaking (min.)	Absorbance of remaining MB solution at the corresponding time	Difference of absorbance (Original absorbance of 2×10^{-5} M MB solution) - (Absorbance of remaining MB solution at the corresponding time)	Amount of solute adsorbed by the sample at the corresponding time $(mg\ g^{-1})$
15	0.167	0.034	0.67
30	0.132	0.069	1.87
60	0.116	0.085	2.19
90	0.113	0.088	2.67
120	0.113	0.088	2.67

Fig. 2.20: Effect of shaking time on the amount of solute (MB) adsorbed from its 2×10^{-5} M solution

MB solution: 3×10^{-5} M

Table 2.17: Absorbance data for 3×10^{-5} M MB solution at different shaking time

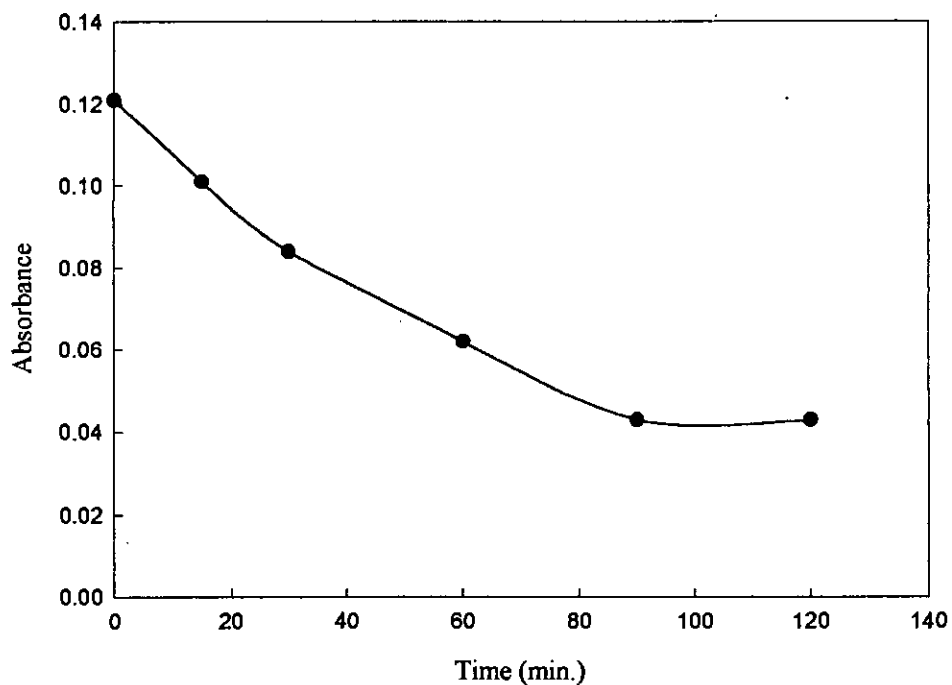| Initial conc. of MB (M)	Amount of sample taken in 100 mL solution to each vessel (g)	Time of shaking (min.)	Corresponding absorbance	Original absorbance
3×10^{-5}	0.133	15	0.215	0.297
		30	0.175	
		60	0.172	
		90	0.169	
		120	0.169	

Fig. 2.21: Effect of shaking time on the absorbance of 3×10^{-5} M MB solution

Table 2.18: Amount of MB adsorbed by per gram of sample from original concentration of 3×10^{-5} M

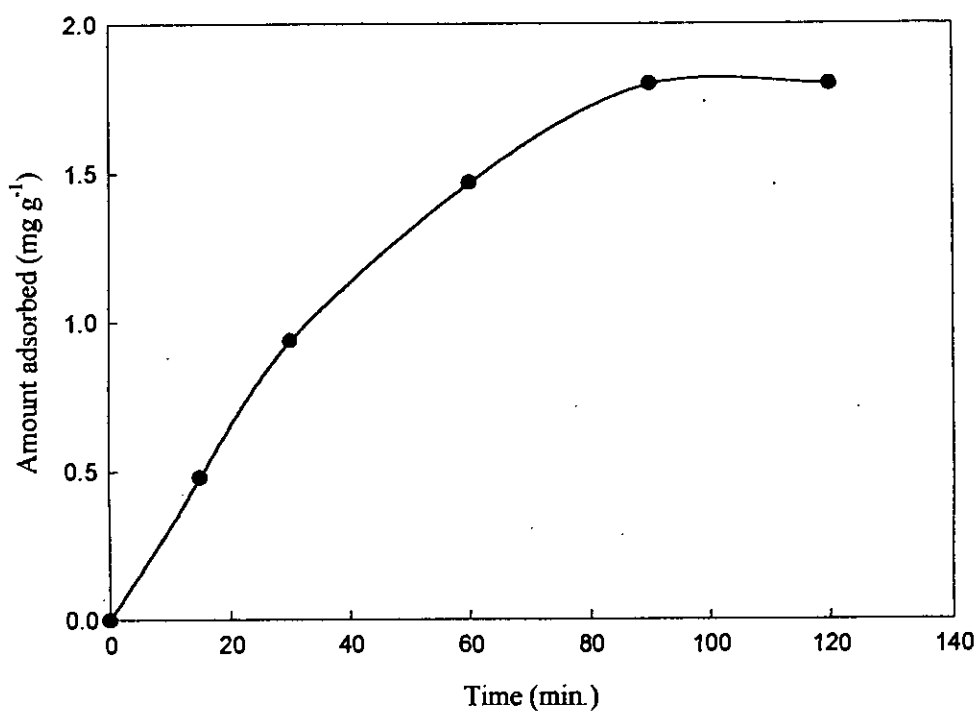| Time of shaking (min.)	Absorbance of remaining MB solution at the corresponding time	Difference of absorbance (Original absorbance of 3×10^{-5} M MB solution) - (Absorbance of remaining MB solution at the corresponding time)	Amount of solute adsorbed by the sample at the corresponding time (mg g^{-1})
15	0.215	0.082	2.19
30	0.175	0.122	3.21
60	0.172	0.125	3.34
90	0.169	0.128	3.47
120	0.169	0.128	3.47

Fig. 2.22: Effect of shaking time on the amount of solute (MB) adsorbed from its 3×10^{-5} M solution

MB solution: 4×10^{-5} M

Table 2.19: Absorbance data for 4×10^{-5} M MB solution at different shaking time

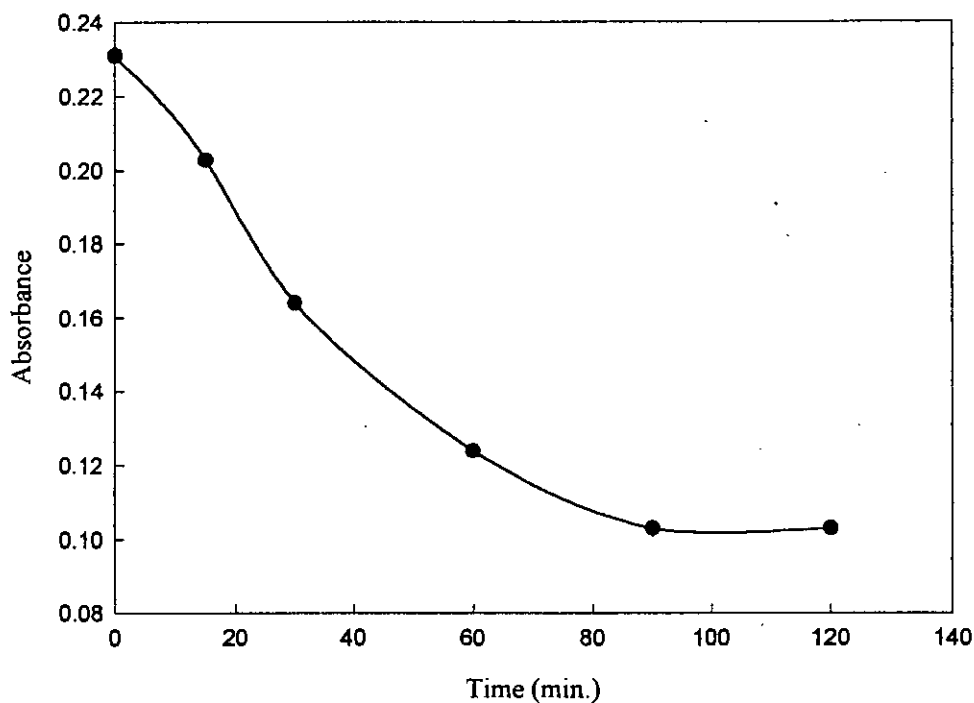| Initial conc. of MB (M)	Amount of sample taken in 100 mL solution to each vessel (g)	Time of shaking (min.)	Corresponding absorbance	Original absorbance
4×10^{-5}	0.133	15	0.254	0.381
		30	0.241	
		60	0.236	
		90	0.233	
		120	0.232	

Fig. 2.23: Effect of shaking time on the absorbance of 4×10^{-5} M MB solution

Table 2.20: Amount of MB adsorbed by per gram of sample from original concentration of 4×10^{-5} M

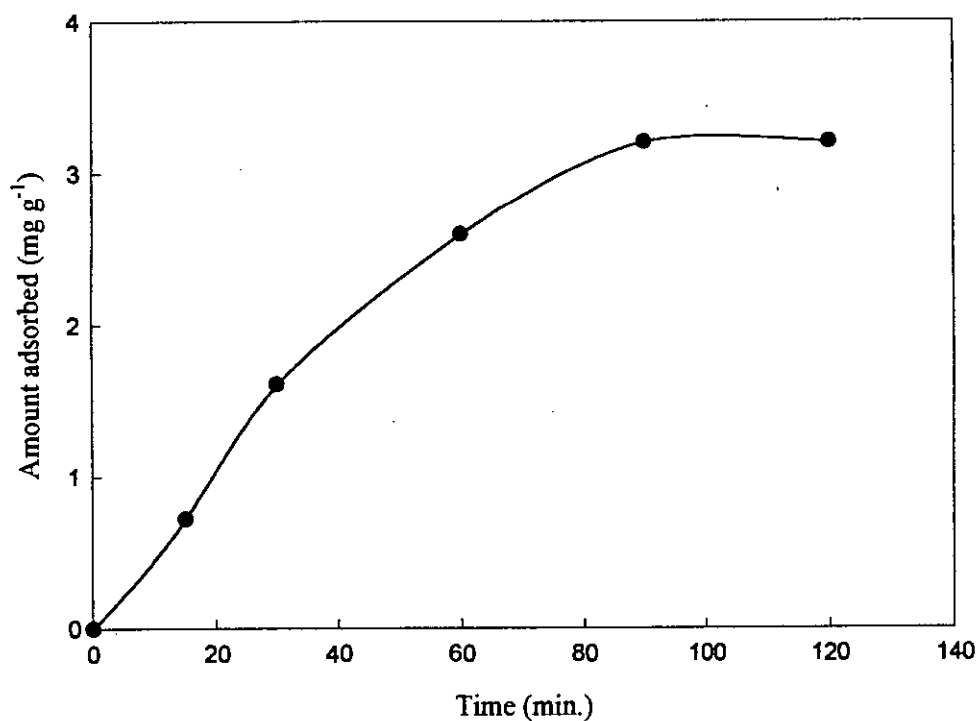| Time of shaking (min.)	Absorbance of remaining MB solution at the corresponding time	Difference of absorbance (Original absorbance of 4×10^{-5} M MB solution) - (Absorbance of remaining MB solution at the corresponding time)	Amount of solute adsorbed by the sample at the corresponding time (mg g^{-1})
15	0.254	0.127	3.34
30	0.241	0.140	3.85
60	0.236	0.145	4.09
90	0.233	0.148	4.14
120	0.232	0.149	4.14

Fig. 2.24: Effect of shaking time on the amount of solute (MB) adsorbed from its 4×10^{-5}M solution

MB solution: 5×10^{-5} M

Table 2.21: Absorbance data for 5×10^{-5} M MB solution at different shaking time

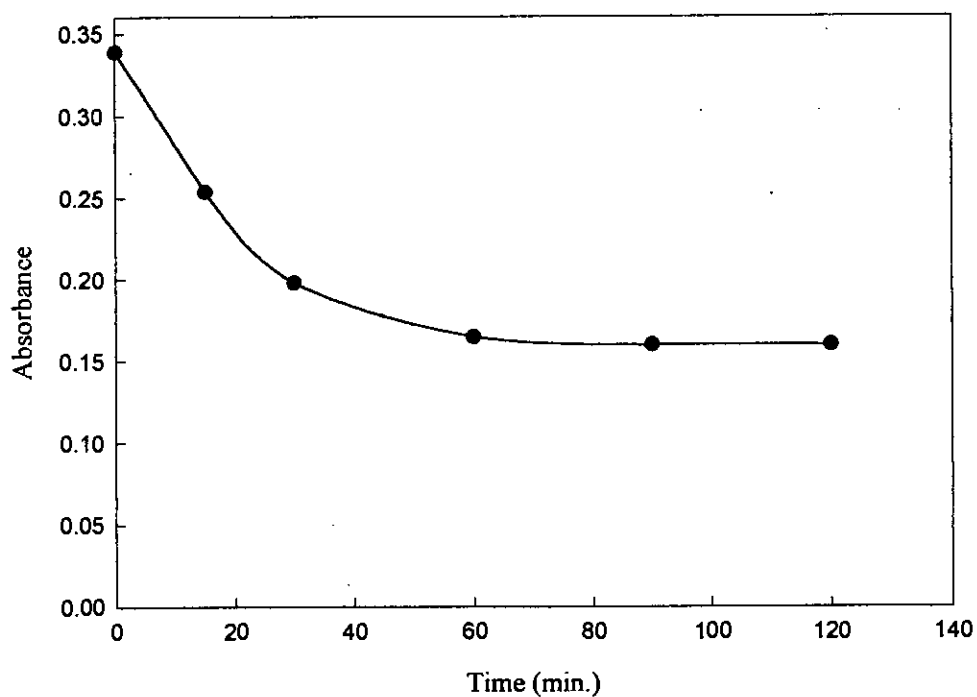| Initial conc. of MB (M)	Amount of sample taken in 100 mL solution to each vessel (g)	Time of shaking (min.)	Corresponding absorbance	Original absorbance
5×10^{-5}	0.133	15	0.325	0.476
		30	0.313	
		60	0.309	
		90	0.302	
		120	0.302	

Fig. 2.25: Effect of shaking time on the absorbance of 5×10^{-5} M MB solution

Table 2.22: Amount of MB adsorbed by per gram of sample from original concentration of 5×10^{-5} M

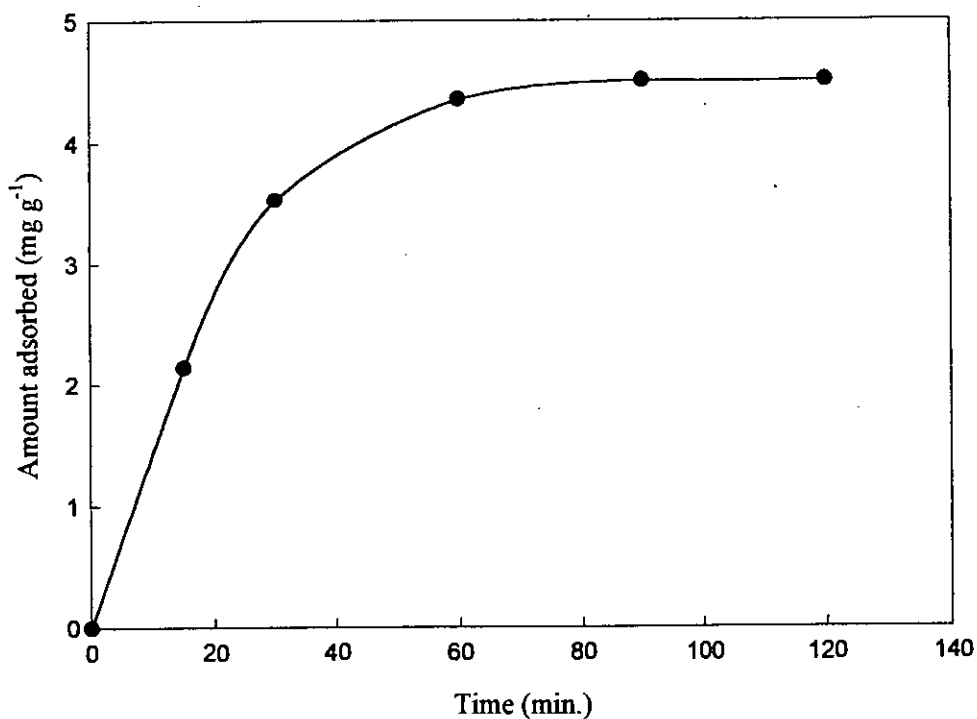| Time of shaking (min.)	Absorbance of remaining MB solution at the corresponding time	Difference of absorbance (Original absorbance of 5×10^{-5} M MB solution) - (Absorbance of remaining MB solution at the corresponding time)	Amount of solute adsorbed by the sample at the corresponding time (mg g^{-1})
15	0.325	0.151	4.01
30	0.313	0.163	4.42
60	0.309	0.167	4.55
90	0.302	0.174	4.80
120	0.302	0.174	4.80
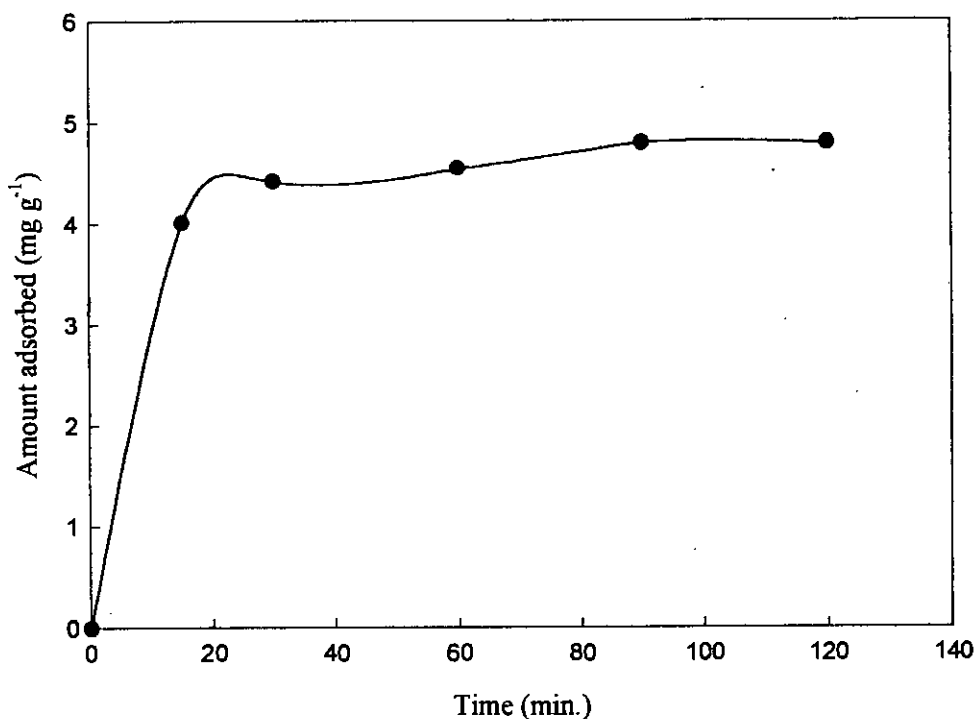
Fig. 2.26: Effect of shaking time on the amount of solute (MB) adsorbed from its 5×10^{-5}M solution

MB solution: 6×10^{-5} M

Table 2.23: Absorbance data for 6×10^{-5} M MB solution at different shaking time

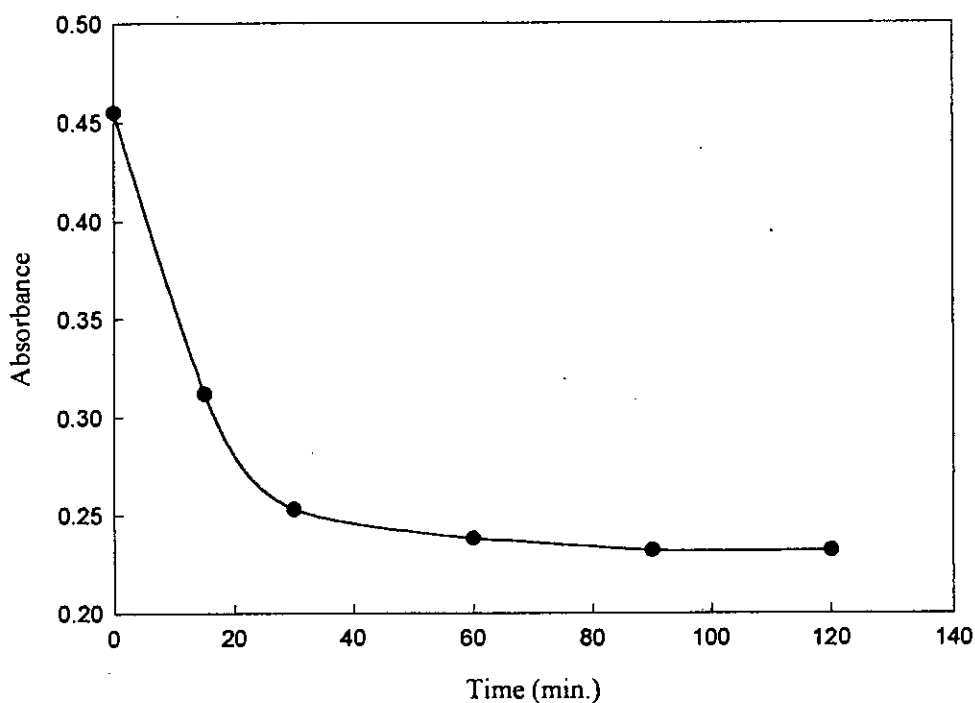| Initial conc. of MB (M)	Amount of sample taken in 100 mL solution to each vessel (g)	Time of shaking (min.)	Corresponding absorbance	Original absorbance
6×10^{-5}	0.133	15	0.426	0.571
		30	0.402	
		60	0.395	
		90	0.393	
		120	0.392	

Fig. 2.27: Effect of shaking time on the absorbance of 6×10^{-5} M MB solution

Table 2.24: Amount of MB adsorbed by per gram of sample from original concentration of 6×10^{-5} M

Time of shaking (min.)	Absorbance of remaining MB solution at the corresponding time	Difference of absorbance (Original absorbance of 6×10^{-5} M MB solution) - (Absorbance of remaining MB solution at the corresponding time)	Amount of solute adsorbed by the sample at the corresponding time (mg g^{-1})
15	0.426	0.145	4.14
30	0.402	0.169	4.68
60	0.395	0.176	4.82
90	0.393	0.178	4.89
120	0.392	0.179	4.95
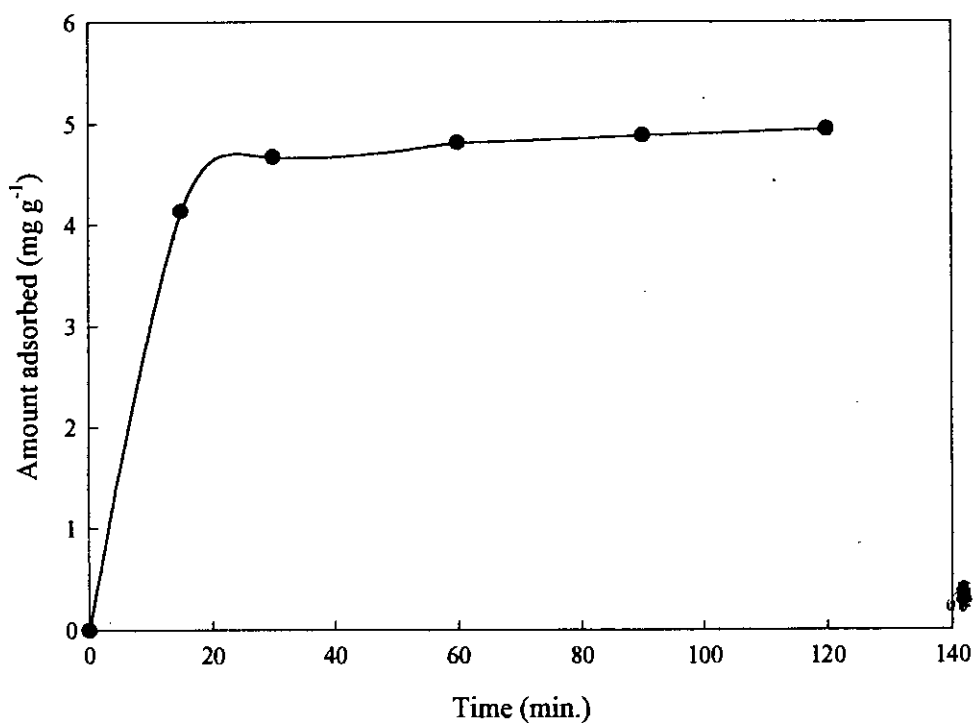
Fig. 2.28: Effect of shaking time on the amount of solute (MB) adsorbed from its 6×10^{-5}M solution

The determination of specific surface area of basic PANI by adsorption method using MB dyestuff

MB solution: 1×10^{-5} M

Table 2.25: Absorbance data for 1×10^{-5} M MB solution at different shaking time

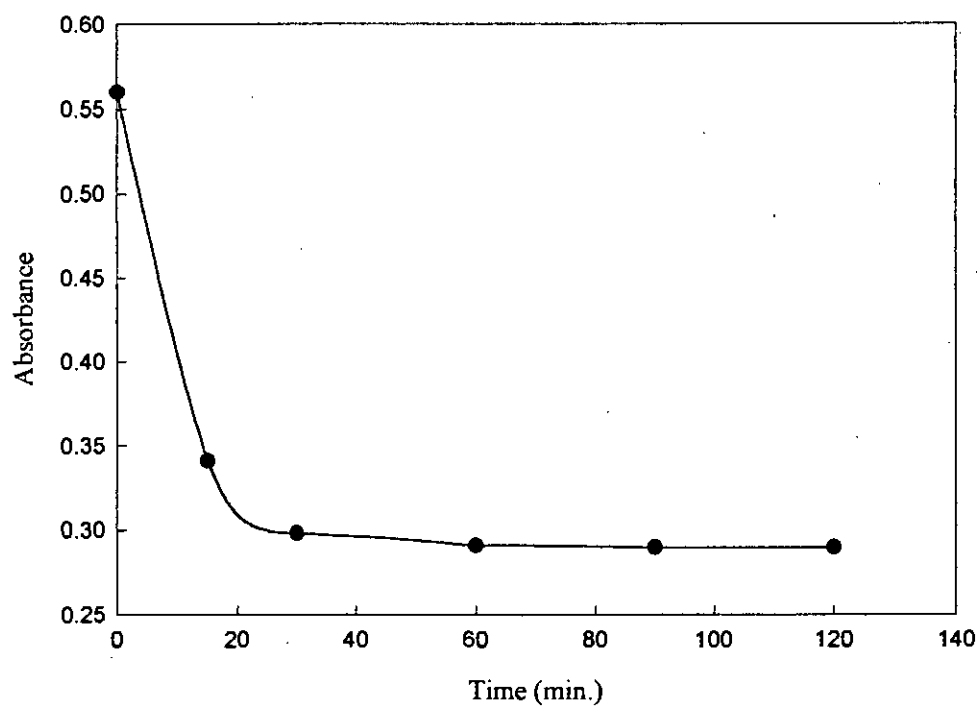| Initial conc. of MB (M)	Amount of sample taken in 100 mL solution to each vessel (g)	Time of shaking (min.)	Corresponding absorbance	Original absorbance
1×10^{-5}	0.133	15	0.084	0.135
		30	0.052	
		60	0.031	
		90	0.020	
		120	0.020	

Fig. 2.29: Effect of shaking time on the absorbance of 1×10^{-5} M MB solution

Table 2.26: Amount of MB adsorbed by per gram of sample from original concentration of 1×10^{-5} M

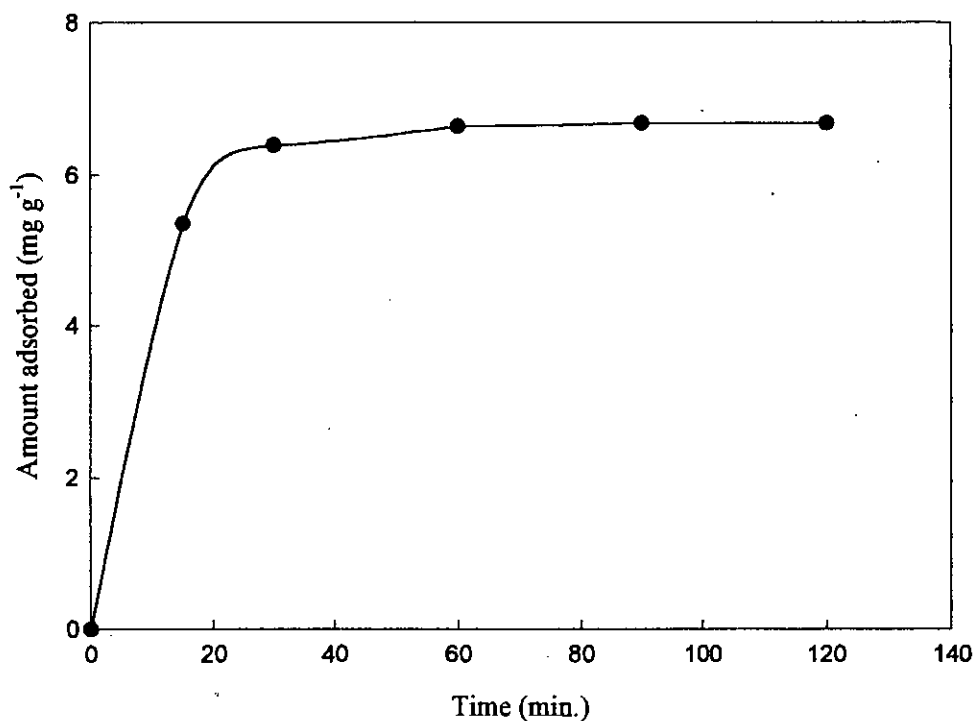| Time of shaking (min.)	Absorbance of remaining MB solution at the corresponding time	Difference of absorbance (Original absorbance of 1×10^{-5} M MB solution) - (Absorbance of remaining MB solution at the corresponding time)	Amount of solute adsorbed by the sample at the corresponding time (mg g^{-1})
15	0.084	0.051	1.20
30	0.052	0.083	1.87
60	0.031	0.104	2.54
90	0.020	0.115	2.60
120	0.020	0.115	2.60

Fig. 2.30: Effect of shaking time on the amount of solute (MB) adsorbed from its 1×10^{-5}M solution

MB solution: 2×10^{-5} M

Table 2.27: Absorbance data for 2×10^{-5} M MB solution at different shaking time

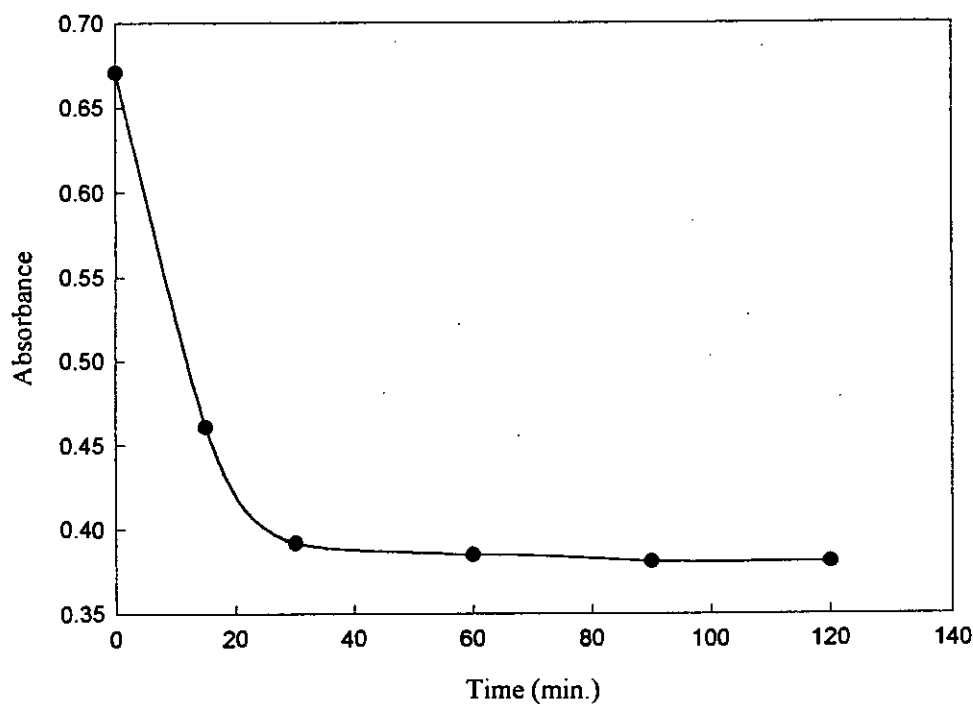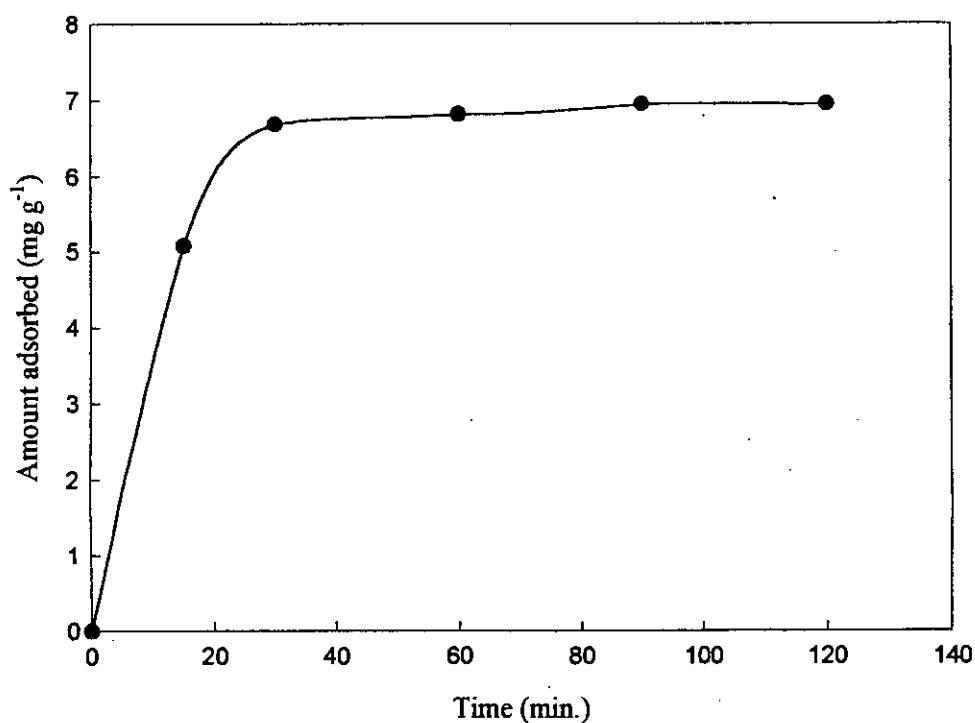| Initial conc. of MB (M)	Amount of sample taken in 100 mL solution to each vessel (g)	Time of shaking (min.)	Corresponding absorbance	Original absorbance
2×10^{-5}	0.133	15	0.103	0.240
		30	0.061	
		60	0.030	
		90	0.025	
		120	0.025	

Fig. 2.31: Effect of shaking time on the absorbance of 2×10^{-5} M MB solution

Table 2.28: Amount of MB adsorbed by per gram of sample from original concentration of 2×10^{-5} M

Time of shaking (min.)	Absorbance of remaining MB solution at the corresponding time	Difference of absorbance (Original absorbance of 2×10^{-5} M MB solution) - (Absorbance of remaining MB solution at the corresponding time)	Amount of solute adsorbed by the sample at the corresponding time $(mg\ g^{-1})$
15	0.103	0.137	3.20
30	0.061	0.179	4.20
60	0.030	0.210	4.95
90	0.025	0.215	5.08
120	0.025	0.215	5.08
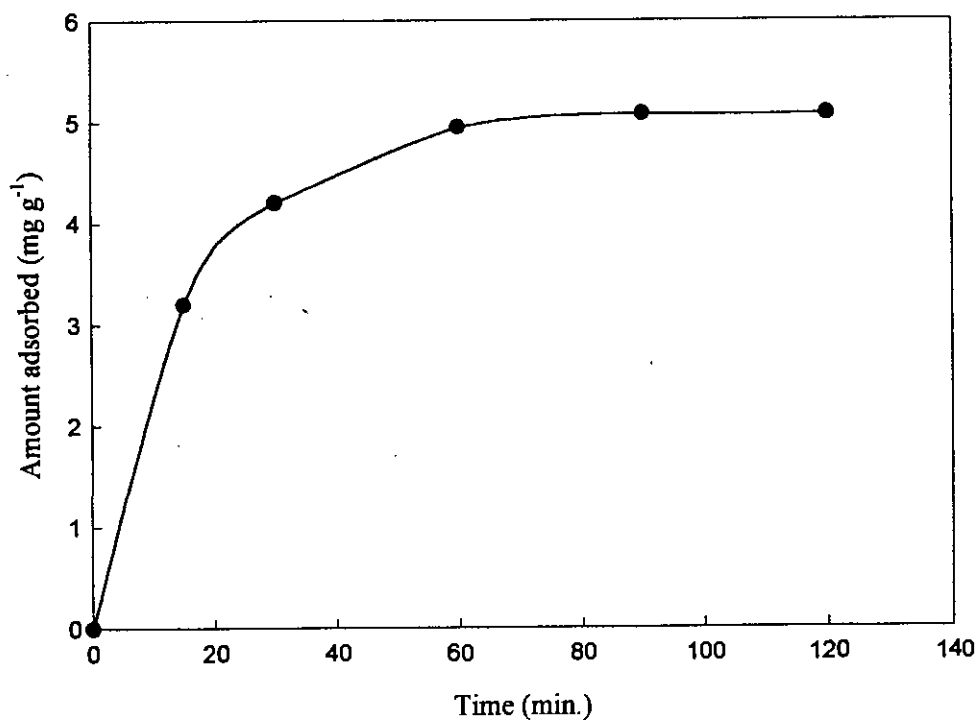
Fig. 2.32: Effect of shaking time on the amount of solute (MB) adsorbed from its 2×10^{-5} M solution

Table 2.30: Amount of MB adsorbed by per gram of sample from original concentration of 3×10^{-5} M

Time of shaking (min.)	Absorbance of remaining MB solution at the corresponding time	Difference of absorbance (Original absorbance of 3×10^{-5} M MB solution) - (Absorbance of remaining MB solution at the corresponding time)	Amount of solute adsorbed by the sample at the corresponding time (mg g^{-1})
15	0.109	0.237	5.80
30	0.061	0.285	6.70
60	0.051	0.295	7.04
90	0.048	0.298	7.22
120	0.048	0.298	7.22

Fig. 2.34: Effect of shaking time on the amount of solute (MB) adsorbed from its 3×10^{-5}M solution

MB solution: 4×10^{-5} M

Table 2.31: Absorbance data for 4×10^{-5} M MB solution at different shaking time

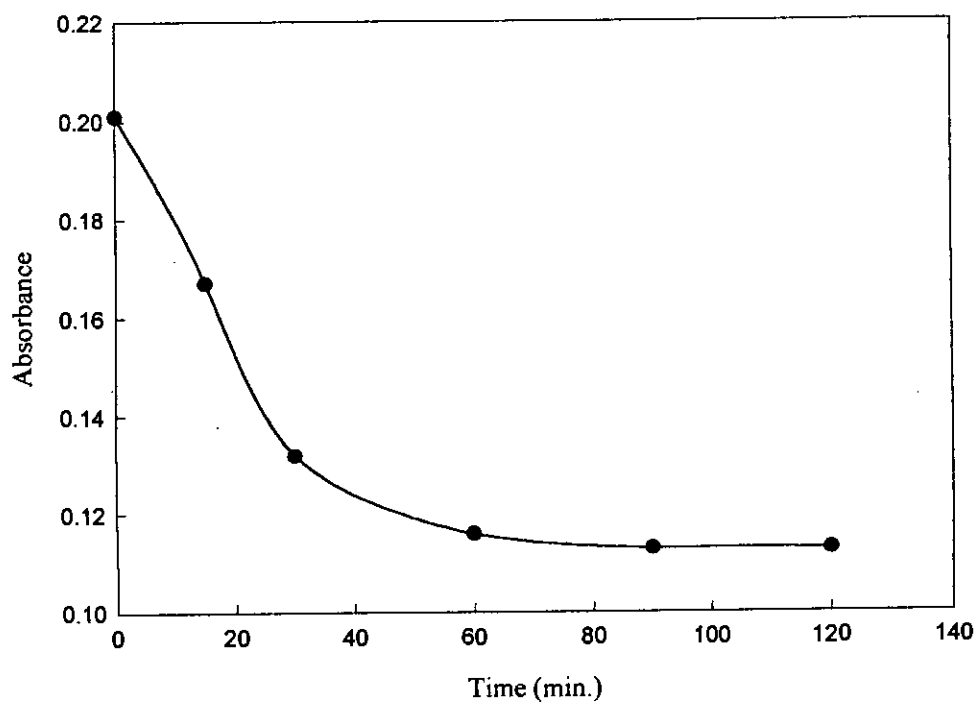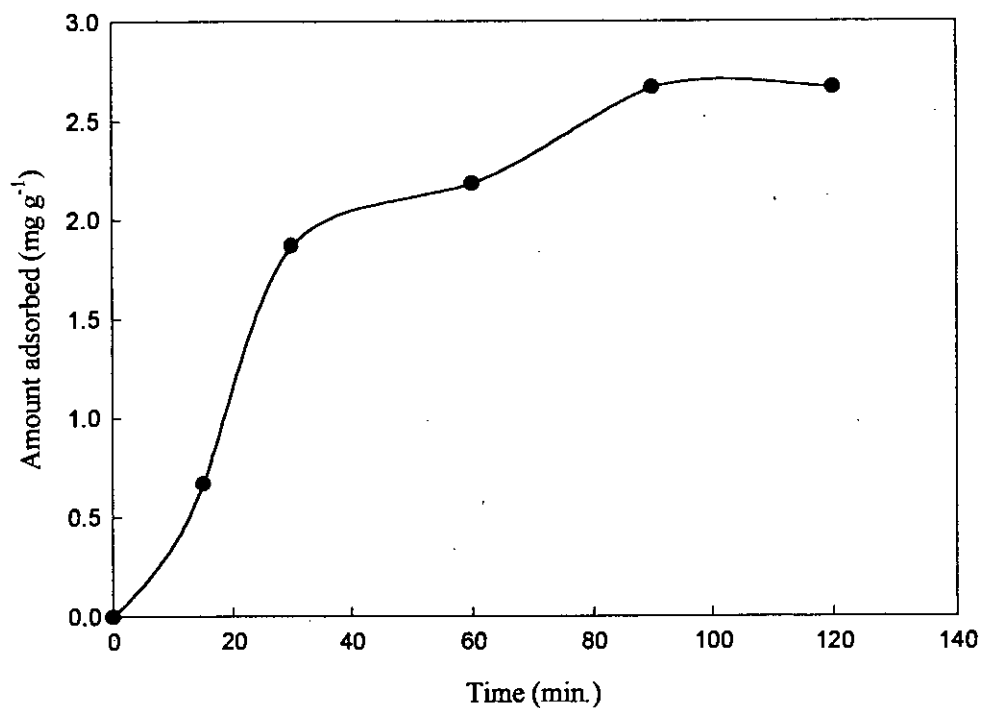| Initial conc. of MB (M)	Amount of sample taken in 100 mL solution to each vessel (g)	Time of shaking (min.)	Corresponding absorbance	Original absorbance
4×10^{-5}	0.133	15	0.121	0.461
		30	0.083	
		60	0.065	
		90	0.061	
		120	0.061	

Fig. 2.35: Effect of shaking time on the absorbance of 4×10^{-5} M MB solution

Table 2.32: Amount of MB adsorbed by per gram of sample from original concentration of 4×10^{-5} M

Time of shaking (min.)	Absorbance of remaining MB solution at the corresponding time	Difference of absorbance (Original absorbance of 4×10^{-5} M MB solution) - (Absorbance of remaining MB solution at the corresponding time)	Amount of solute adsorbed by the sample at the corresponding time (mg g^{-1})
15	0.121	0.340	8.16
30	0.083	0.378	9.02
60	0.065	0.396	9.42
90	0.061	0.400	9.50
120	0.061	0.400	9.50

Fig. 2.36: Effect of shaking time on the amount of solute (MB) adsorbed from its 4×10^{-5} M solution

MB solution: 5×10^{-5} M

Table 2.33: Absorbance data for 5×10^{-5} M MB solution at different shaking time

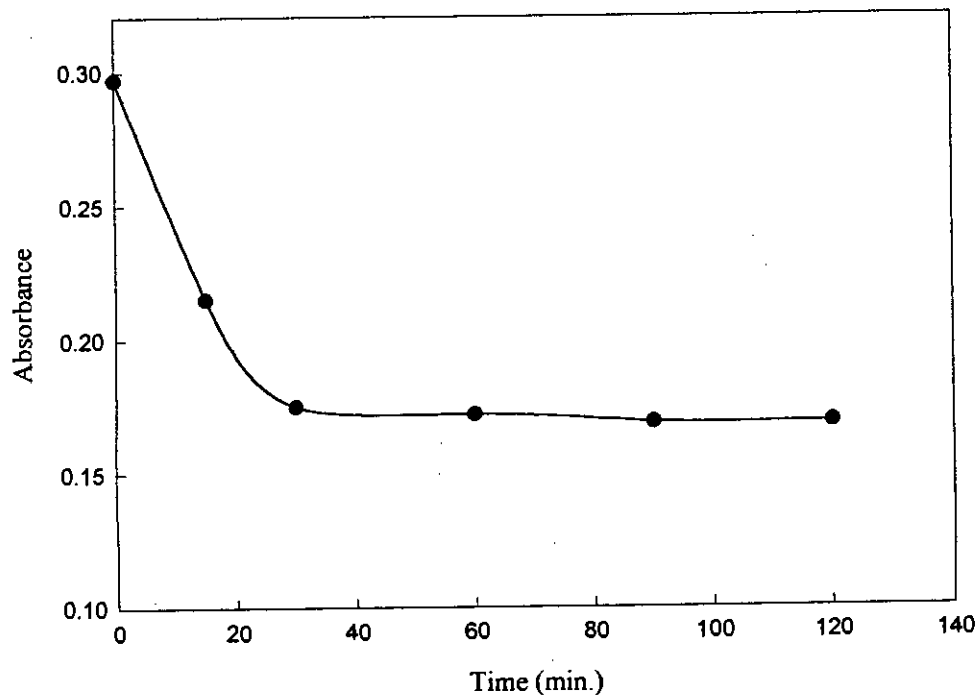| Initial conc. of MB (M)	Amount of sample taken in 100 mL solution to each vessel (g)	Time of shaking (min.)	Corresponding absorbance	Original absorbance
5×10^{-5}	0.133	15	0.217	0.575
		30	0.142	
		60	0.113	
		90	0.103	
		120	0.103	

Fig. 2.37: Effect of shaking time on the absorbance of 5×10^{-5} M MB solution

Table 2.34: Amount of MB adsorbed by per gram of sample from original concentration of 5×10^{-5} M

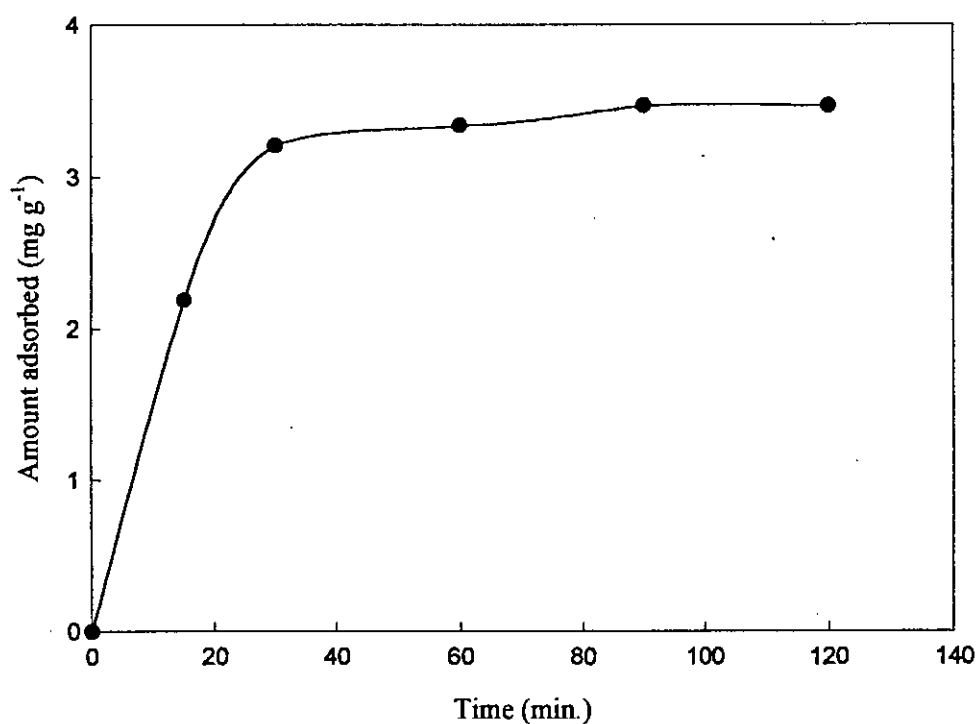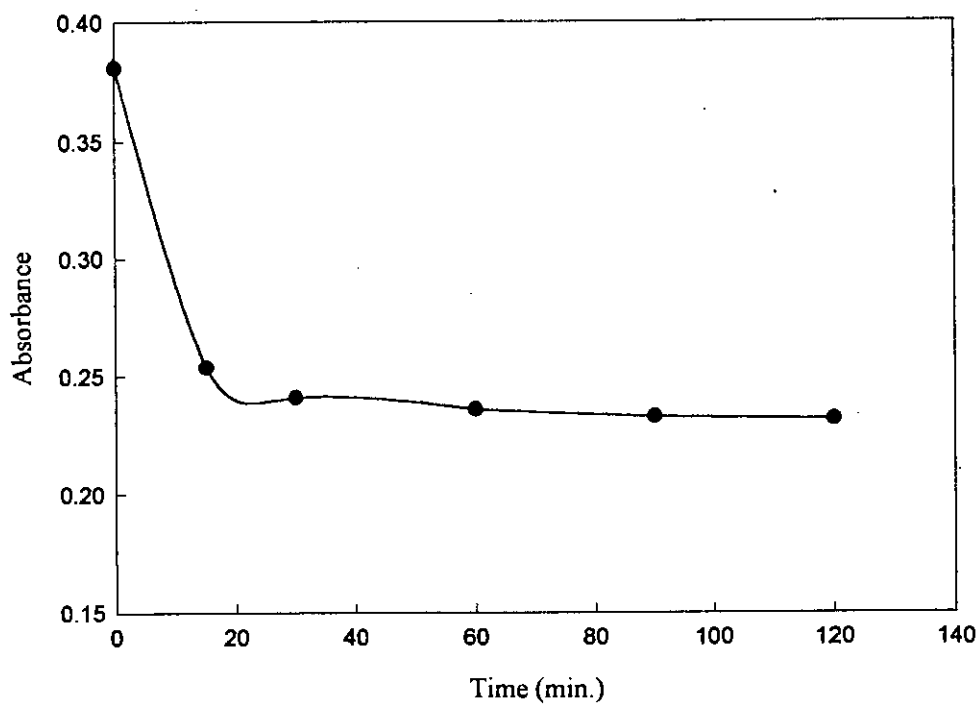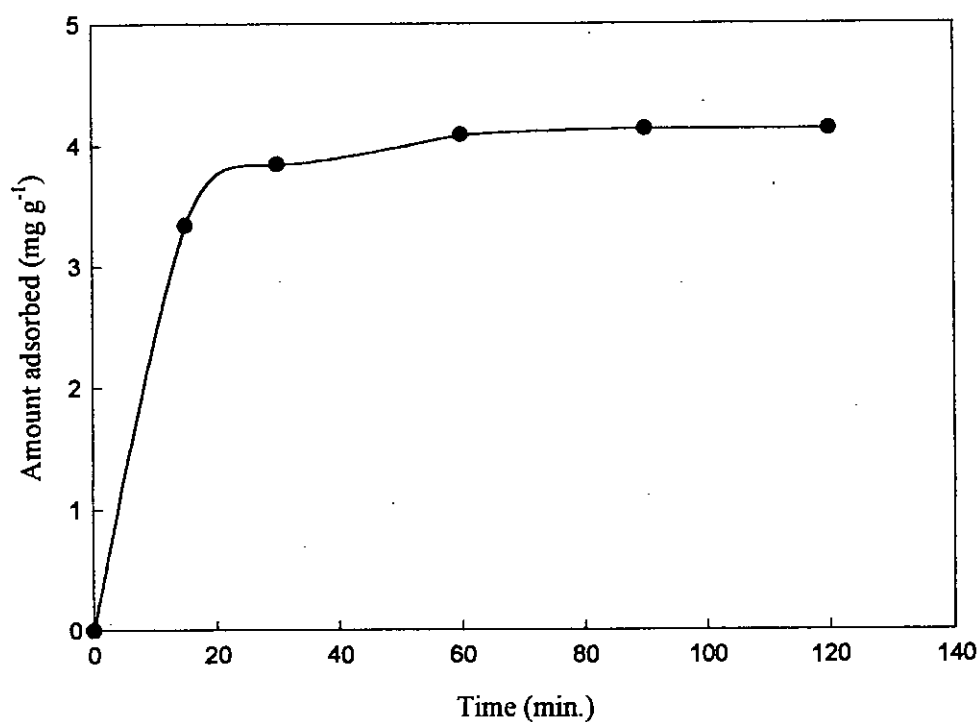| Time of shaking (min.)	Absorbance of remaining MB solution at the corresponding time	Difference of absorbance (Original absorbance of 5×10^{-5} M MB solution) - (Absorbance of remaining MB solution at the corresponding time)	Amount of solute adsorbed by the sample at the corresponding time (mg g^{-1})
15	0.217	0.358	8.78
30	0.142	0.433	10.43
60	0.113	0.462	11.30
90	0.103	0.472	11.80
120	0.103	0.472	11.80

Fig. 2.38: Effect of shaking time on the amount of solute (MB) adsorbed from its 5×10^{-5}M solution

MB solution: 6×10^{-5} M

Table 2.35: Absorbance data for 6×10^{-5} M MB solution at different shaking time

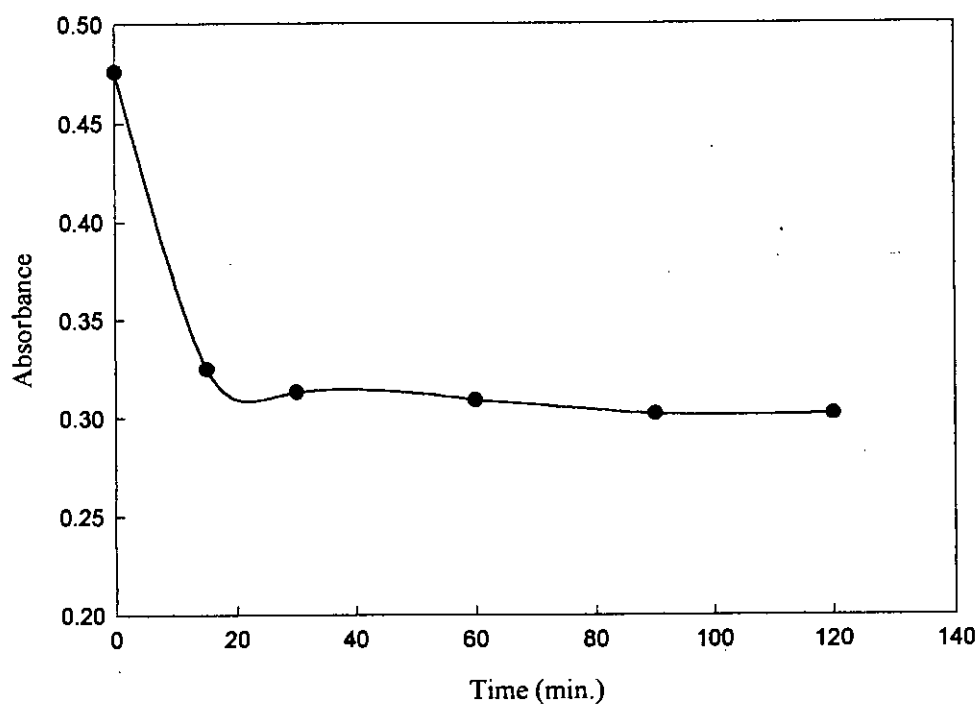| Initial conc. of MB (M)	Amount of sample taken in 100 mL solution to each vessel (g)	Time of shaking (min.)	Corresponding absorbance	Original absorbance
6×10^{-5}	0.133	15	0.315	0.676
		30	0.201	
		60	0.145	
		90	0.140	
		120	0.140	

Fig. 2.39: Effect of shaking time on the absorbance of 6×10^{-5} M MB solution

Table 2.36: Amount of MB adsorbed by per gram of sample from original concentration of 6×10^{-5} M

Time of shaking (min.)	Absorbance of remaining MB solution at the corresponding time	Difference of absorbance (Original absorbance of 6×10^{-5} M MB solution) - (Absorbance of remaining MB solution at the corresponding time)	Amount of solute adsorbed by the sample at the corresponding time (mg g^{-1})
15	0.315	0.361	8.70
30	0.201	0.475	11.37
60	0.145	0.531	12.58
90	0.140	0.536	12.90
120	0.140	0.536	12.90

Fig. 2.40: Effect of shaking time on the amount of solute (MB) adsorbed from its 6×10^{-5}M solution

The determination of specific surface area of acidic PANI-SiO$_2$ by adsorption method using MB dyestuff

MB solution: 1×10^{-5} M

Table 2.37: Absorbance data for 1×10^{-5} M MB solution at different shaking time

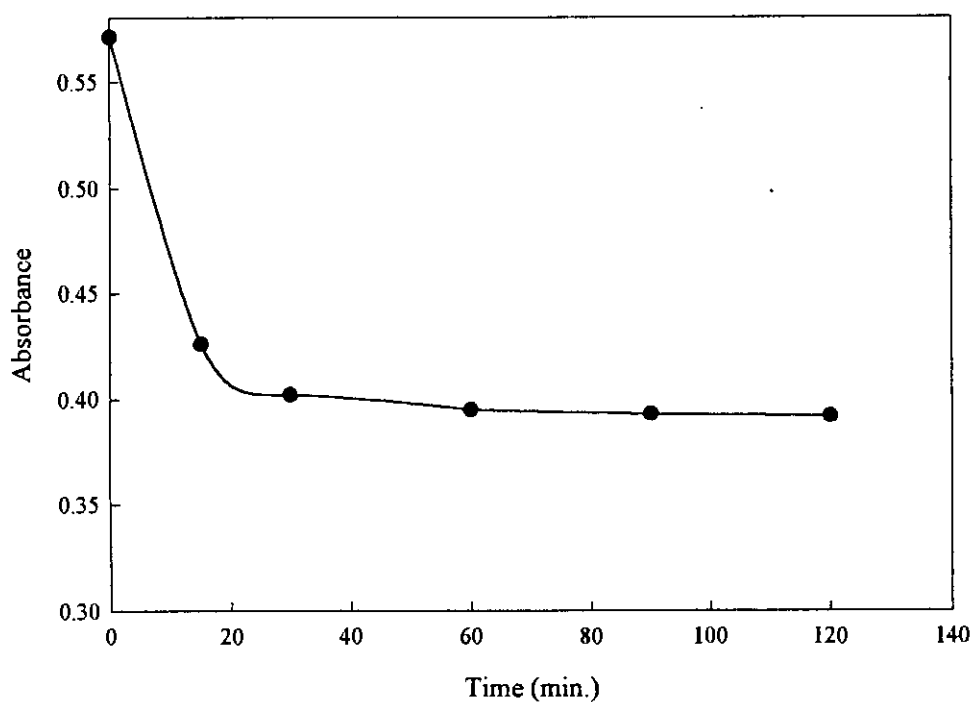| Initial conc. of MB (M)	Amount of sample taken in 100 mL solution to each vessel (g)	Time of shaking (min.)	Corresponding absorbance	Original absorbance
1×10^{-5}	0.133	15	0.095	0.121
		30	0.062	
		60	0.031	
		90	0.021	
		120	0.021	

Fig. 2.41: Effect of shaking time on the absorbance of 1×10^{-5} M MB solution

Table 2.38: Amount of MB adsorbed by per gram of sample from original concentration of 1×10^{-5} M

Time of shaking (min.)	Absorbance of remaining MB solution at the corresponding time	Difference of absorbance (Original absorbance of 1×10^{-5} M MB solution) - (Absorbance of remaining MB solution at the corresponding time)	Amount of solute adsorbed by the sample at the corresponding time (mg g^{-1})
15	0.095	0.026	0.54
30	0.062	0.059	1.47
60	0.031	0.090	2.16
90	0.021	0.100	2.40
120	0.021	0.100	2.40

Fig. 2.42: Effect of shaking time on the amount of solute (MB) adsorbed from its 1×10^{-5}M solution

MB solution: 2×10^{-5} M

Table 2.39: Absorbance data for 2×10^{-5} M MB solution at different shaking time

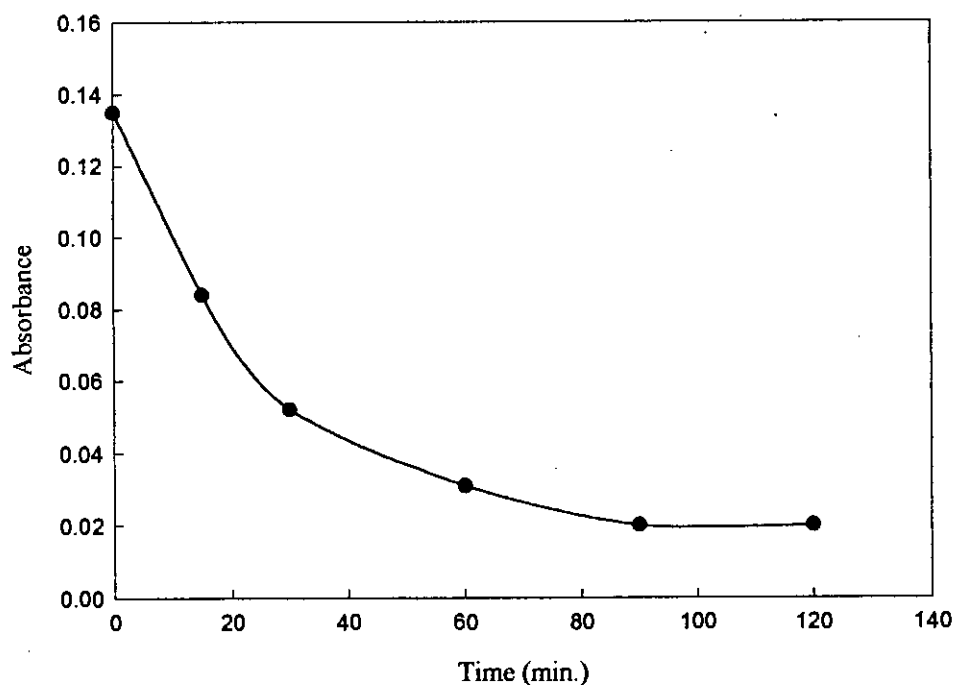| Initial conc. of MB (M)	Amount of sample taken in 100 mL solution to each vessel (g)	Time of shaking (min.)	Corresponding absorbance	Original absorbance
2×10^{-5}	0.133	15	0.165	0.231
		30	0.095	
		60	0.065	
		90	0.054	
		120	0.053	

Fig. 2.43: Effect of shaking time on the absorbance of 2×10^{-5} M MB solution

Table 2.40: Amount of MB adsorbed by per gram of sample from original concentration of 2×10^{-5} M

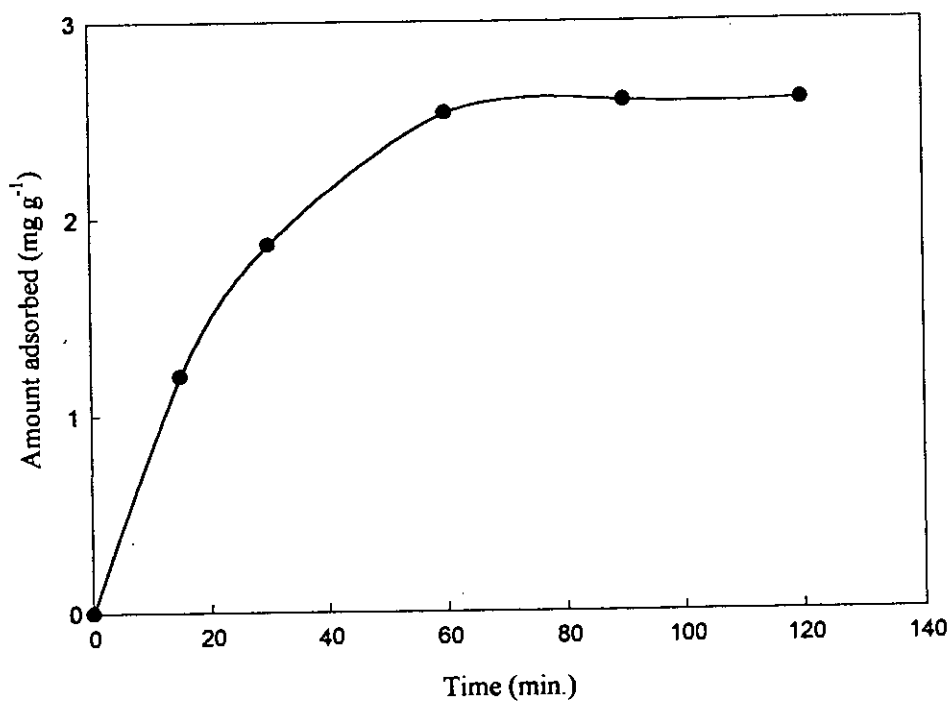| Time of shaking (min.)	Absorbance of remaining MB solution at the corresponding time	Difference of absorbance (Original absorbance of 2×10^{-5} M MB solution) - (Absorbance of remaining MB solution at the corresponding time)	Amount of solute adsorbed by the sample at the corresponding time (mg g^{-1})
15	0.165	0.066	1.65
30	0.095	0.136	3.21
60	0.065	0.166	4.01
90	0.054	0.177	4.28
120	0.053	0.178	4.28

Fig. 2.44: Effect of shaking time on the amount of solute (MB) adsorbed from its 2×10^{-5}M solution

MB solution: 3×10^{-5} M

Table 2.41: Absorbance data for 3×10^{-5} M MB solution at different shaking time

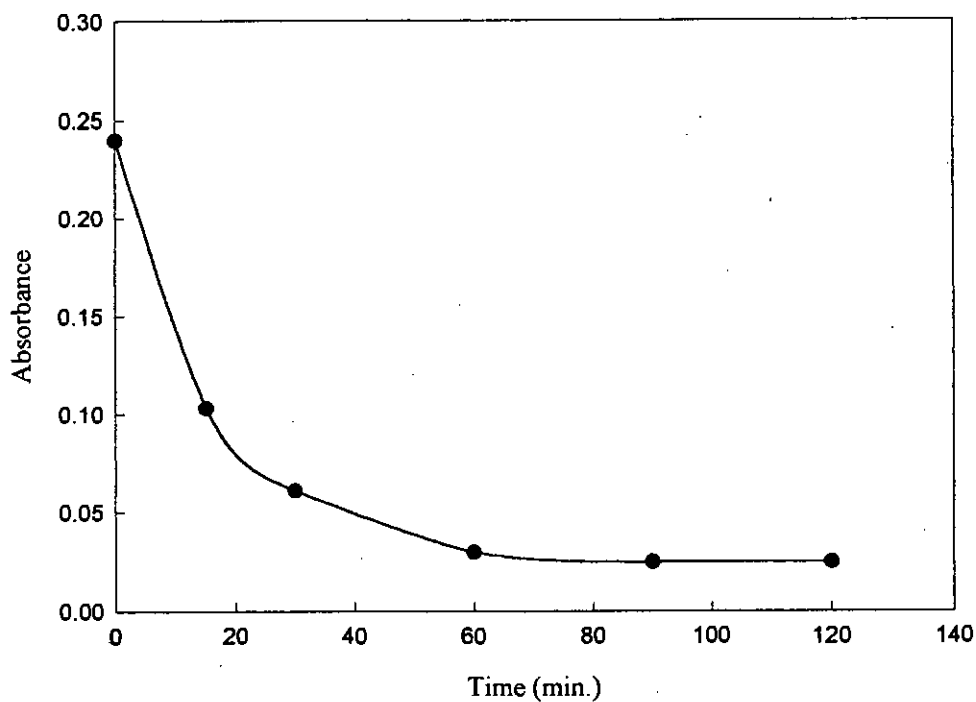| Initial conc. of MB (M)	Amount of sample taken in 100 mL solution to each vessel (g)	Time of shaking (min.)	Corresponding absorbance	Original absorbance
3×10^{-5}	0.133	15	0.232	0.339
		30	0.153	
		60	0.102	
		90	0.095	
		120	0.095	

Fig. 2.45: Effect of shaking time on the absorbance of 3×10^{-5} M MB solution

Table 2.42: Amount of MB adsorbed by per gram of sample from original concentration of 3×10^{-5} M

Time of shaking (min.)	Absorbance of remaining MB solution at the corresponding time	Difference of absorbance (Original absorbance of 3×10^{-5} M MB solution) - (Absorbance of remaining MB solution at the corresponding time)	Amount of solute adsorbed by the sample at the corresponding time ($mg\ g^{-1}$)
15	0.232	0.107	2.67
30	0.153	0.186	4.55
60	0.102	0.237	5.75
90	0.095	0.244	6.02
120	0.095	0.244	6.02

Fig. 2.46: Effect of shaking time on the amount of solute (MB) adsorbed from its 3×10^{-5}M solution

MB solution: 4×10^{-5} M

Table 2.43: Absorbance data for 4×10^{-5} M MB solution at different shaking time

Initial conc. of MB (M)	Amount of sample taken in 100 mL solution to each vessel (g)	Time of shaking (min.)	Corresponding absorbance	Original absorbance
4×10^{-5}	0.133	15	0.315	0.455
		30	0.203	
		60	0.165	
		90	0.150	
		120	0.149	
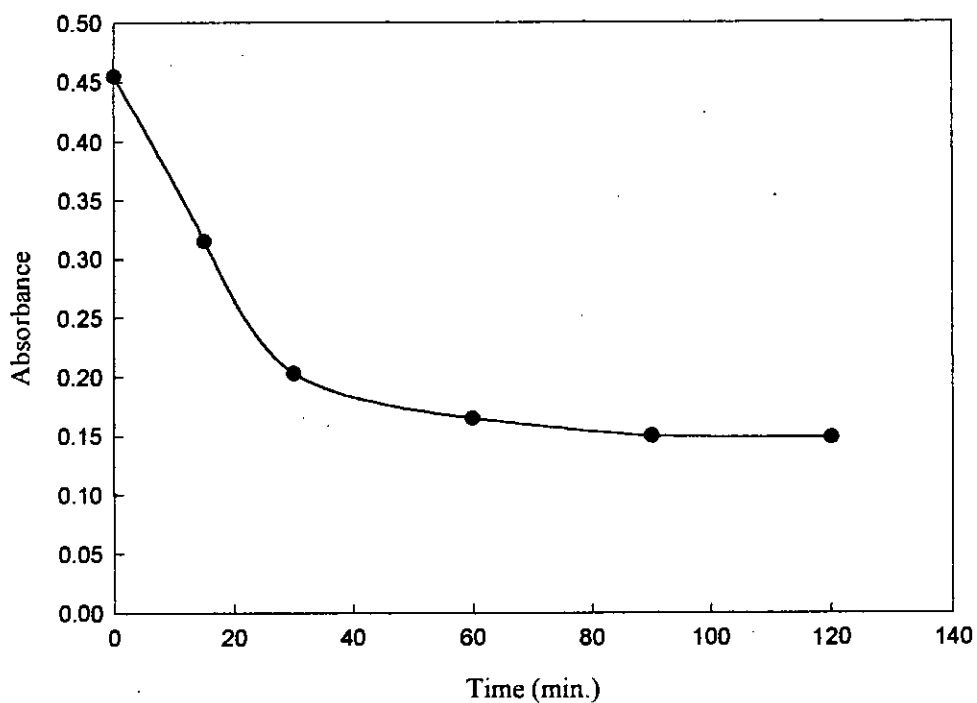
Fig. 2.47: Effect of shaking time on the absorbance of 4×10^{-5} M MB solution

Table 2.44: Amount of MB adsorbed by per gram of sample from original concentration of 4×10^{-5} M

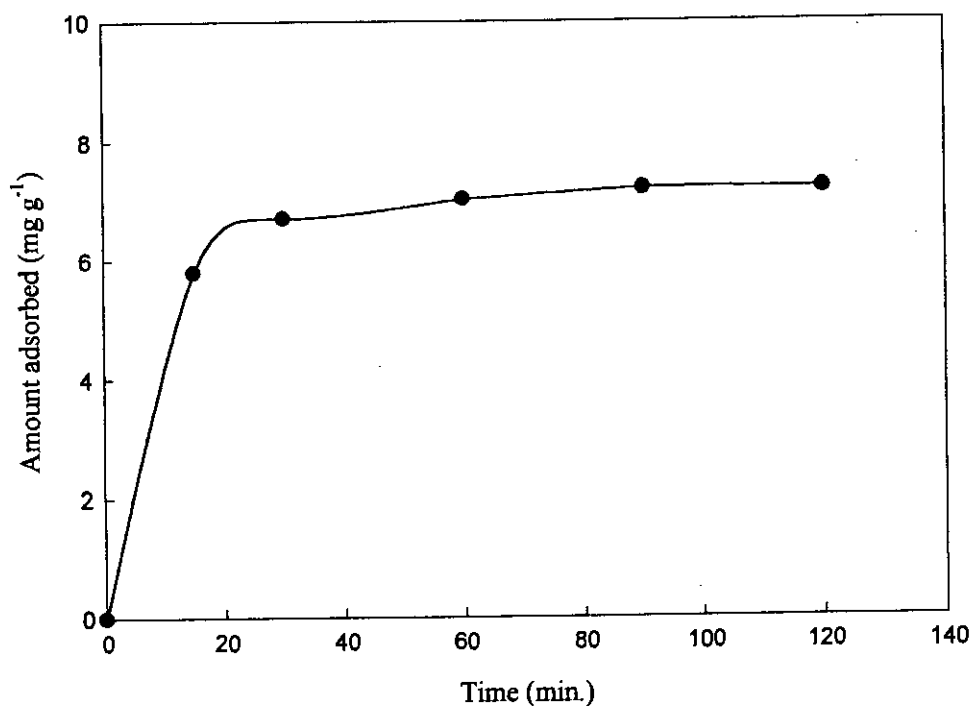| Time of shaking (min.)	Absorbance of remaining MB solution at the corresponding time	Difference of absorbance (Original absorbance of 4×10^{-5} M MB solution) - (Absorbance of remaining MB solution at the corresponding time)	Amount of solute adsorbed by the sample at the corresponding time (mg g^{-1})
15	0.315	0.140	3.48
30	0.203	0.252	6.50
60	0.165	0.290	7.22
90	0.150	0.305	7.60
120	0.149	0.306	7.60

Fig. 2.48: Effect of shaking time on the amount of solute (MB) adsorbed from its 4×10^{-5} M solution

MB solution: 5×10^{-5} M

Table 2.45: Absorbance data for 5×10^{-5} M MB solution at different shaking time

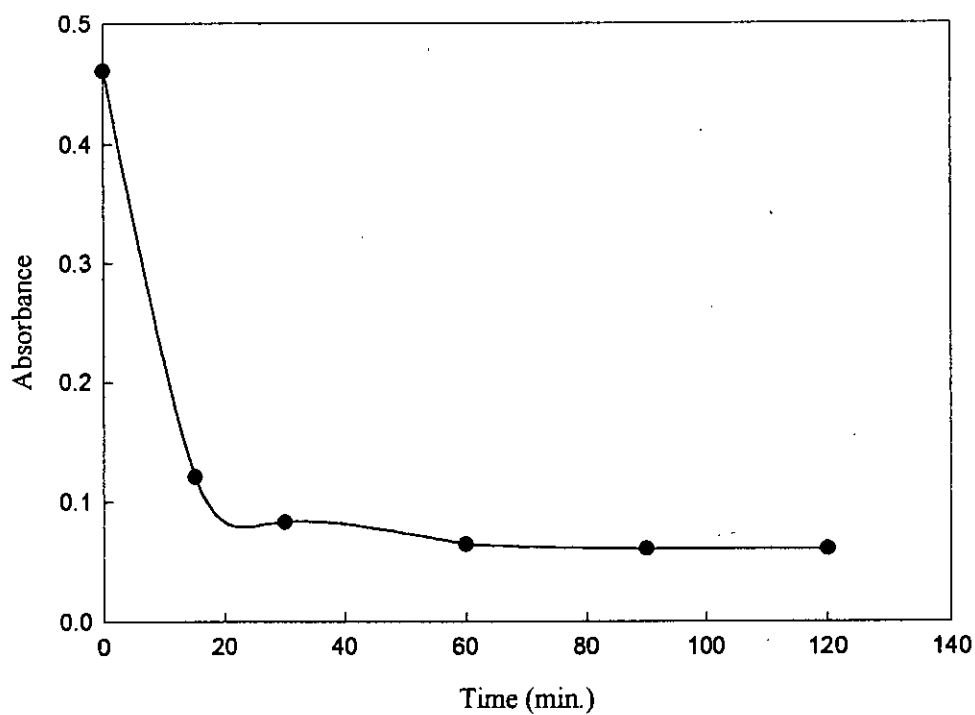| Initial conc. of MB (M)	Amount of sample taken in 100 mL solution to each vessel (g)	Time of shaking (min.)	Corresponding absorbance	Original absorbance
5×10^{-5}	0.133	15	0.399	0.560
		30	0.285	
		60	0.215	
		90	0.205	
		120	0.204	

Fig. 2.49: Effect of shaking time on the absorbance of 5×10^{-5} M MB solution

Table 2.46: Amount of MB adsorbed by per gram of sample from original concentration of 5×10^{-5} M

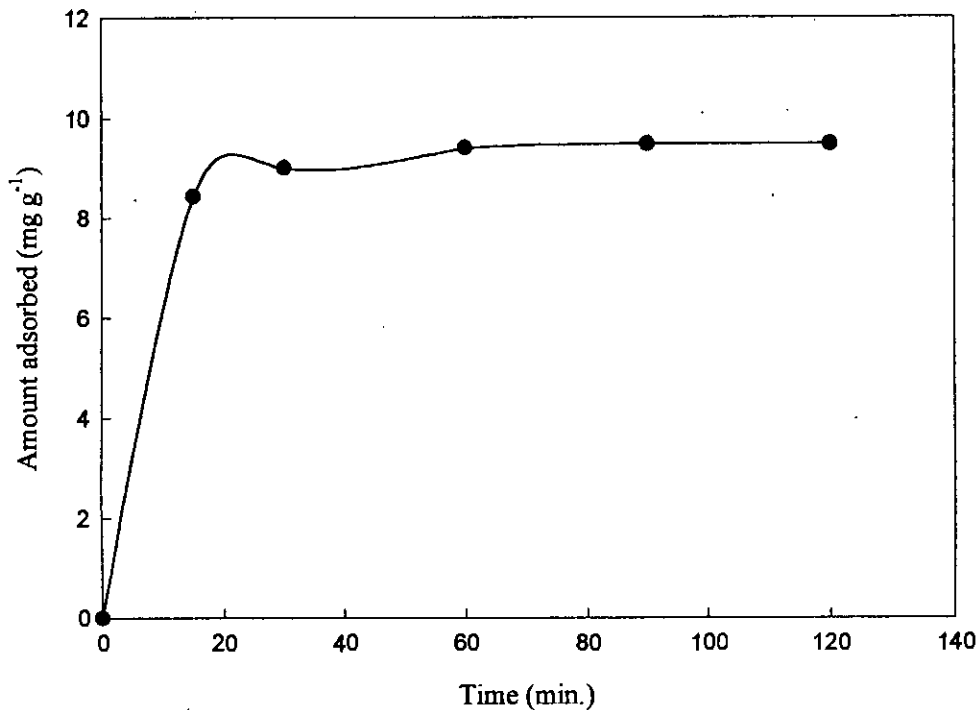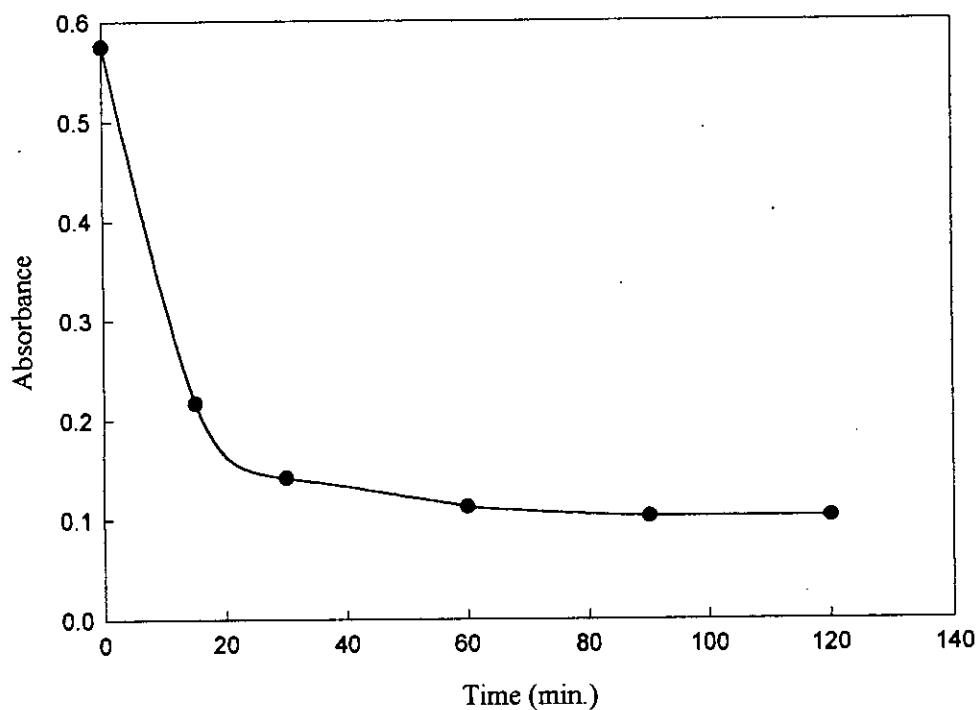| Time of shaking (min.)	Absorbance of remaining MB solution at the corresponding time	Difference of absorbance (Original absorbance of 5×10^{-5} M MB solution) - (Absorbance of remaining MB solution at the corresponding time)	Amount of solute adsorbed by the sample at the corresponding time (mg g^{-1})
15	0.399	0.161	3.75
30	0.285	0.275	6.69
60	0.215	0.345	8.56
90	0.205	0.355	8.83
120	0.204	0.356	8.83

Fig. 2.50: Effect of shaking time on the amount of solute (MB) adsorbed from its 5×10^{-5} M solution

MB solution: 6×10^{-5} M

Table 2.47: Absorbance data for 6×10^{-5} M MB solution at different shaking time

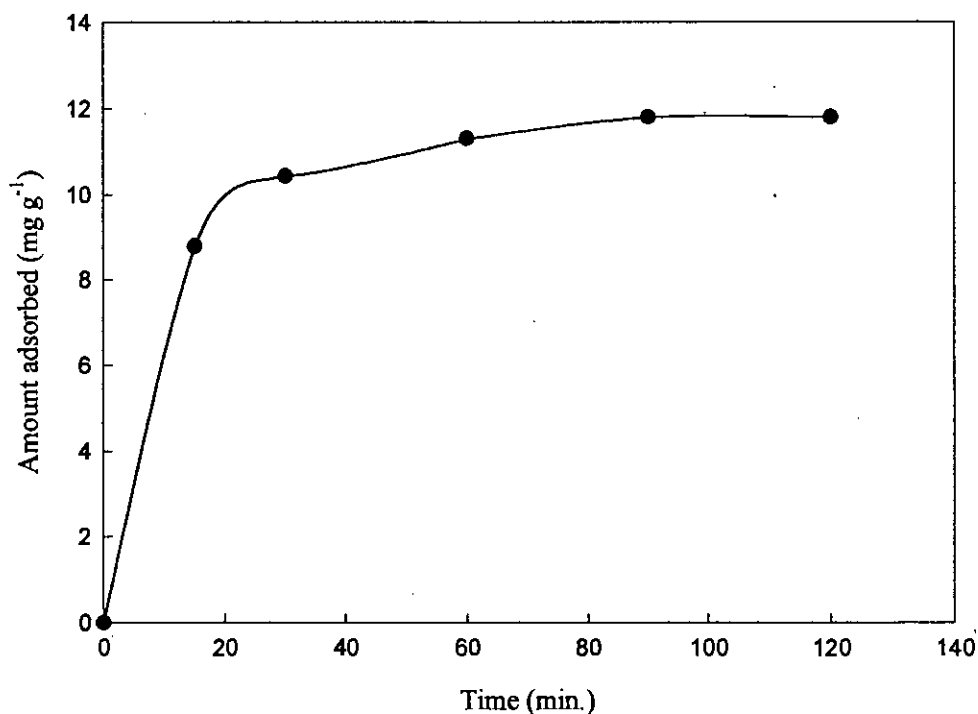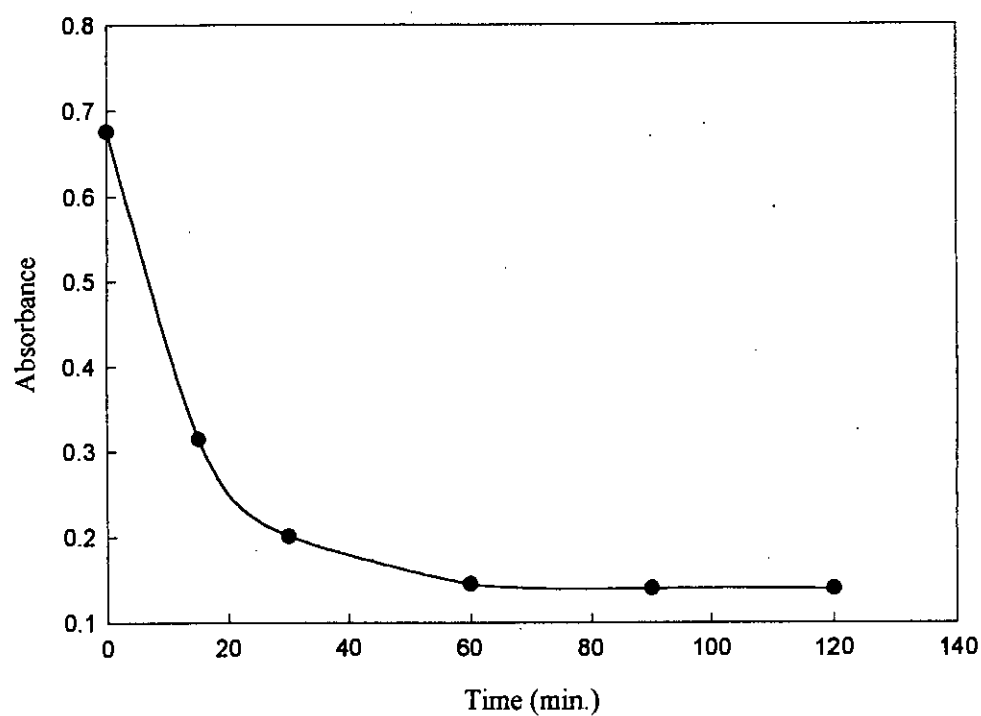| Initial conc. of MB (M)	Amount of sample taken in 100 mL solution to each vessel (g)	Time of shaking (min.)	Corresponding absorbance	Original absorbance
6×10^{-5}	0.133	15	0.452	0.671
		30	0.331	
		60	0.298	
		90	0.295	
		120	0.293	

Fig. 2.51: Effect of shaking time on the absorbance of 6×10^{-5} M MB solution

Table 2.48: Amount of MB adsorbed by per gram of sample from original concentration of $6\times10^{-5}\,M$

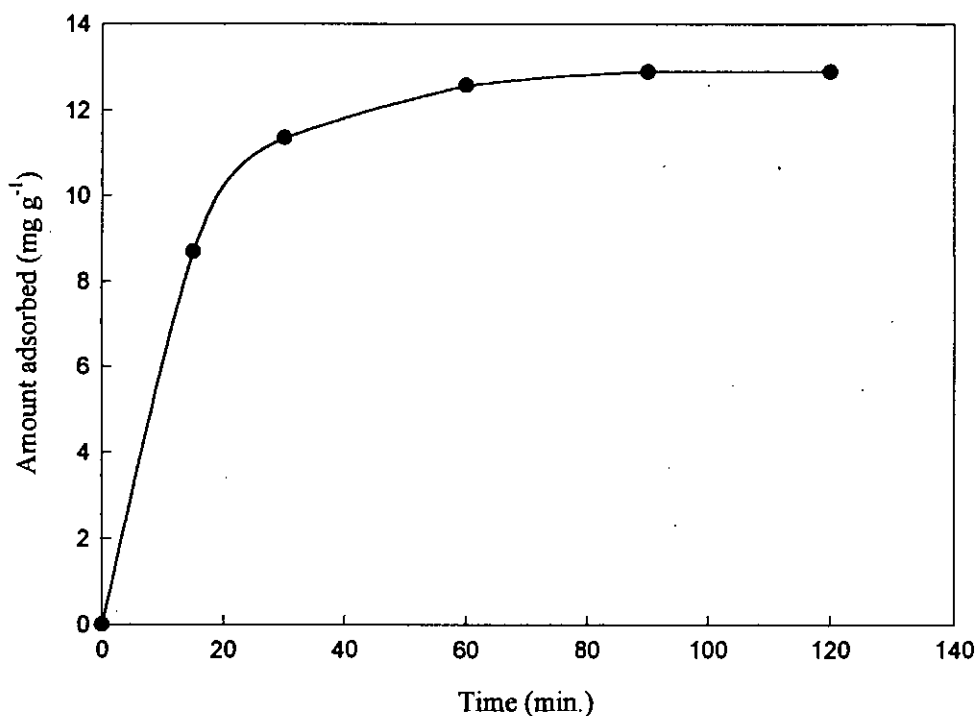| Time of shaking (min.)	Absorbance of remaining MB solution at the corresponding time	Difference of absorbance (Original absorbance of 6×10^{-5} M MB solution) - (Absorbance of remaining MB solution at the corresponding time)	Amount of solute adsorbed by the sample at the corresponding time $(mg\ g^{-1})$
15	0.452	0.219	5.14
30	0.331	0.340	7.76
60	0.298	0.373	8.83
90	0.295	0.376	9.04
120	0.293	0.378	9.09

Fig. 2.52: Effect of shaking time on the amount of solute (MB) adsorbed from its $6\times10^{-5}M$ solution

The determination of specific surface area of neutral PANI-SiO₂ by adsorption method using MB dyestuff

MB solution: 1×10^{-5} M

Table 2.49: Absorbance data for 1×10^{-5} M MB solution at different shaking time

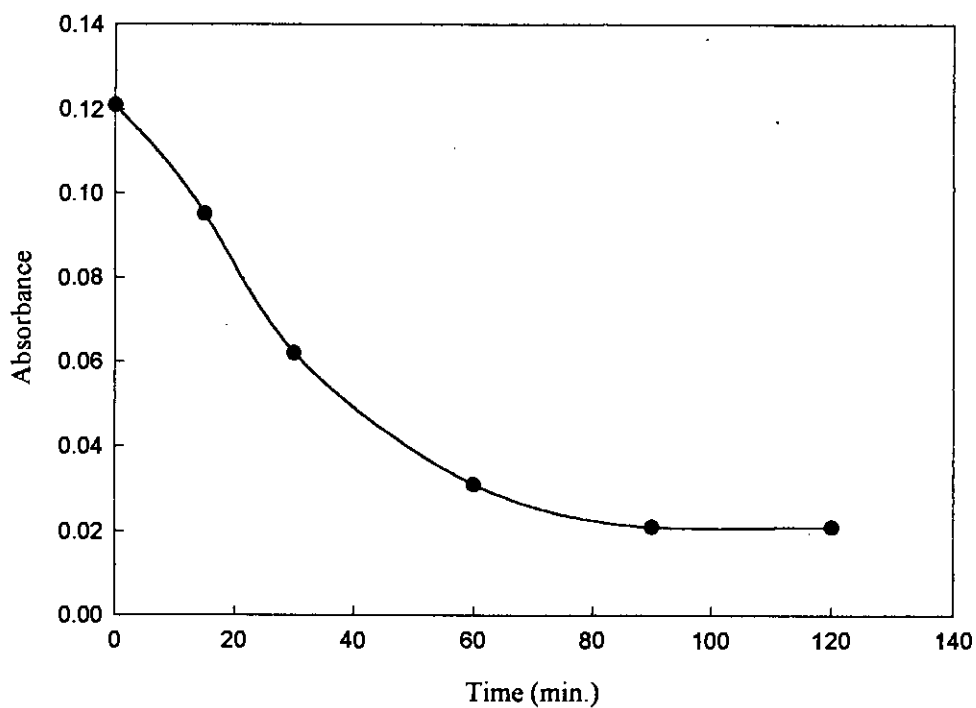| Initial conc. of MB (M)	Amount of sample taken in 100 mL solution to each vessel (g)	Time of shaking (min.)	Corresponding absorbance	Original absorbance
1×10^{-5}	0.133	15	0.081	0.101
		30	0.052	
		60	0.031	
		90	0.022	
		120	0.022	

Fig. 2.53: Effect of shaking time on the absorbance of 1×10^{-5} M MB solution

Table 2.50: Amount of MB adsorbed by per gram of sample from original concentration of 1×10^{-5} M

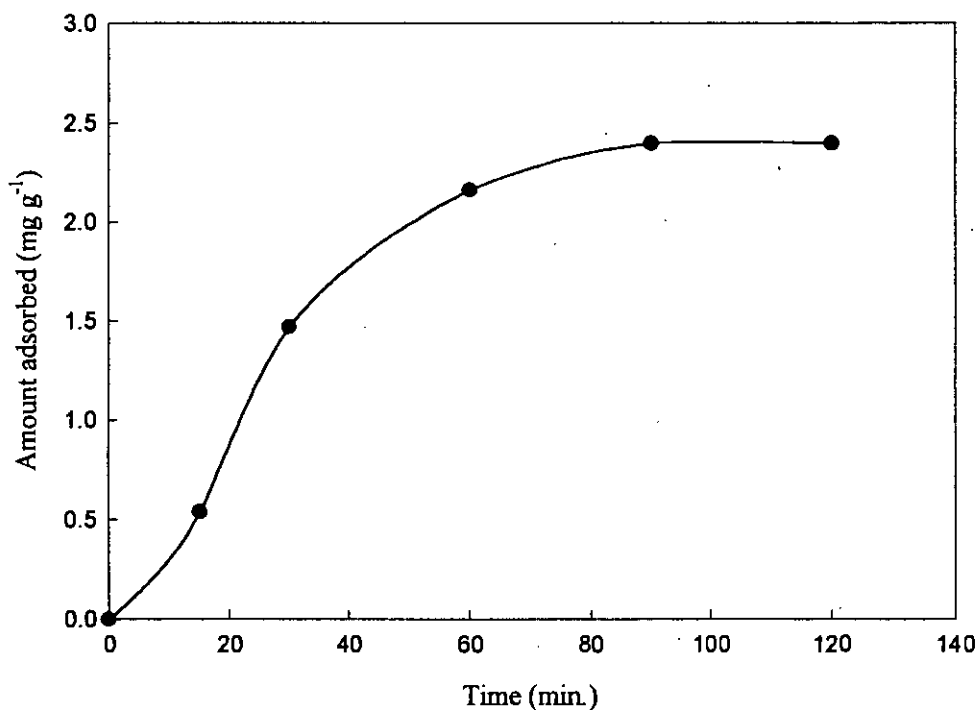| Time of shaking (min.)	Absorbance of remaining MB solution at the corresponding time	Difference of absorbance (Original absorbance of 1×10^{-5} M MB solution) - (Absorbance of remaining MB solution at the corresponding time)	Amount of solute adsorbed by the sample at the corresponding time (mg g^{-1})
15	0.081	0.020	0.59
30	0.052	0.049	1.41
60	0.031	0.070	2.22
90	0.022	0.079	2.27
120	0.022	0.079	2.27

Fig. 2.54: Effect of shaking time on the amount of solute (MB) adsorbed from its 1×10^{-5}M solution

MB solution: 2×10^{-5} M

Table 2.51: Absorbance data for 2×10^{-5} M methylene blue solution at different shaking time

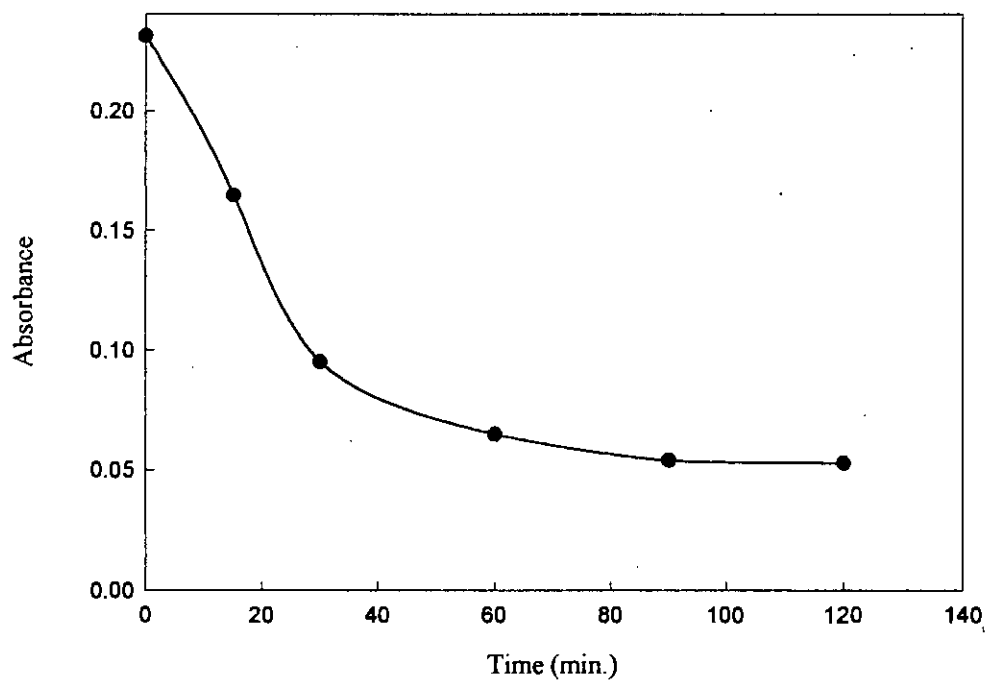| Initial conc. of MB (M)	Amount of sample taken in 100 mL solution to each vessel (g)	Time of shaking (min.)	Corresponding absorbance	Original absorbance
2×10^{-5}	0.133	15	0.123	0.201
		30	0.083	
		60	0.061	
		90	0.059	
		120	0.058	

Fig. 2.55: Effect of shaking time on the absorbance of 2×10^{-5} M MB solution

Table 2.52: Amount of MB adsorbed by per gram of sample from original concentration of 2×10^{-5} M

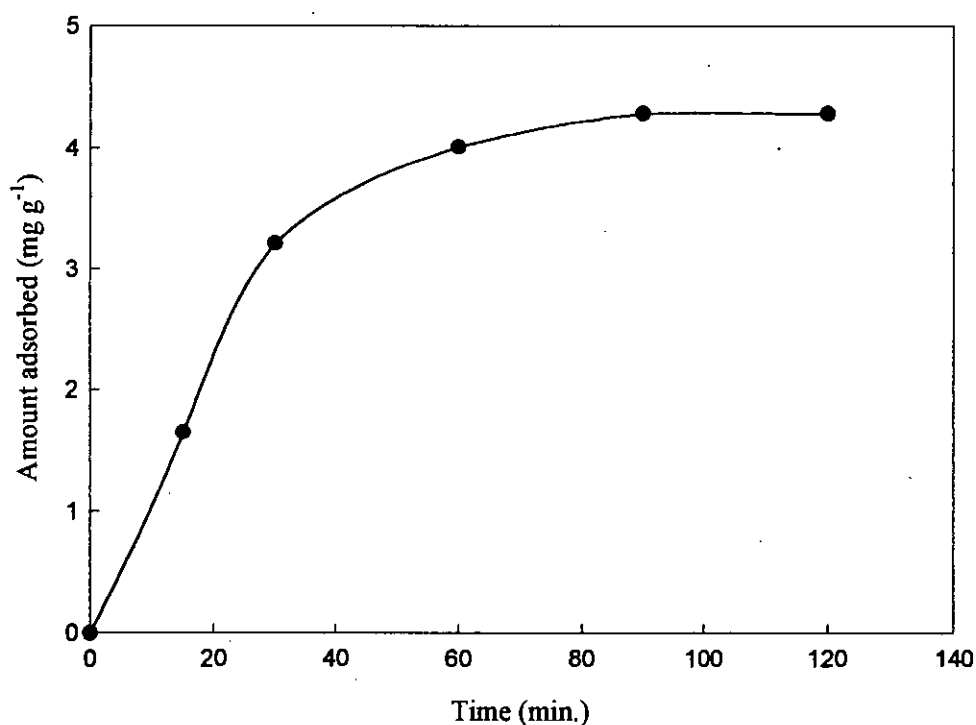| Time of shaking (min.)	Absorbance of remaining MB solution at the corresponding time	Difference of absorbance (Original absorbance of 2×10^{-5} M MB solution) - (Absorbance of remaining MB solution at the corresponding time)	Amount of solute adsorbed by the sample at the corresponding time (mg g^{-1})
15	0.123	0.078	2.14
30	0.083	0.118	3.16
60	0.061	0.140	3.77
90	0.059	0.142	3.96
120	0.058	0.143	4.01

Fig. 2.56: Effect of shaking time on the amount of solute (MB) adsorbed from its 2×10^{-5}M solution

MB solution: 3×10^{-5} M

Table 2.53: Absorbance data for 3×10^{-5} M MB solution at different shaking time

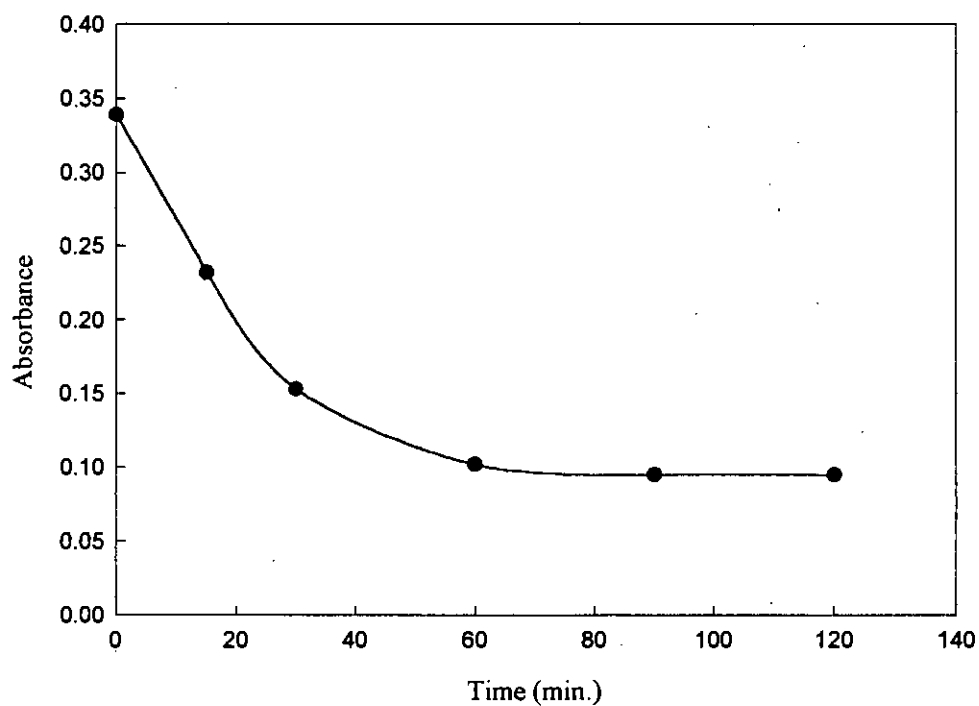| Initial conc. of MB (M)	Amount of sample taken in 100 mL solution to each vessel (g)	Time of shaking (min.)	Corresponding absorbance	Original absorbance
3×10^{-5}	0.133	15	0.153	0.297
		30	0.110	
		60	0.096	
		90	0.089	
		120	0.089	

Fig. 2.57: Effect of shaking time on the absorbance of 3×10^{-5} M MB solution

Table 2.54: Amount of MB adsorbed by per gram of sample from original concentration of 3×10^{-5} M

Time of shaking (min.)	Absorbance of remaining MB solution at the corresponding time	Difference of absorbance (Original absorbance of 3×10^{-5} M MB solution) - (Absorbance of remaining MB solution at the corresponding time)	Amount of solute adsorbed by the sample at the corresponding time (mg g^{-1})
15	0.153	0.144	3.74
30	0.110	0.187	5.08
60	0.096	0.201	5.48
90	0.089	0.208	5.75
120	0.089	0.208	5.75
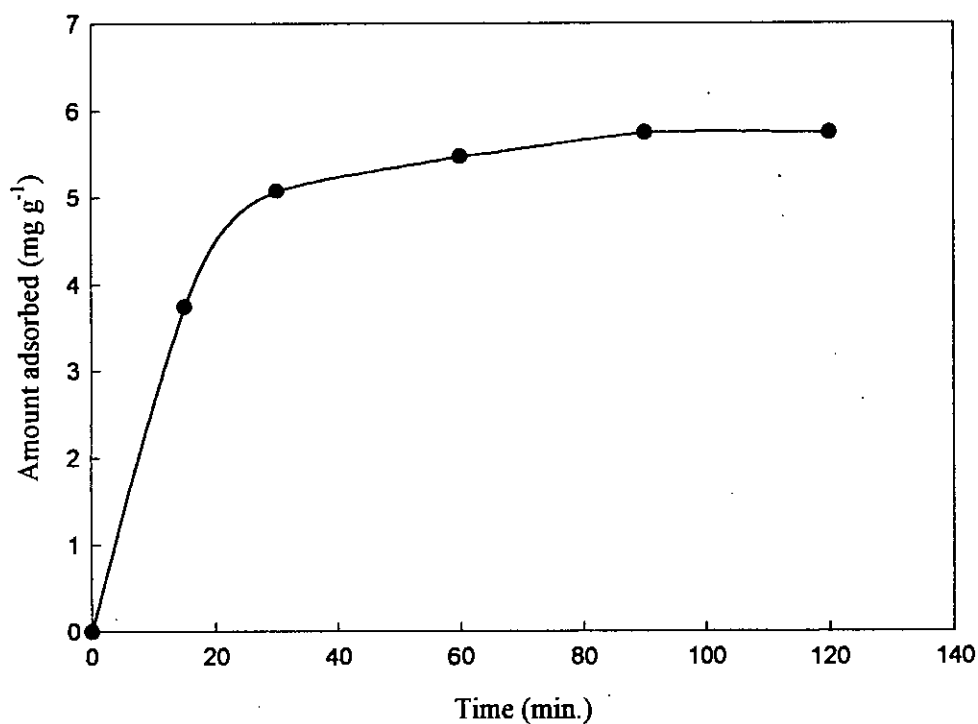
Fig. 2.58: Effect of shaking time on the amount of solute (MB) adsorbed from its 3×10^{-5}M solution

Table 2.56: Amount of MB adsorbed by per gram of sample from original concentration of 4×10^{-5} M

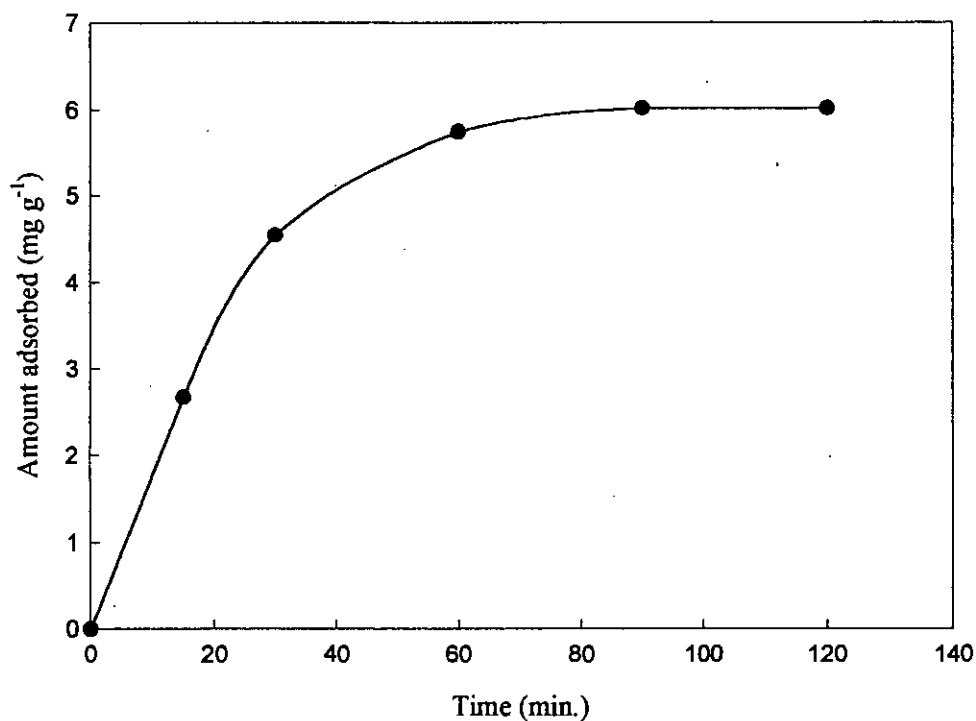| Time of shaking (min.)	Absorbance of remaining MB solution at the corresponding time	Difference of absorbance (Original absorbance of 4×10^{-5} M MB solution) - (Absorbance of remaining MB solution at the corresponding time)	Amount of solute adsorbed by the sample at the corresponding time (mg g^{-1})
15	0.251	0.130	3.61
30	0.185	0.196	5.49
60	0.153	0.228	6.29
90	0.143	0.238	6.95
120	0.143	0.238	6.95

Fig. 2.60: Effect of shaking time on the amount of solute (MB) adsorbed from its 4×10^{-5}M solution

MB solution: 5×10^{-5} M

Table 2.57: Absorbance data for 5×10^{-5} M MB solution at different shaking time

Initial conc. of MB (M)	Amount of sample taken in 100 mL solution to each vessel (g)	Time of shaking (min.)	Corresponding absorbance	Original absorbance
5×10^{-5}	0.133	15	0.314	0.476
		30	0.224	
		60	0.205	
		90	0.199	
		120	0.198	
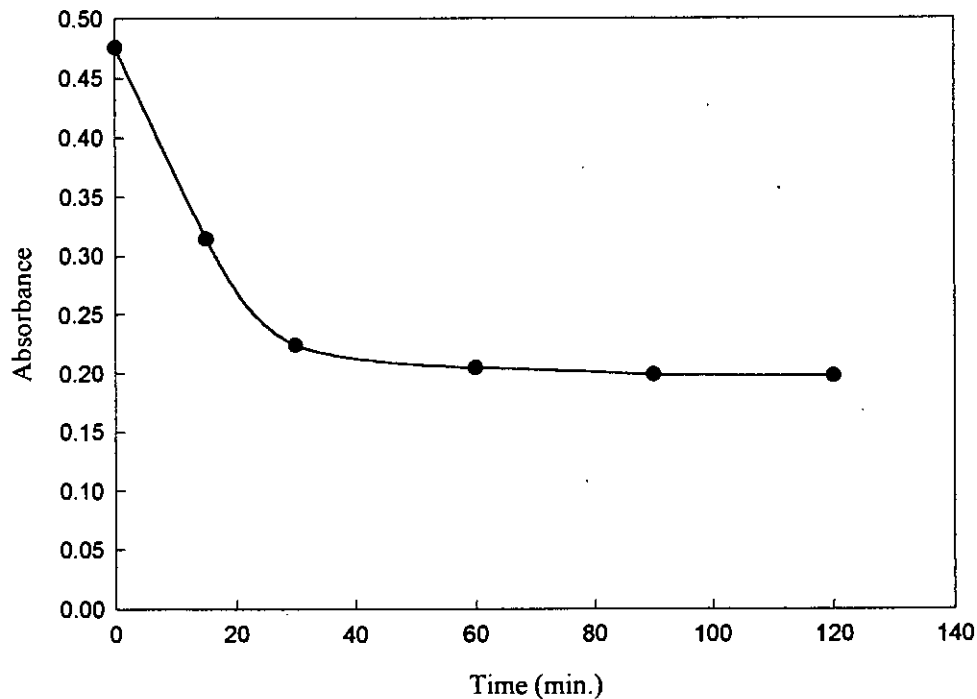
Fig. 2.61: Effect of shaking time on the absorbance of 5×10^{-5} M MB solution

Table 2.58: Amount of MB adsorbed by per gram of sample from original concentration of 5×10^{-5} M

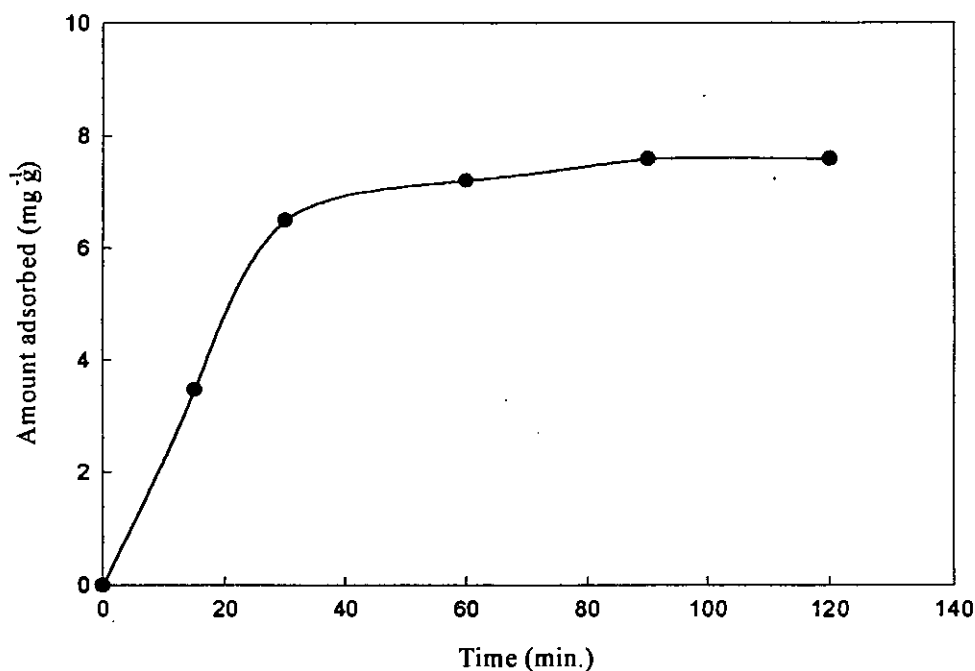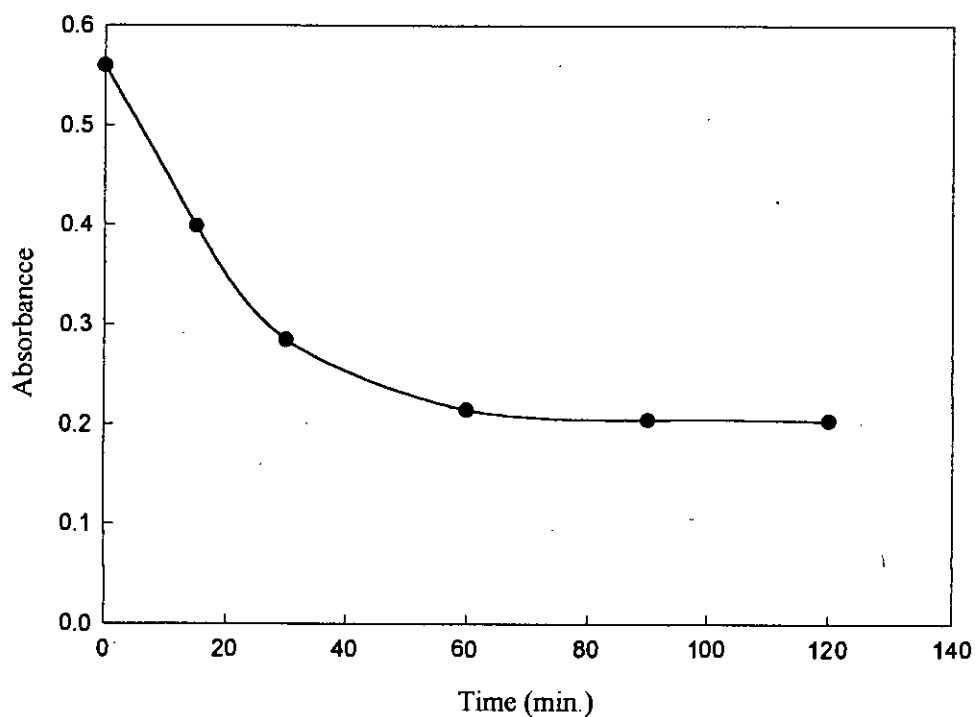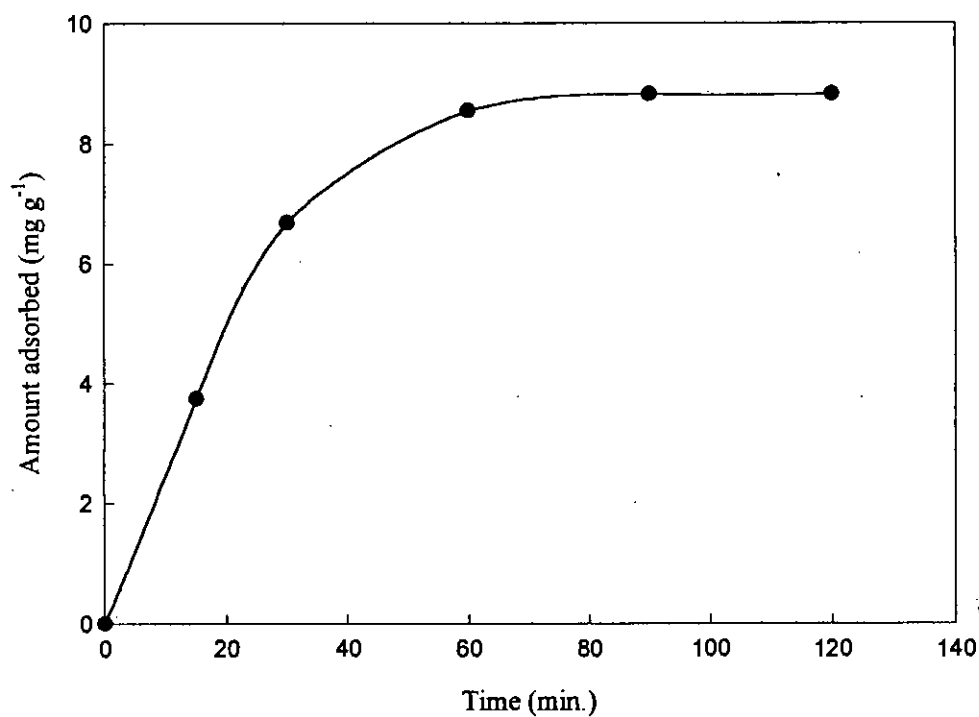| Time of shaking (min.)	Absorbance of remaining MB solution at the corresponding time	Difference of absorbance (Original absorbance of 5×10^{-5} M MB solution) - (Absorbance of remaining MB solution at the corresponding time)	Amount of solute adsorbed by the sample at the corresponding time (mg g^{-1})
15	0.314	0:162	4.28
30	0.224	0.252	6.96
60	0.205	0.271	7.49
90	0.199	0.277	7.76
120	0.198	0.278	7.76
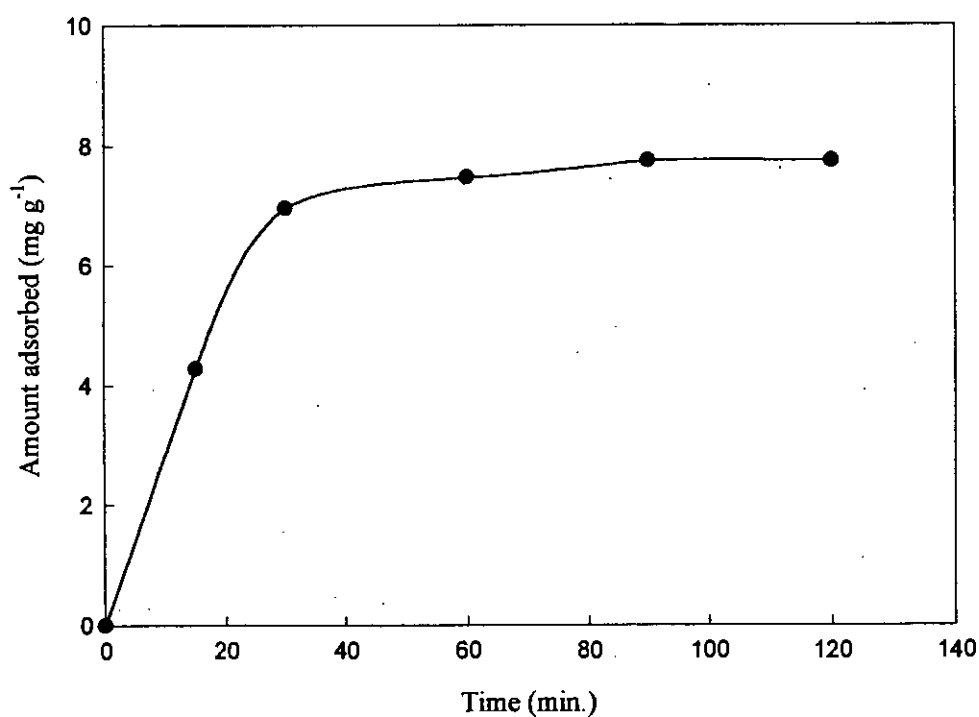
Fig. 2.62: Effect of shaking time on the amount of solute (MB) adsorbed from its 5×10^{-5} M solution

MB solution: 6×10^{-5} M

Table 2.59: Absorbance data for 6×10^{-5} M MB solution at different shaking time

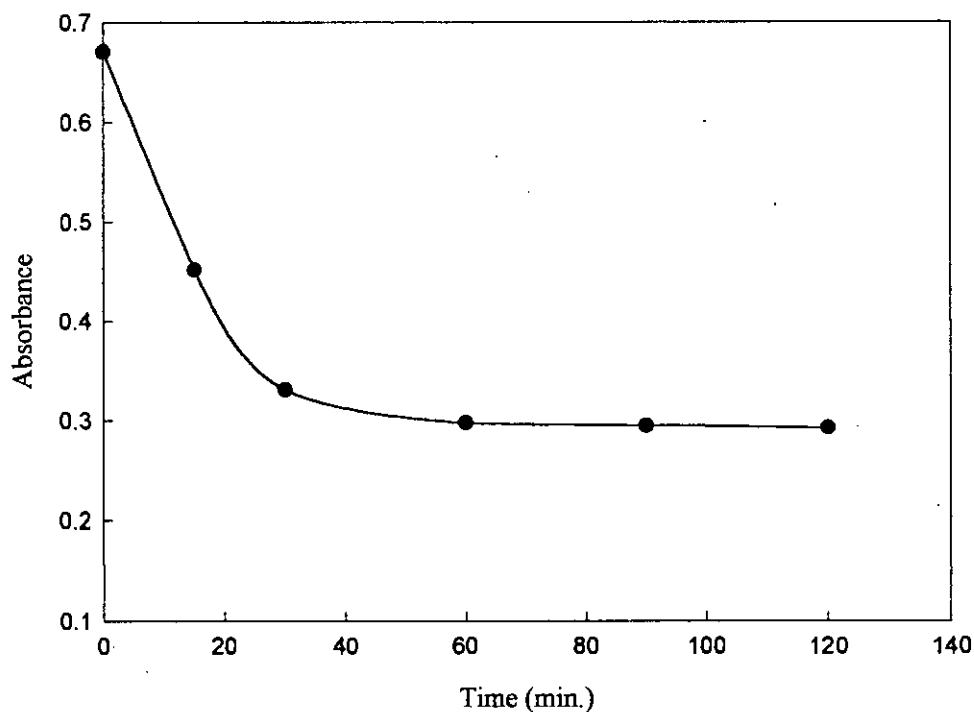| Initial conc. of MB (M)	Amount of sample taken in 100 mL solution to each vessel (g)	Time of shaking (min.)	Corresponding absorbance	Original absorbance
6×10^{-5}	0.133	15	0.384	0.571
		30	0.298	
		60	0.283	
		90	0.280	
		120	0.280	

Fig. 2.63: Effect of shaking time on the absorbance of 6×10^{-5} M MB solution

Table 2.60: Amount of MB adsorbed by per gram of sample from original concentration of 6×10^{-5} M

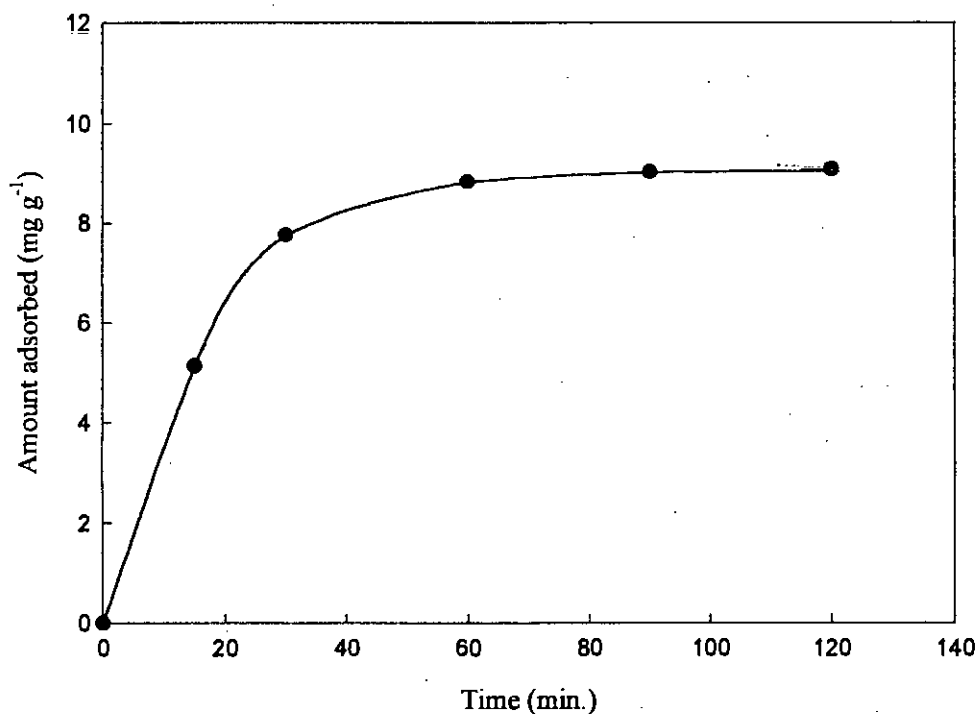| Time of shaking (min.)	Absorbance of remaining MB solution at the corresponding time	Difference of absorbance (Original absorbance of 6×10^{-5} M MB solution) - (Absorbance of remaining MB solution at the corresponding time)	Amount of solute adsorbed by the sample at the corresponding time (mg g^{-1})
15	0.384	0.187	5.16
30	0.298	0.273	7.36
60	0.283	0.288	7.68
90	0.280	0.291	8.02
120	0.280	0.291	8.02
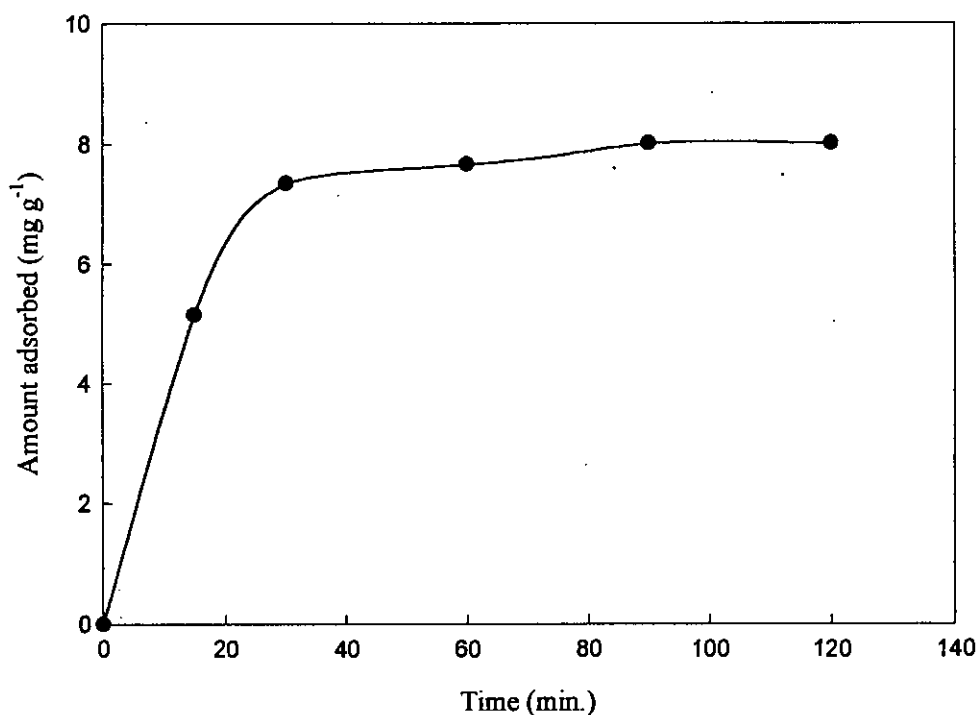
Fig. 2.64: Effect of shaking time on the amount of solute (MB) adsorbed from its 6×10^{-5} M solution

The determination of specific surface area of basic PANI-SiO₂ by adsorption method using MB dyestuff

MB solution: 1×10^{-5} M

Table 2.61: Absorbance data for 1×10^{-5} M MB solution at different shaking time

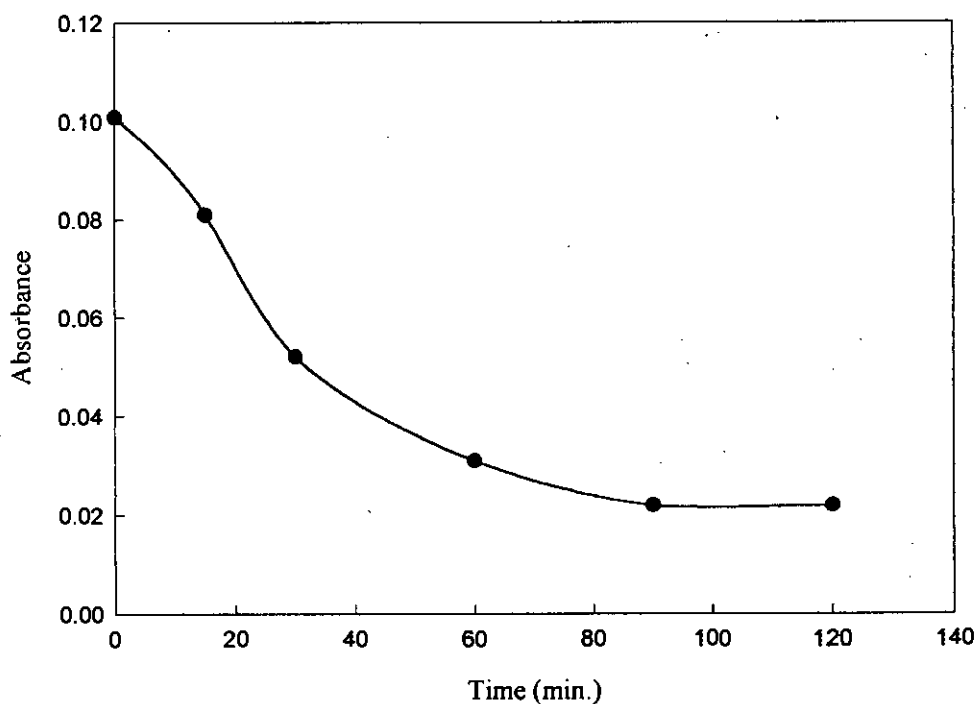| Initial conc. of MB (M)	Amount of sample taken in 100 mL solution to each vessel (g)	Time of shaking (min.)	Corresponding absorbance	Original absorbance
1×10^{-5}	0.133	15	0.080	0.135
		30	0.040	
		60	0.008	
		90	0.002	
		120	0.002	
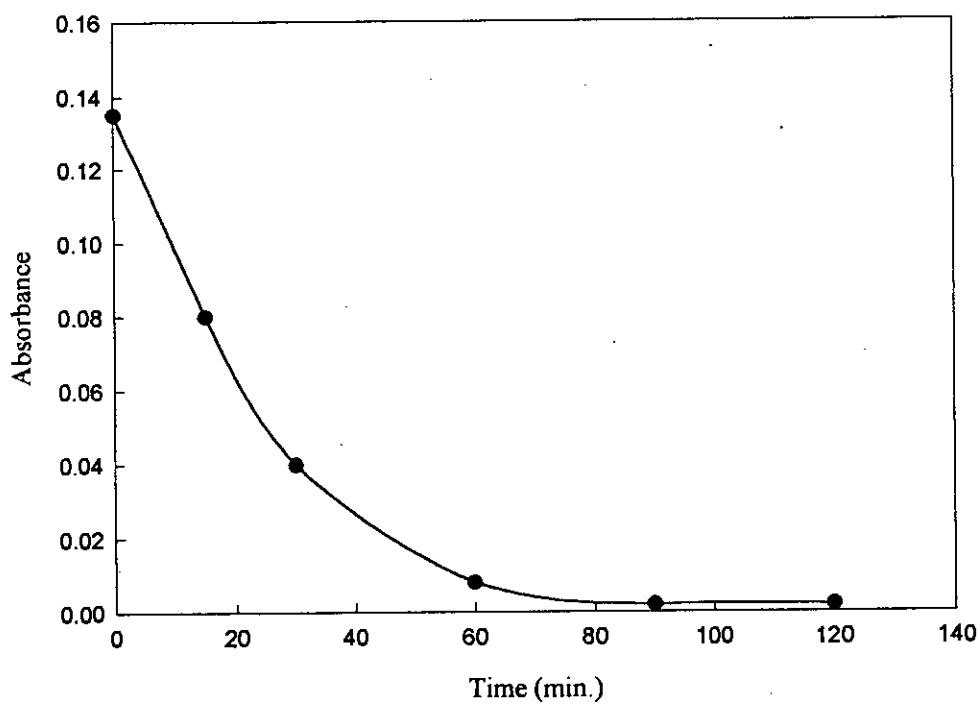
Fig. 2.65: Effect of shaking time on the absorbance of 1×10^{-5} M MB solution

Table 2.62: Amount of MB adsorbed by per gram of sample from original concentration of 1×10^{-5} M

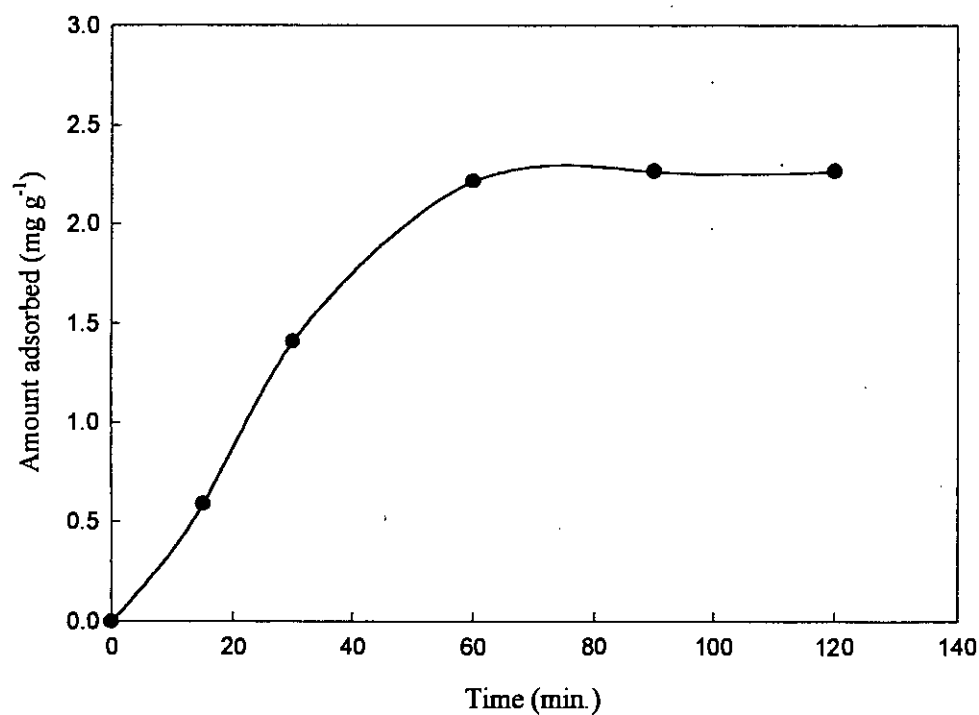| Time of shaking (min.)	Absorbance of remaining MB solution at the corresponding time	Difference of absorbance (Original absorbance of 1×10^{-5} M MB solution) - (Absorbance of remaining MB solution at the corresponding time)	Amount of solute adsorbed by the sample at the corresponding time (mg g^{-1})
15	0.080	0.055	0.75
30	0.040	0.095	1.69
60	0.008	0.127	2.54
90	0.002	0.133	2.60
120	0.002	0.133	2.60
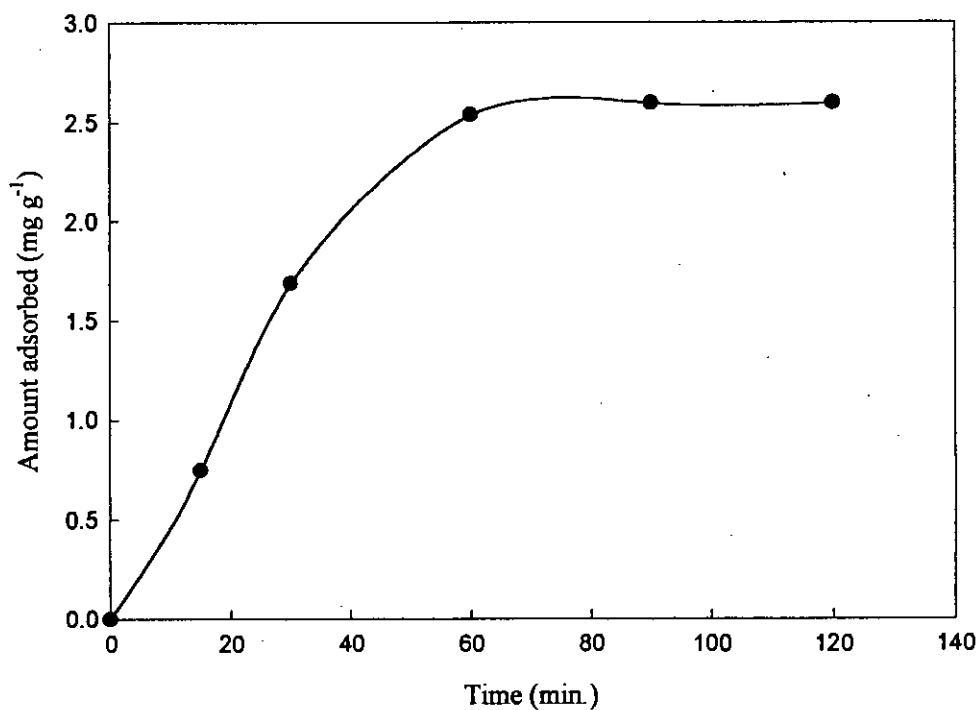
Fig. 2.66: Effect of shaking time on the amount of solute (MB) adsorbed from its 1×10^{-5}M solution

MB solution: 2×10^{-5} M

Table 2.63: Absorbance data for 2×10^{-5} M MB solution at different shaking time

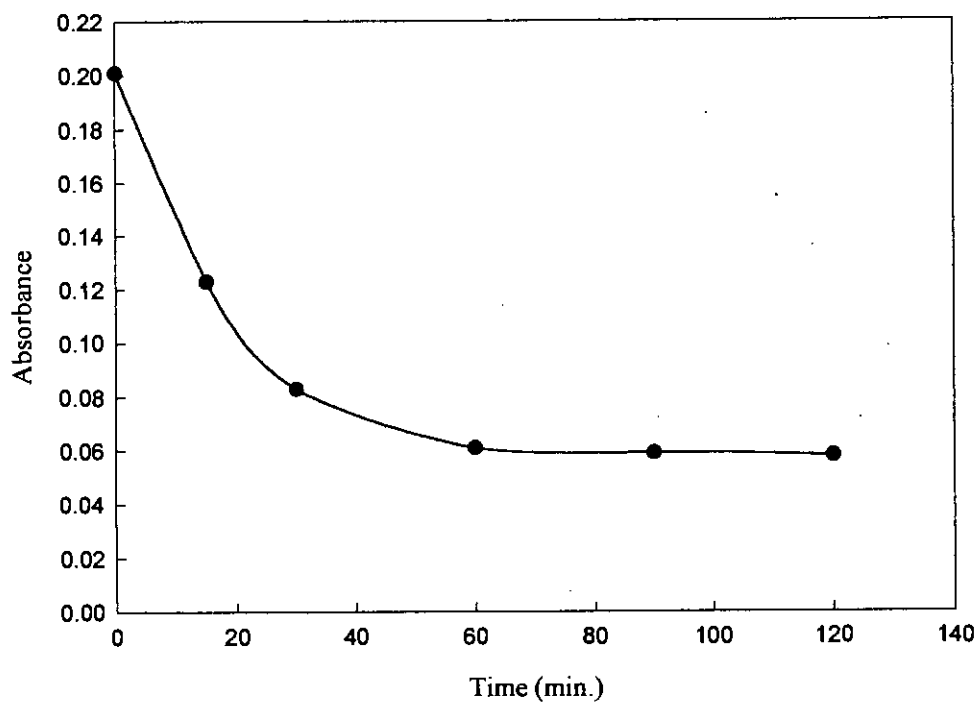| Initial conc. of MB (M)	Amount of sample taken in 100 mL solution to each vessel (g)	Time of shaking (min.)	Corresponding absorbance	Original absorbance
2×10^{-5}	0.133	15	0.144	0.240
		30	0.060	
		60	0.021	
		90	0.010	
		120	0.010	
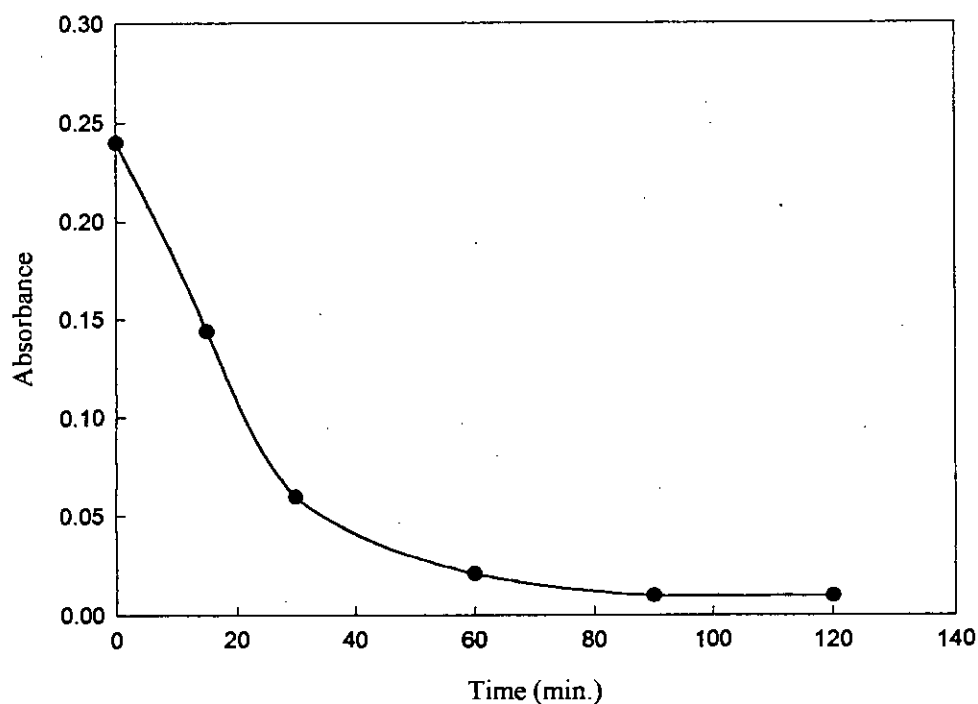
Fig. 2.67: Effect of shaking time on the absorbance of 2×10^{-5} M MB solution

Table 2.64: Amount of MB adsorbed by per gram of sample from original concentration of 2×10^{-5} M

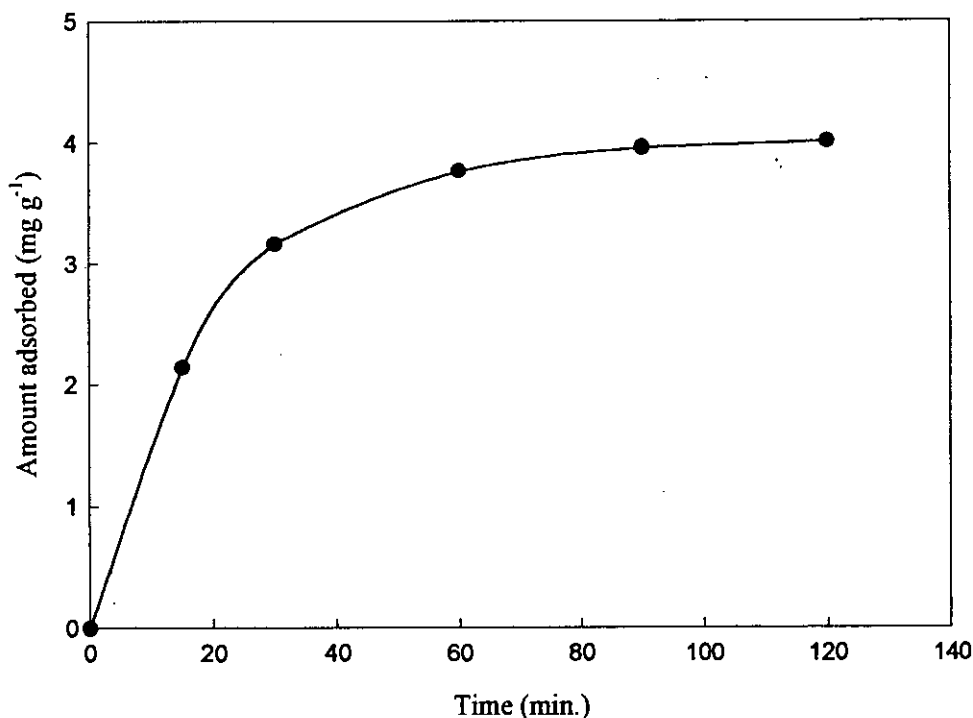| Time of shaking (min.)	Absorbance of remaining MB solution at the corresponding time	Difference of absorbance (Original absorbance of 2×10^{-5} M MB solution) - (Absorbance of remaining MB solution at the corresponding time)	Amount of solute adsorbed by the sample at the corresponding time (mg g^{-1})
15	0.144	0.096	1.87
30	0.060	0.180	3.83
60	0.021	0.219	4.87
90	0.010	0.230	5.22
120	0.010	0.230	5.22
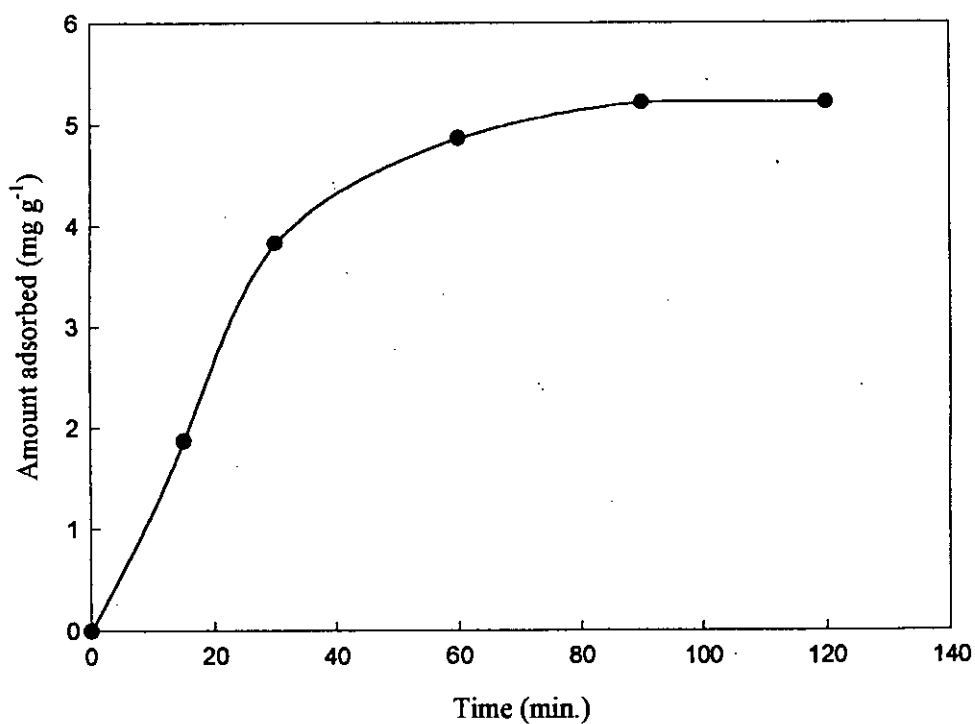
Fig. 2.68: Effect of shaking time on the amount of solute (MB) adsorbed from its 2×10^{-5}M solution

MB solution: 3×10^{-5} M

Table 2.65: Absorbance data for 3×10^{-5} M MB solution at different shaking time

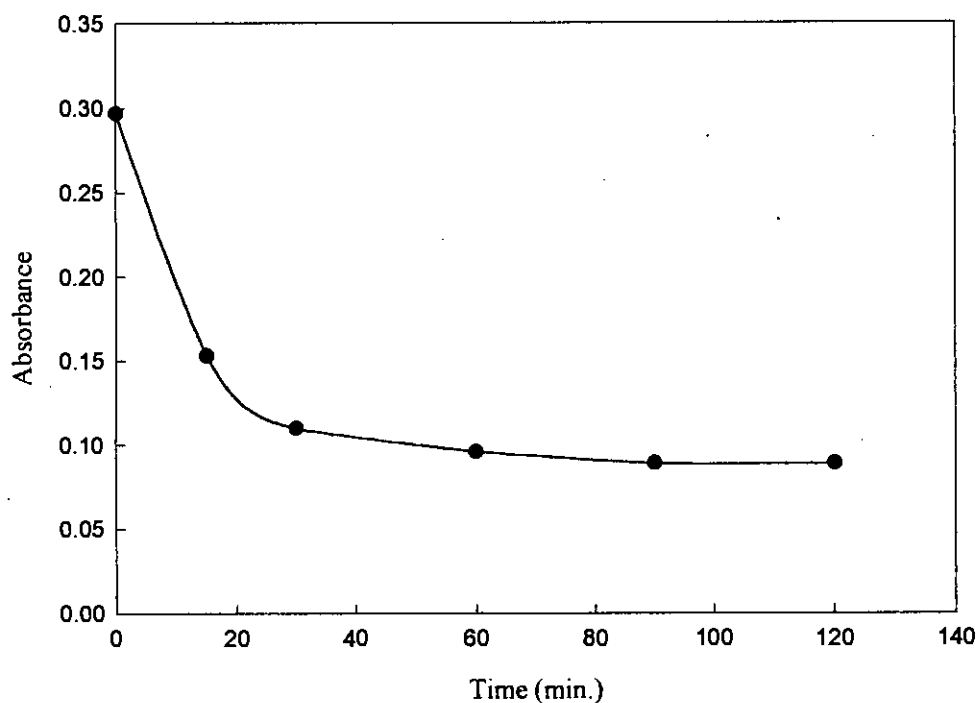| Initial conc. of MB (M)	Amount of sample taken in 100 mL solution to each vessel (g)	Time of shaking (min.)	Corresponding absorbance	Original absorbance
3×10^{-5}	0.133	15	0.121	0.346
		30	0.065	
		60	0.022	
		90	0.018	
		120	0.018	
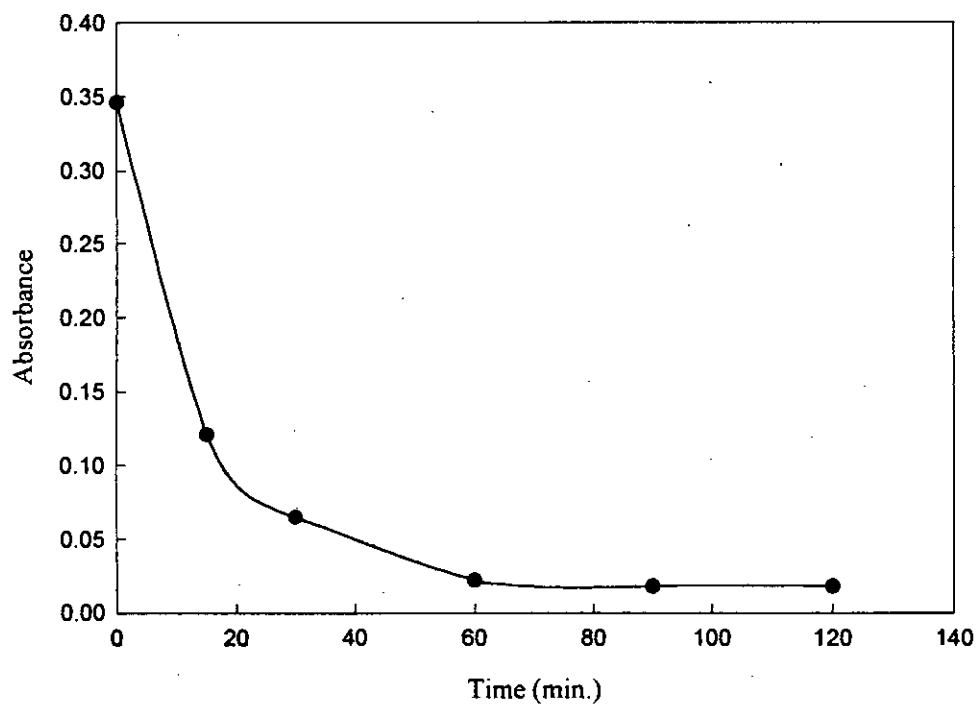
Fig. 2.69: Effect of shaking time on the absorbance of 3×10^{-5} M MB solution

Table 2.66: Amount of MB adsorbed by per gram of sample from original concentration of 3×10^{-5} M

Time of shaking (min.)	Absorbance of remaining MB solution at the corresponding time	Difference of absorbance (Original absorbance of 3×10^{-5} M MB solution) - (Absorbance of remaining MB solution at the corresponding time)	Amount of solute adsorbed by the sample at the corresponding time (mg g^{-1})
15	0.121	0.225	5.08
30	0.065	0.281	6.37
60	0.022	0.324	7.47
90	0.018	0.328	7.79
120	0.018	0.328	7.79
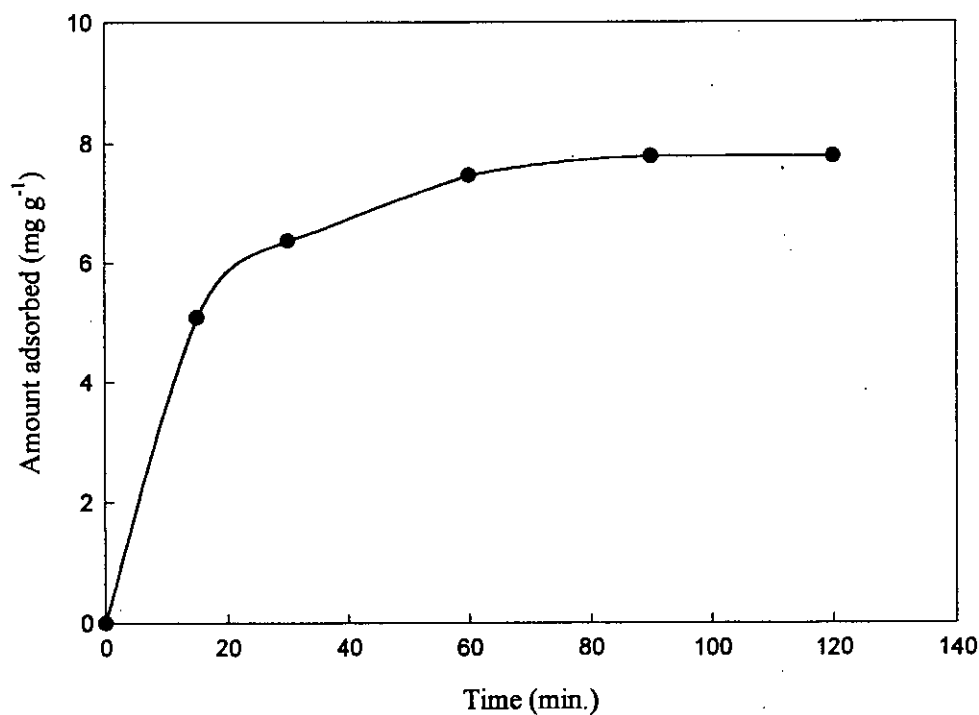
Fig. 2.70: Effect of shaking time on the amount of solute (MB) adsorbed from its 3×10^{-5} M solution

MB solution: 4×10^{-5} M

Table 2.67: Absorbance data for 4×10^{-5} M MB solution at different shaking time

Initial conc. of MB (M)	Amount of sample taken in 100 mL solution to each vessel (g)	Time of shaking (min.)	Corresponding absorbance	Original absorbance
4×10^{-5}	0.133	15	0.185	0.461
		30	0.068	
		60	0.032	
		90	0.021	
		120	0.020	
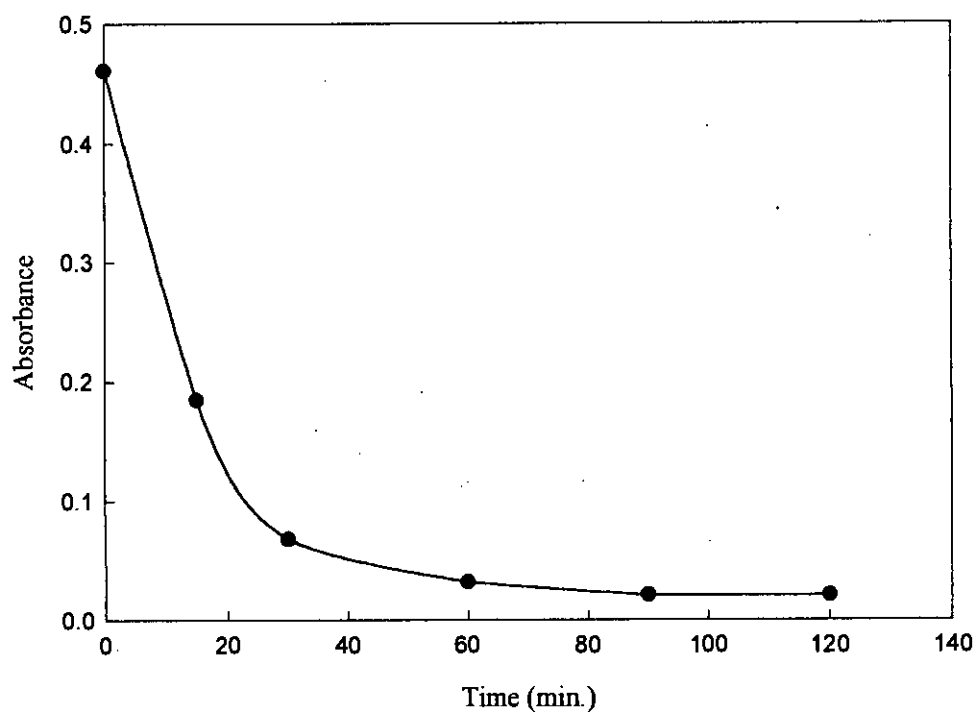
Fig. 2.71: Effect of shaking time on the absorbance of 4×10^{-5} M MB solution

Table 2.68: Amount of MB adsorbed by per gram of sample from original concentration of 4×10^{-5} M

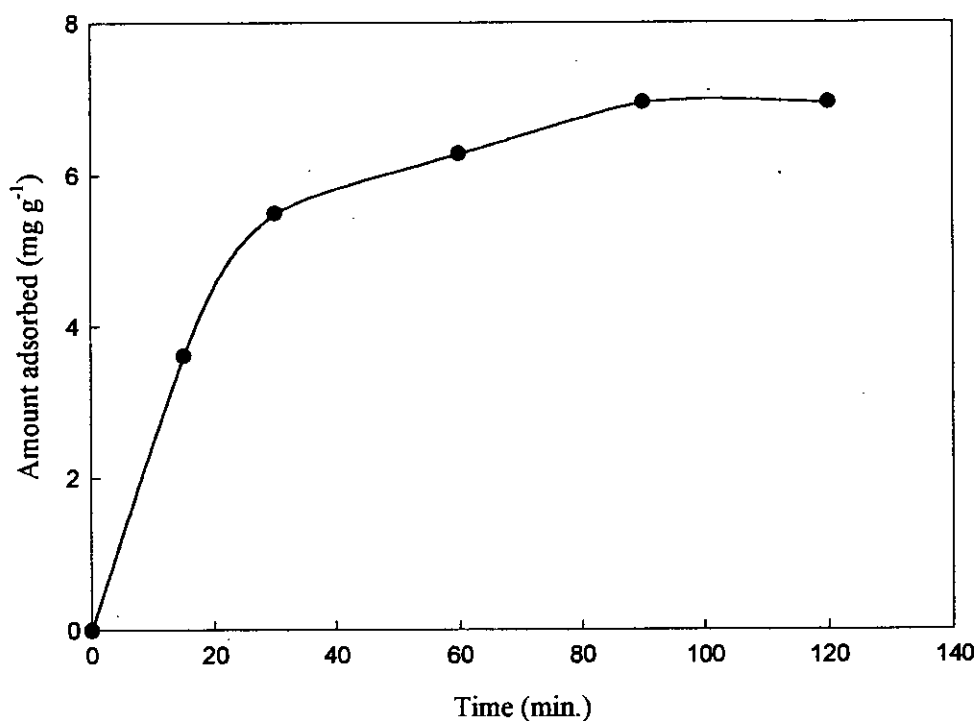| Time of shaking (min.)	Absorbance of remaining MB solution at the corresponding time	Difference of absorbance (Original absorbance of 4×10^{-5} M MB solution) - (Absorbance of remaining MB solution at the corresponding time)	Amount of solute adsorbed by the sample at the corresponding time (mg g^{-1})
15	0.185	0.276	6.34
30	0.068	0.393	8.96
60	0.032	0.429	9.90
90	0.021	0.440	10.30
120	0.020	0.441	10.30
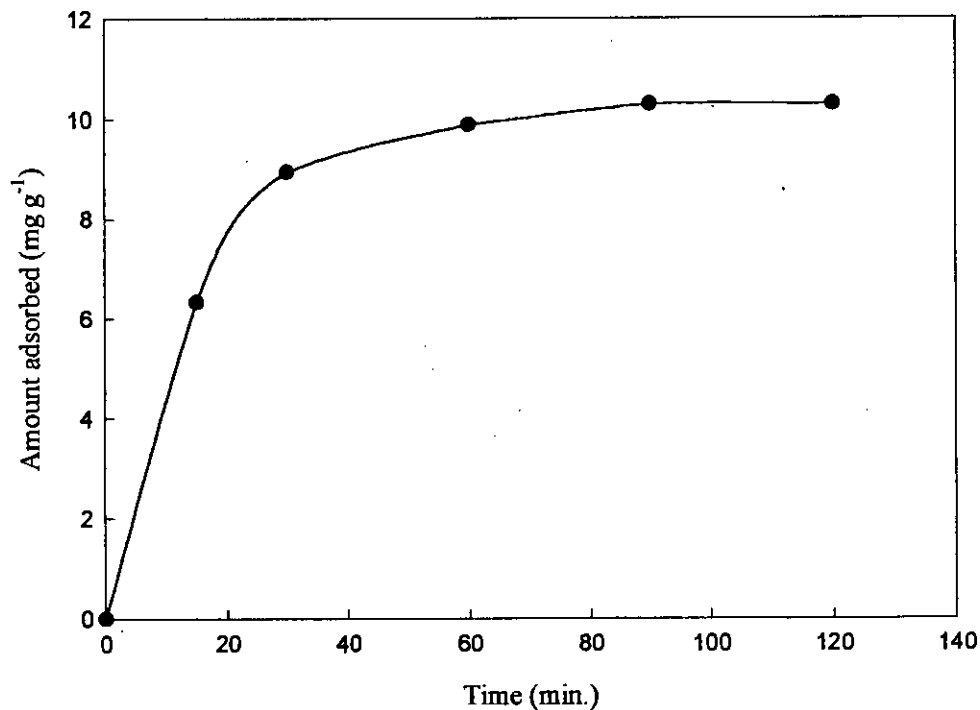
Fig. 2.72: Effect of shaking time on the amount of solute (MB) adsorbed from its 3×10^{-5}M solution

MB solution: 5×10^{-5} M

Table 2.69: Absorbance data for 5×10^{-5} M MB solution at different shaking time

Initial conc. of MB (M)	Amount of sample taken in 100 mL solution to each vessel (g)	Time of shaking (min.)	Corresponding absorbance	Original absorbance
5×10^{-5}	0.133	15	0.196	0.575
		30	0.074	
		60	0.042	
		90	0.031	
		120	0.031	
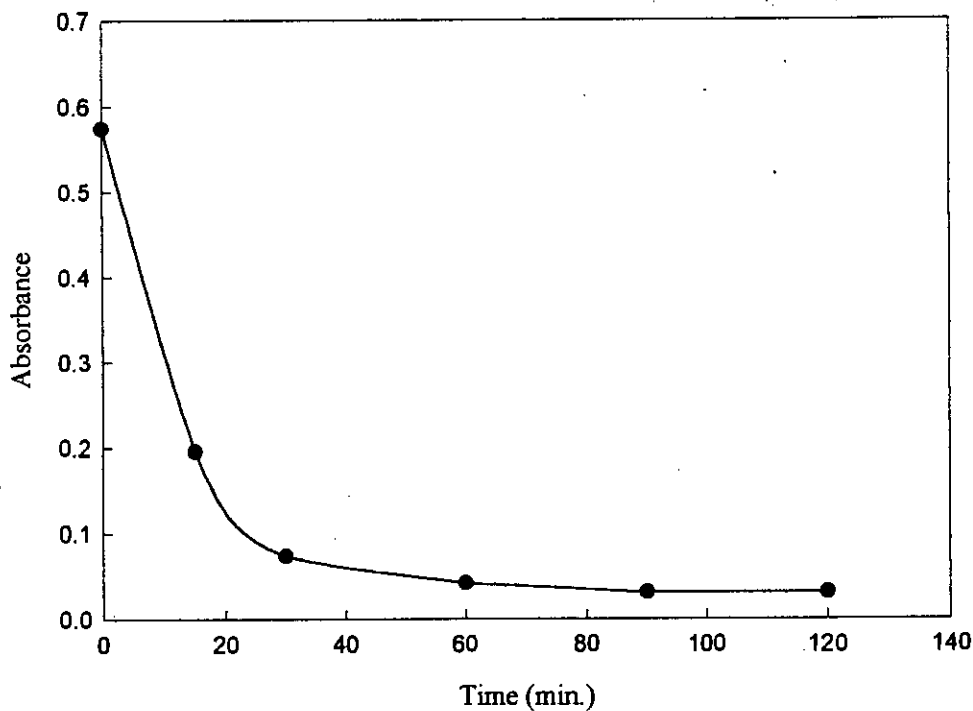
Fig. 2.73: Effect of shaking time on the absorbance of 5×10^{-5} M MB solution

MB solution: 6×10^{-5} M

Table 2.71: Absorbance data for 6×10^{-5} M MB solution at different shaking time

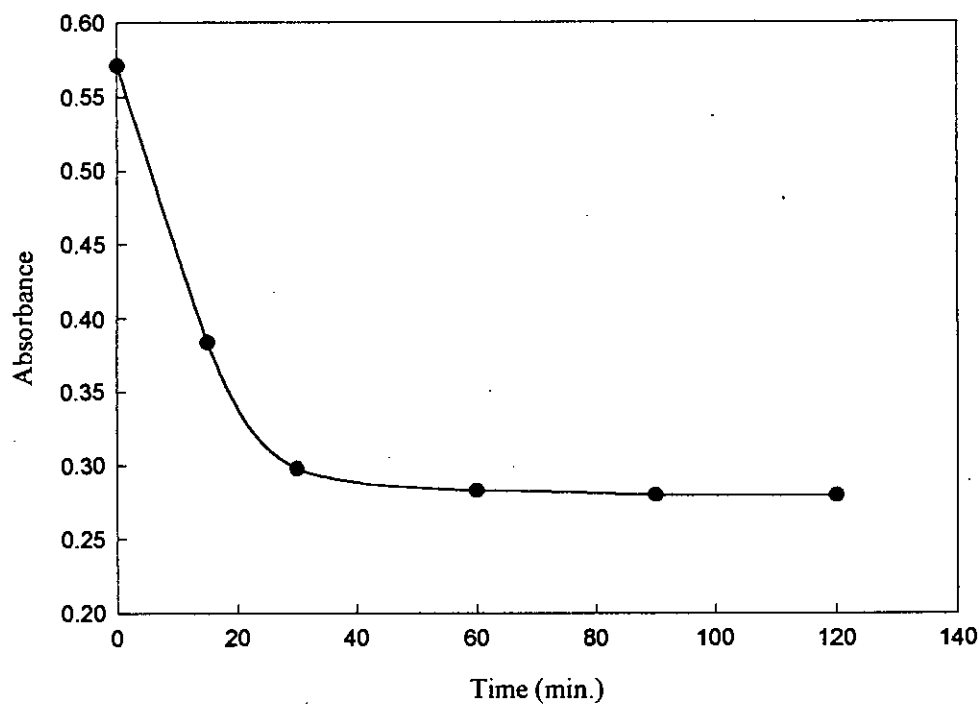| Initial conc. of MB (M)	Amount of sample taken in 100 mL solution to each vessel (g)	Time of shaking (min.)	Corresponding absorbance	Original absorbance
6×10^{-5}	0.133	15	0.196	0.676
		30	0.067	
		60	0.065	
		90	0.060	
		120	0.058	
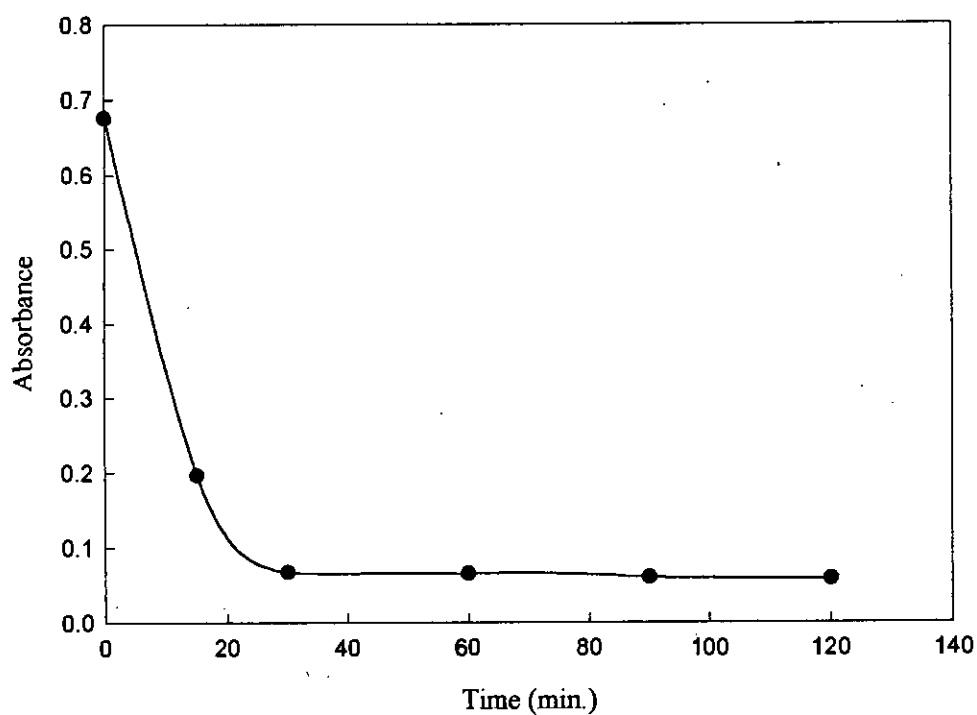
Fig. 2.75: Effect of shaking time on the absorbance of 6×10^{-5} M MB solution

Table 2.72: Amount of MB adsorbed by per gram of sample from original concentration of 6×10^{-5} M

Time of shaking (min.)	Absorbance of remaining MB solution at the corresponding time	Difference of absorbance (Original absorbance of 6×10^{-5} M MB solution) - (Absorbance of remaining MB solution at the corresponding time)	Amount of solute adsorbed by the sample at the corresponding time $(mg\ g^{-1})$
15	0.196	0.480	11.43
30	0.067	0.609	14.32
60	0.065	0.611	14.40
90	0.060	0.616	14.66
120	0.058	0.618	14.70
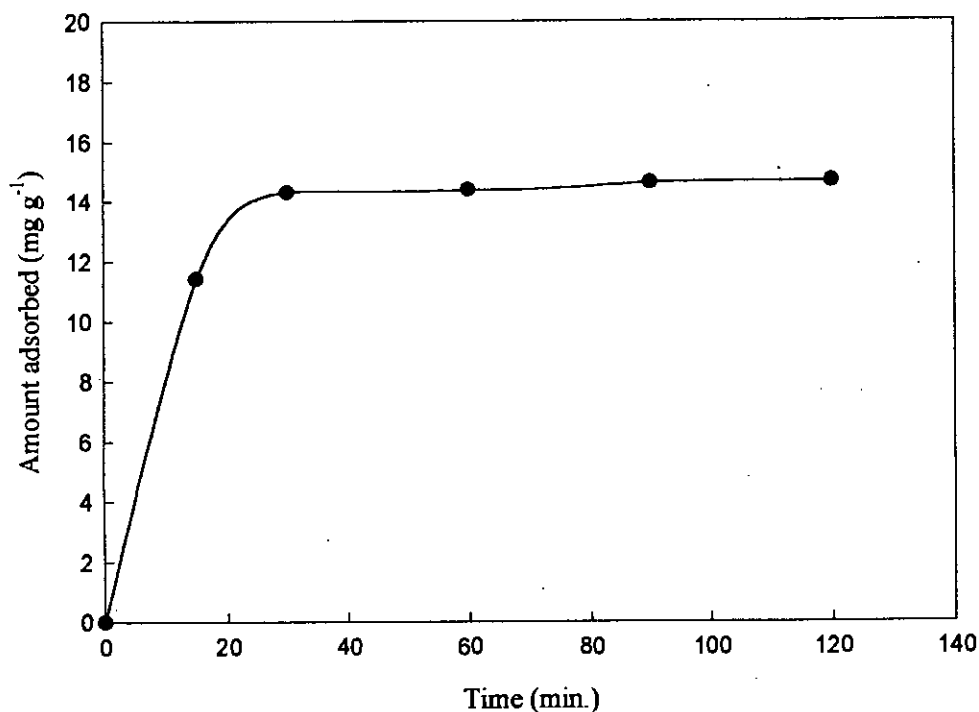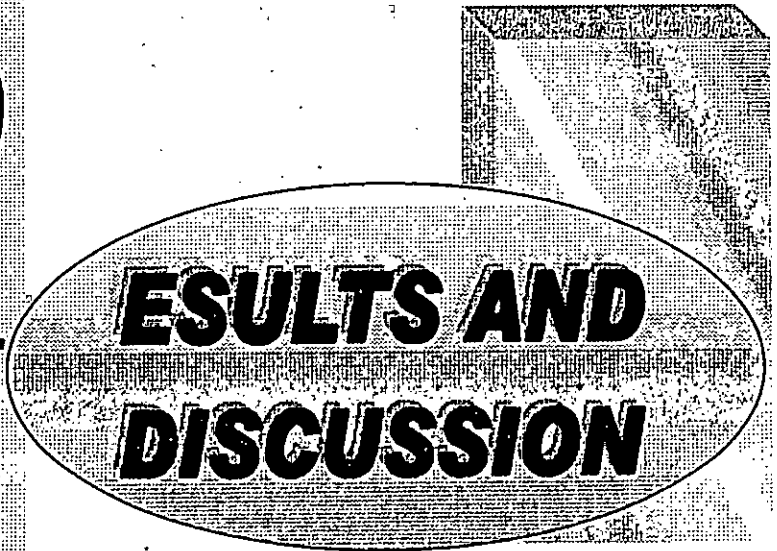
Fig. 2.76: Effect of shaking time on the amount of solute (MB) adsorbed from its 6×10^{-5}M solution
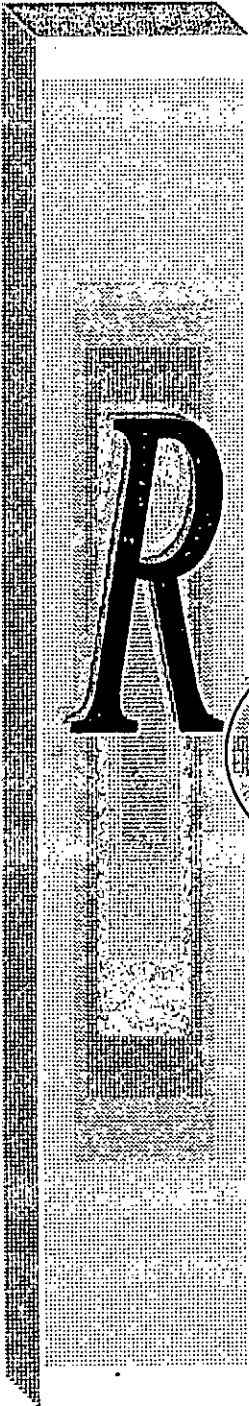
RESULTS AND DISCUSSION

3.1 Polymerization Mechanisms and Structure of PANI

The wide variety of methods[59-70] employed for the preparation of PANI leads to the formation of products whose nature and properties differ greatly. According to most authors, the first step in the oxidation of aniline is the formation of a radical cation, which is independent of the pH of the synthesis medium (be it acidic or basic), and is the governing criteria for the polymerization reaction. In the subsequent steps, radical cation coupling of aniline leads to the formation of PANI (Fig. 1.2).

PANI can be prepared in the four idealized forms shown in Fig. 3.1, at least when it's synthesis and any subsequent treatment are carried out in aqueous media. These forms may be interconverted at will by chemical and/or electrochemical oxidation or reduction. A given "A" form, *e.g.* 1A, may be converted to a given "S" form, *e.g.* 1S by treatment with an aqueous protonic acid, such as HCl. The acid may be removed to regenerate the "A" form by treating the "S" form with an aqueous solution of a base, such as aq. NH_3.

In the present investigation, PANI was synthesized chemically as a dark blue/black powder $[(=(C_6H_4)=N-(C_6H_4)-N(H)=)^+Cl^-]_x$, (form 2S) by treating a solution of aqueous HCl containing dissolve aniline, with the oxidizing agent, ammonia peroxydisulfate, $(NH_4)S_2O_8$. Protonation was completed by treating the powder with 0.1M aqueous HCl solution (pH = 1.09) for over night followed by drying initially in air and then under vacuum at room temperature for 3 days to remove water and free HCl. Hence, we designated this powder *"acidic PANI"*. The "2S" form was converted to the "2A" form, a dark purple / black powder by treating over night with a 0.1M aq. NH_3 solution (pH = 10.15) followed by drying in air and under vacuum as mentioned for the pervious sample.

Fig.3.1: Illustration of the idealized forms of PANI.

This sample is termed as "*basic* PANI". The **2S** form was washed with double distilled water (pH = 6.95) until the pH of the washed out water reached the pH value of 6.95 and then kept over night in the distilled water. This sample is termed as "*neutral* PANI" and may correspond to any form in between **2A** and **2S**. The **2A** form (*basic* PANI) fully de-protonated, the "*neutral* PANI" could be less de-protonated compared to that of *basic* PANI that treated with aq. NH_3. Level of protonation in its structures results in different physical properties and specific surface area. The different characterizations of the studied PANI samples are discussed in the section 3.3.

3.2 Silica-Stabilized Conducting Polymer Colloids

The preparation of stable colloidal dispersions of conducting polymers using polymeric surfactants[71-75] attracted special attention of the material scientists. A wide variety of oxidants is feasible in the chemical polymerization of conducting polymers: H_2O_2[76], $FeCl_3$[77], $(NH_4)_2S_2O_8$[78] are well established reagents. When aniline is oxidized in the presence of colloidal silica, colloidal $PANI/SiO_2$ composites are produced. In this synthesis the precipitating PANI was adsorbed as an insoluble thin layer onto the high surface area silica substrate particles. This

outer layer of PANI is non-solvated and acts as a binder, effectively 'gluing' the silica particles together.

Recently, it has been reported that stable PANI colloids can be prepared in aqueous media in the presence of small silica particles i.e. using particulate rather than polymeric dispersants. Most of the colloidal silica has a negative surface charge. Since PANI chains are polycations[79-80], the attractive electrostatic interaction may play a certain role in the formation of PANI/SiO$_2$ particles.

3.3 Characterization of the Prepared Substrates

3.3.1 IR spectral analysis

IR spectroscopic studies were carried out in order to get some qualitative information on the synthesized acidic-PANI, basic-PANI, neutral-PANI and PANI/SiO$_2$ substrates. The results are described below:

Figures 3.2-3.5 give IR spectra of the PANI obtained after treating with various aqueous solutions having (a) pH = 6.95 (b) pH = 1.09 and (c) pH = 10.15, and PAN/SiO$_2$ while the tentative assignment of the spectra are listed in a tabular form (Table 3.1) presented later.

The main absorption peaks are almost at the same position but their relative intensities obviously change with the solution pH with which PANI was treated. It can be seen form Fig.3.2 that the main effects of HCl treatment are: (i) The intensity of the 1262 cm^{-1} peak is increased (ii) with the 1171 cm^{-1} peak growing, another peak appears at 1140 cm^{-1}.

After treating with aq. NH$_3$, the spectrum (Fig. 3.4) substantially returns to the original shape except the additional bands formed at 3445 and 1490 cm^{-1} due to the NH$_4$Cl.

Figure 3.5 shows the IR spectrum of the PANI/SiO$_2$. The absorption peaks of the composite film at 3090, 1629–1558, 1487 and 707 cm^{-1}, are characteristics of the various modes of the

C–H and C–C bonds of the aromatic nuclei. The peaks at 3545, 3395, and 3230 cm^{-1} correspond to the stretching of the N–H bonds; those at 1296 and 1227 cm^{-1} correspond to the stretching of the C–N bonds of the secondary aromatic amines, and the peaks at 1629 cm^{-1} correspond to the stretching of the C=N bonds[81-83]. The region 1151–1071 seems to be the characteristic peak of Si–O bond. The IR spectrum of PANI/SiO$_2$ samples indeed shows several peaks in this region and may indicate the presence of SiO$_2$ into the PANI matrix.

Therefore, the IR spectra of the above studied samples clearly exhibited absorption bands attributable to both the polymers and silica components. It is the worthwhile to mention here that the observed IR spectra are consistent with the previous studies[84-90] and discuss below according to the frequency region:
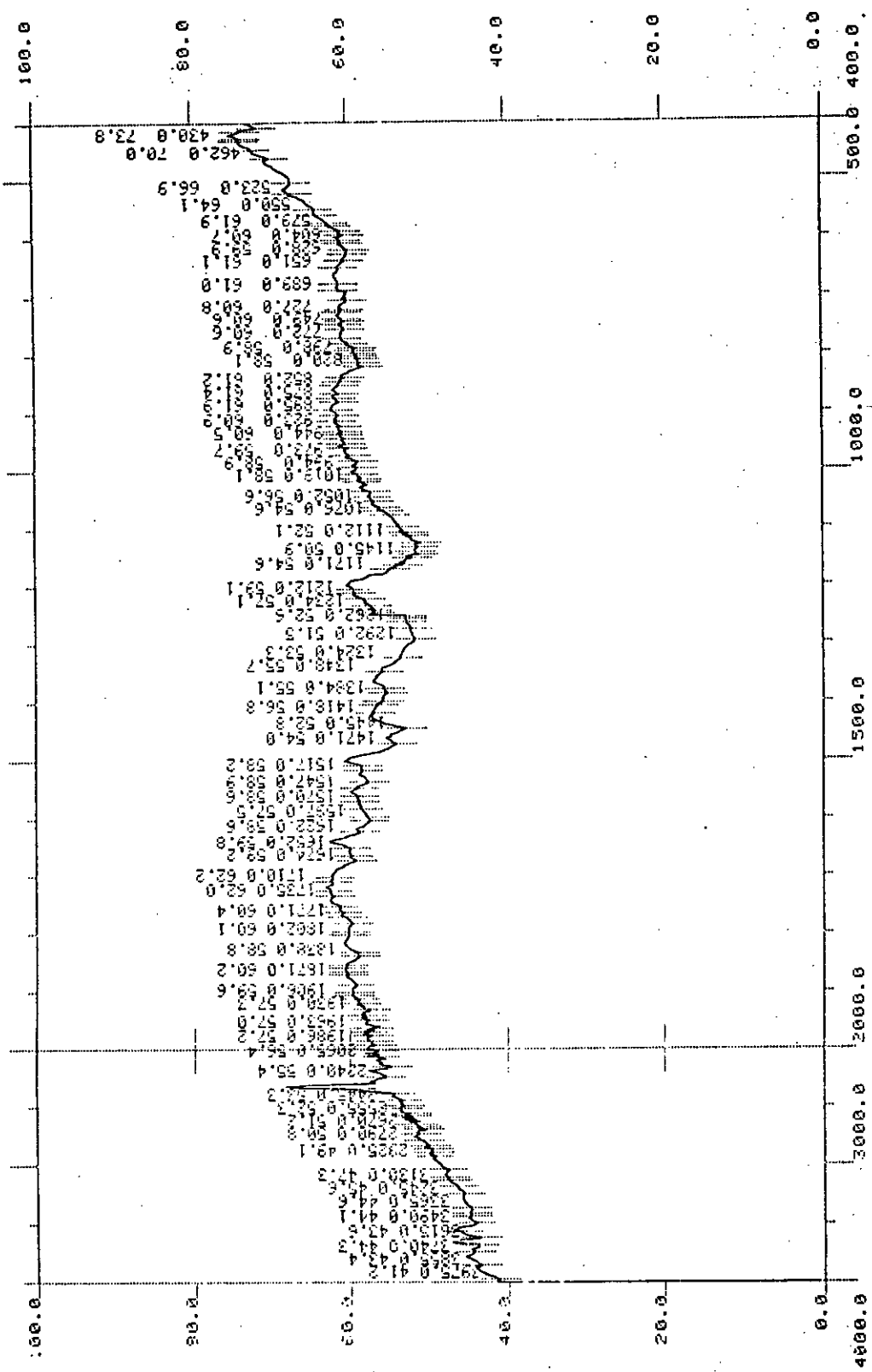
Fig. 3.2: IR spectrum of acidic-PANI.
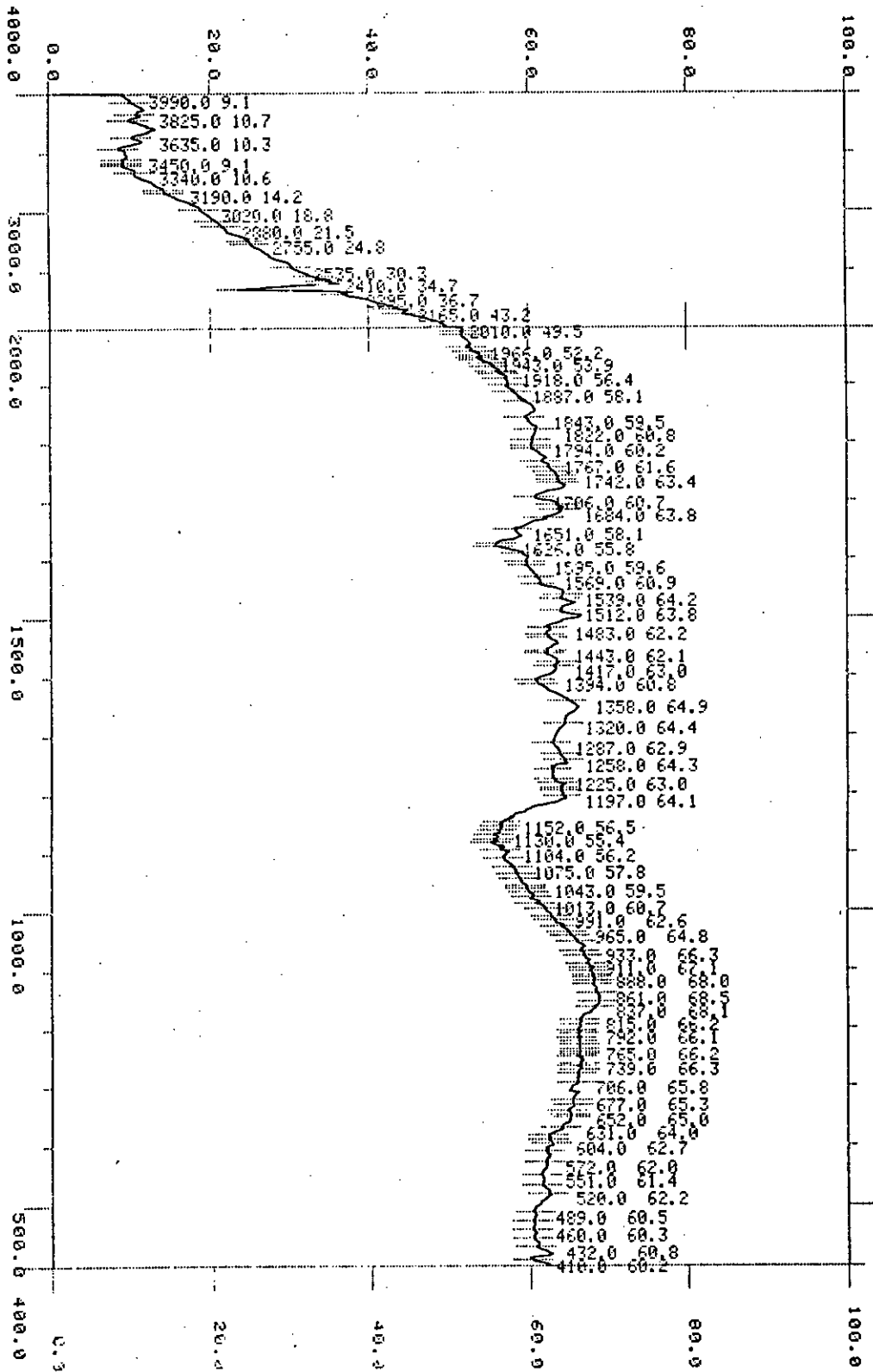
Fig. 3.3: IR spectrum of neutral-PANI.
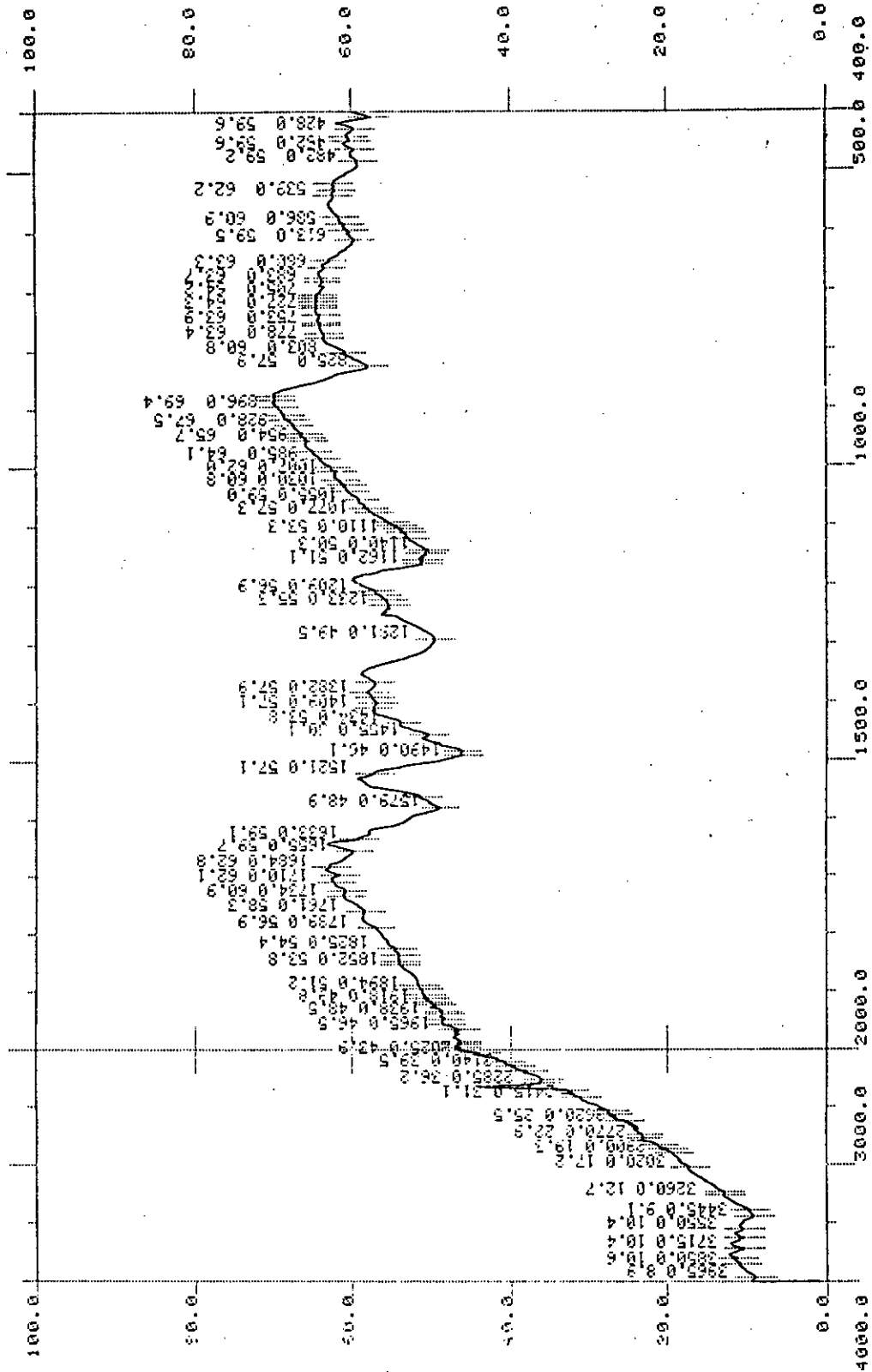
Fig. 3.4: IR spectrum of basic-PANI.
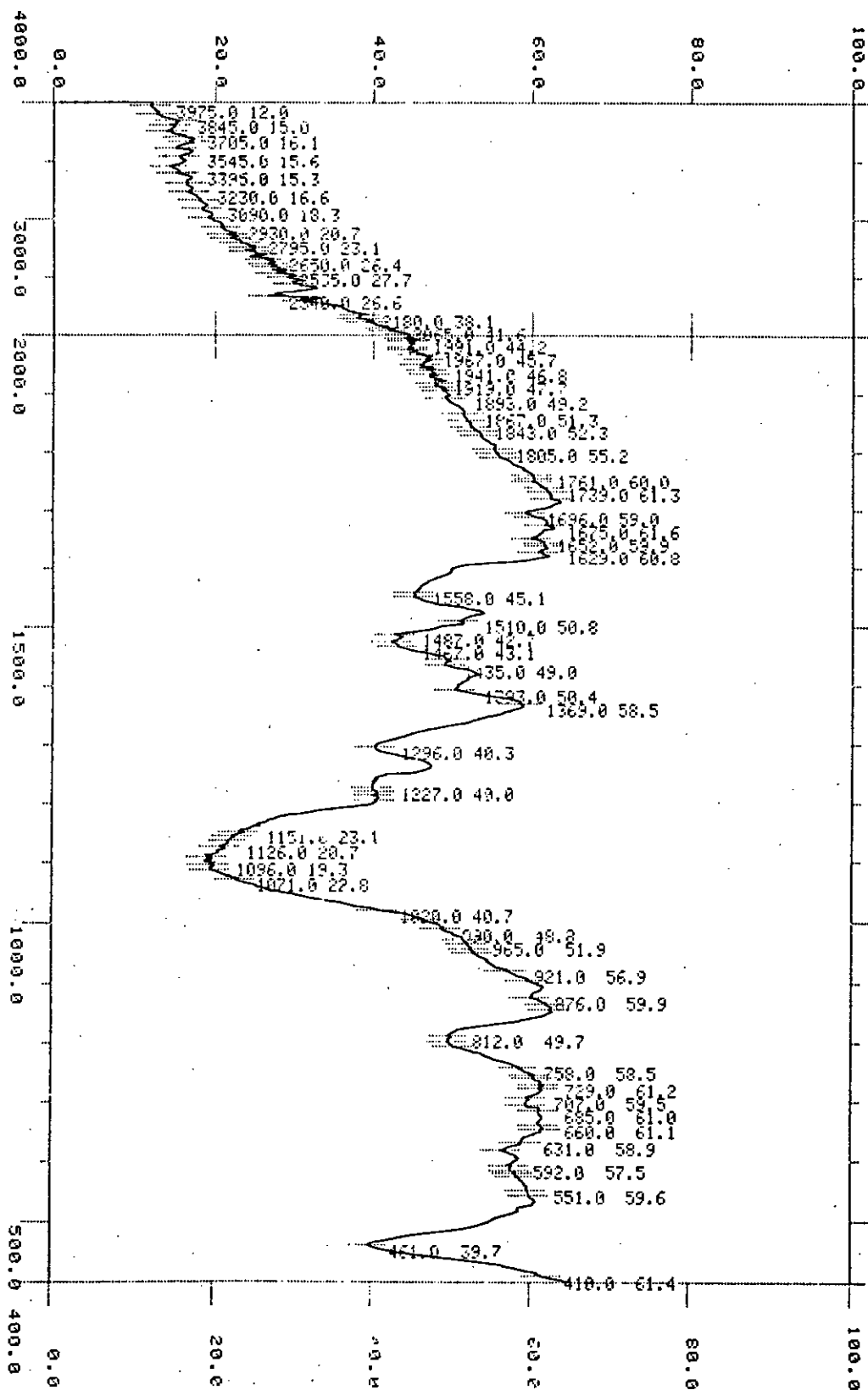
Fig. 3.5 IR spectrum of PANI/SiO₂

(a) 3500-3100 cm^{-1}

This is the N-H stretching region. The absorption of PANI in this region is rather weak. The main absorption peaks are located at 3380 and 3310 cm^{-1}, with shoulders at 3460 and 3170 cm^{-1}. With increasing HCl concentration in the polymerization system, the peak at 3380 cm^{-1} increases and the shoulder at 3170 cm^{-1} decreases.

(b) 3100- 2800 cm^{-1}

This is the C-H stretching region. The absorption of PANI in this region is even weaker, but it is observable at 3050 – 3030 and 2960 – 2850 cm^{-1}. With increase of HCl concentration in the polymerization system, the relative intensity of the 3040 cm^{-1} decreases indicating that the number of H atoms bonded to benzene ring is reduced. This implies that Cl substitution occurs and thus strengthening of the C-Cl stretching band at 810 cm^{-1} occurs.

(c) 1600-1450 cm^{-1}

Aromatic ring breathing, N-H deformation and C=N stretching all give absorption in this region. In general, The N-H deformation band is very weak. A 1, 4- substituted benzene ring may give absorption band at 1600-1580 and 1510-1500 cm^{-1}. However, the former is very weak and even observable if the two substituents are the same and the latter is strong in the IR in this range. Therefore, it is reasonable to assign the band at 1510 cm^{-1} mainly to benzoid ring (B) stretching in PANI. Based on the following arguments, we consider the 1587 cm^{-1} band as a characteristic band of nitrogen quinone (Q).

(d) 1400-1240 cm^{-1}

This is the C-N stretching region for aromatic amines. The intrinsic PANI shows three peaks: medium absorption at 1240 cm^{-1} and weak ones at 1380 and 1240 cm^{-1}. The 1315 cm^{-1} peak is rapidly strengthened by HCl treatment. Here it would be worthy to point out that the reaction mechanism of PANI with HCl may involve the structure $\overset{+}{=}NH$ and $\overset{\bullet +}{-NH}$. The introduction

of the positive charge leads to a great increases in molecular dipolar moment and thus IR activity. This is why all peaks in this region grow obviously during HCl doping or treatment. The band at 1160 and 1140 was referred as "electronic like band" and was considered as a measure of the degree of delocalization of electrons on PANI and thus are the characteristic peaks of PANI conductivity. The band at 1160 and 1140 cm^{-1} be assigned separately: 1160 cm^{-1} to intrinsic structure and 1140 cm^{-1} to the doped (HCl treated) structure. The 1140 cm^{-1} band is a vibrational mode of B-NH = Q or $B\overset{\bullet+}{-}NH-B$ which is formed in doping reactions. This may be attributed to the existence of the positive charge and the distribution of the dihedral angle between the B and Q rings.

(e) 1220-500 cm^{-1}

This is the region of in-plane and out-of-plane bending of C-H bonds on aromatic rings. The main absorption bands for intrinsic PANI are located at 1160 and 830 cm^{-1} and some weak bands can be observed. It is easy to judge the substitution pattern on the benzene ring from the frequencies of these peaks. For example, 1220, 1105, 1010 and 830 cm^{-1} stands for 1,4-substitution, 1115, 1060, 960, 895 and 850 cm^{-1} for 1, 2, 4-substitution and 740 and 690 cm^{-1} for 1,2- or mono-substitution.

In summary, tentative assignment of the IR spectra of PANI and PANI/SiO$_2$ are listed in Table-3.1 and 3.2.

Table-3.1: Tentative assignment of the IR spectra of PANI sample.

Frequency (cm^{-1})	Assignment*
3715	presence of H_2O
3550	NH_2 asym. str.
3445	NH_2 sym. str., NH str
3260	=NH str.
1579	str. of N=Q=N
1521	str. of N–B–N
1455	str. of benzene ring
1382	C–N str. in QB_tQ
1291	C–N str. in QB_cQ, QBB, BBQ
1233	C–N str. in BBB
1162	a mode of N=Q=N
1140	a mode of Q=$\overset{+}{N}$H-B or B-$\overset{+}{N}$H-B
1110	C–H *ip* on 1,4-ring
1076	
1030	C–H *ip* on 1,2,4-ring
985	
954	
928	C–H *op* on 1,2,4-ring
896	
825	C–H *ip* on 1,4-ring
753	C–H *ip* on 1,2-ring
683	
613	aromatic ring deformation
482	
462	

* Abbrevations: asym = asymmetric, sym = symmetric, str = stretching, *ip* = in-plane bending, *op* = out-of-plane bending, Q = quinoid unit, B = benzoid unit, B_t= *trans* benzoid unit, B_c= *cis* benzoid unit.

Table-3.2: Tentative assignment of the IR spectra of PANI/SiO$_2$ sample.

Frequency (cm^{-1})	Assignment*
3705	Presence of H$_2$O
3545	NH$_2$ asym. str.
3395	NH$_2$ sym. str., NH str
3230	=NH str.
1558	str. of N=Q=N
1510	str. of N–B–N
1467	str. of benzene ring
1369	C–N str. in QB$_t$Q
1296	C–N str. in QB$_c$Q, QBB, BBQ
1227	C–N str. in BBB
1151	a mode of N=Q=N
1126	a mode of Q=$\overset{+}{N}$H-B or B-$\overset{+}{N}$H-B
1096	
1071	presence of SiO$_2$
1020	
990	C–H *ip* on 1,2,4-ring
965	
921	
876	C–H *op* on 1,2,4-ring
812	C–H *ip* on 1,4-ring
758	
685	C–H *ip* on 1,2-ring
631	
551	aromatic ring deformation
461	

3.3.2 X- ray diffraction pattern

Structural analysis by X-ray can provide information on the intermolecular arrangement, i.e. the level of crystallinity of a material. Both the PANI and PANI/SiO$_2$ samples prepared chemically were examined for their structural analysis in the powdered state by using wide angle X-ray diffraction. The scattering patterns as function of the Bragg angle, 2θ at $\lambda = 1.54$ A$^\circ$ for the studied substrate powders are presented in Fig. 3.6-3.9.

The results show that the patterns consist of only diffuse x-ray scattering i.e., the peaks appear in the pattern are responsible for the amorphous nature of the sample. It is important to note that the X-ray pattern of the bulk polymer PANI treated at different pH and that of the PANI/SiO$_2$ seems to be indifferent. This observation clearly indicates that silica particles have no influence on the structure even it incorporated to the matrix. Therefore, the diffraction patterns of the PANI/SiO$_2$ are mostly dominated by the response made by the polymer component. Most of the conducting polymers are reported to be extremely poor crystalline[91]. During polymerization, although most of the aniline units are linked through the 1,4-position, a significant unit is coupled through other positions. This introduces defects in the hypothetical ideal linear chain arrangement of the polymer and also causes some cross-linking of the polymer and consequently results in a significant decrease in the crystallographic order of the chains[92, 93]. As a result, the polymer loses its crystallinity and leads diffuse diffraction pattern as exhibited in Fig. 3.6-3.9. Other well-studied conducting polymer PPY, has also been reported to be amorphous in nature[94]. Effort is still paying for achieving the better PANI structure. Indeed, results of few studies have already been appeared and reported to be claimed the crystalline structure of PANI[95, 96].
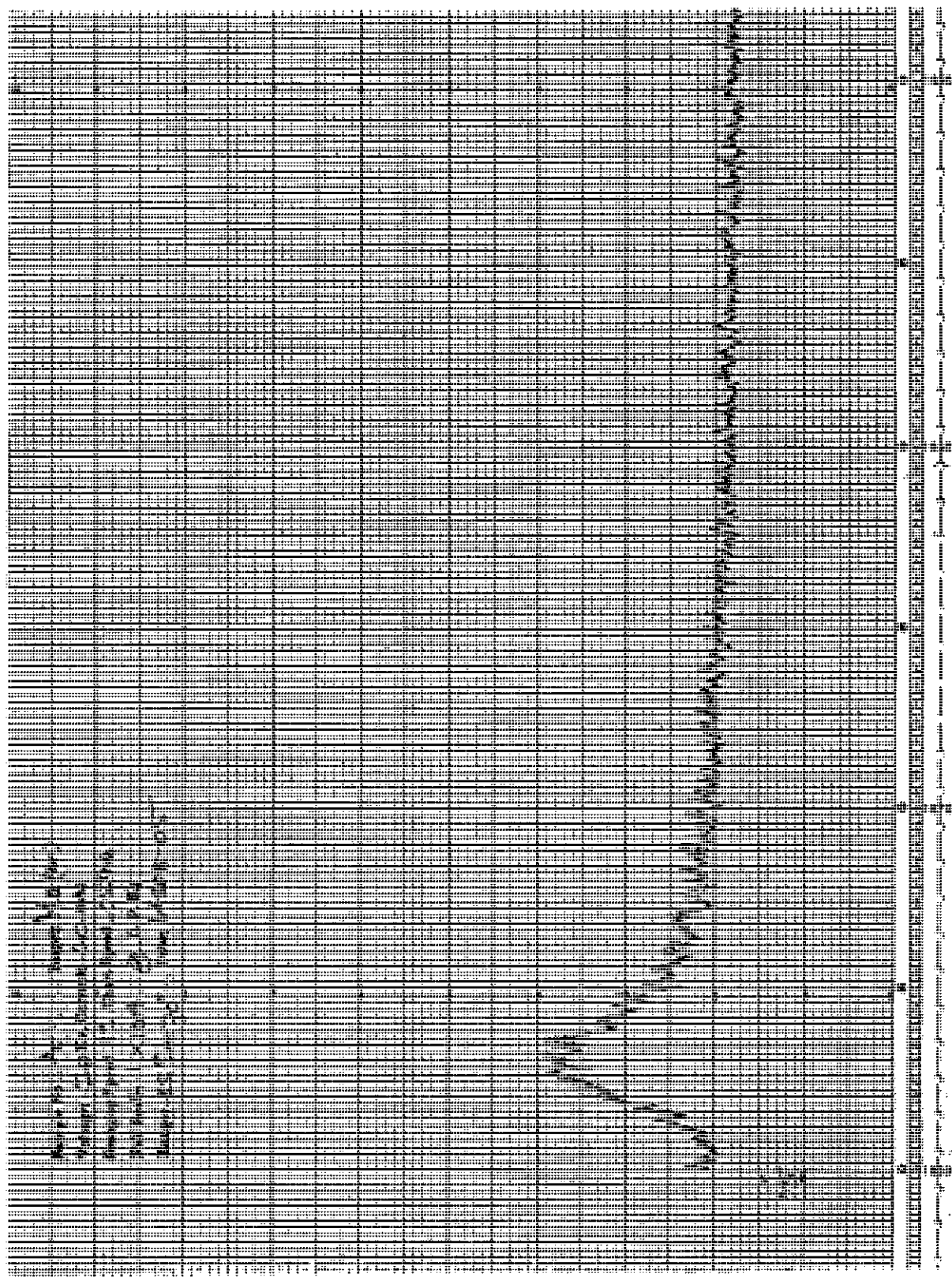
Fig. 3.6: XRD pattern of acidic-PANI.
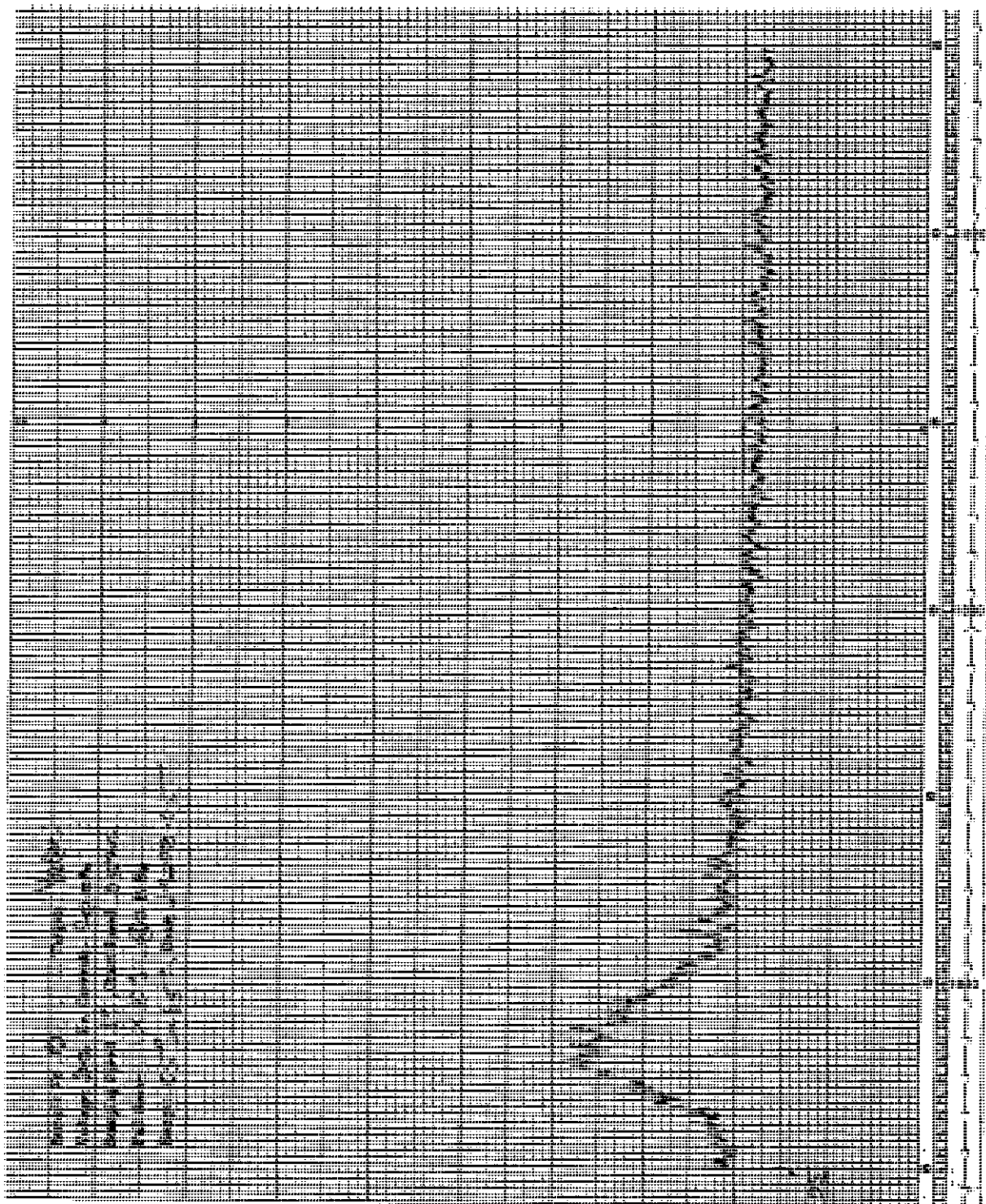
Fig. 3.7: XRD pattern of neutral-PANI
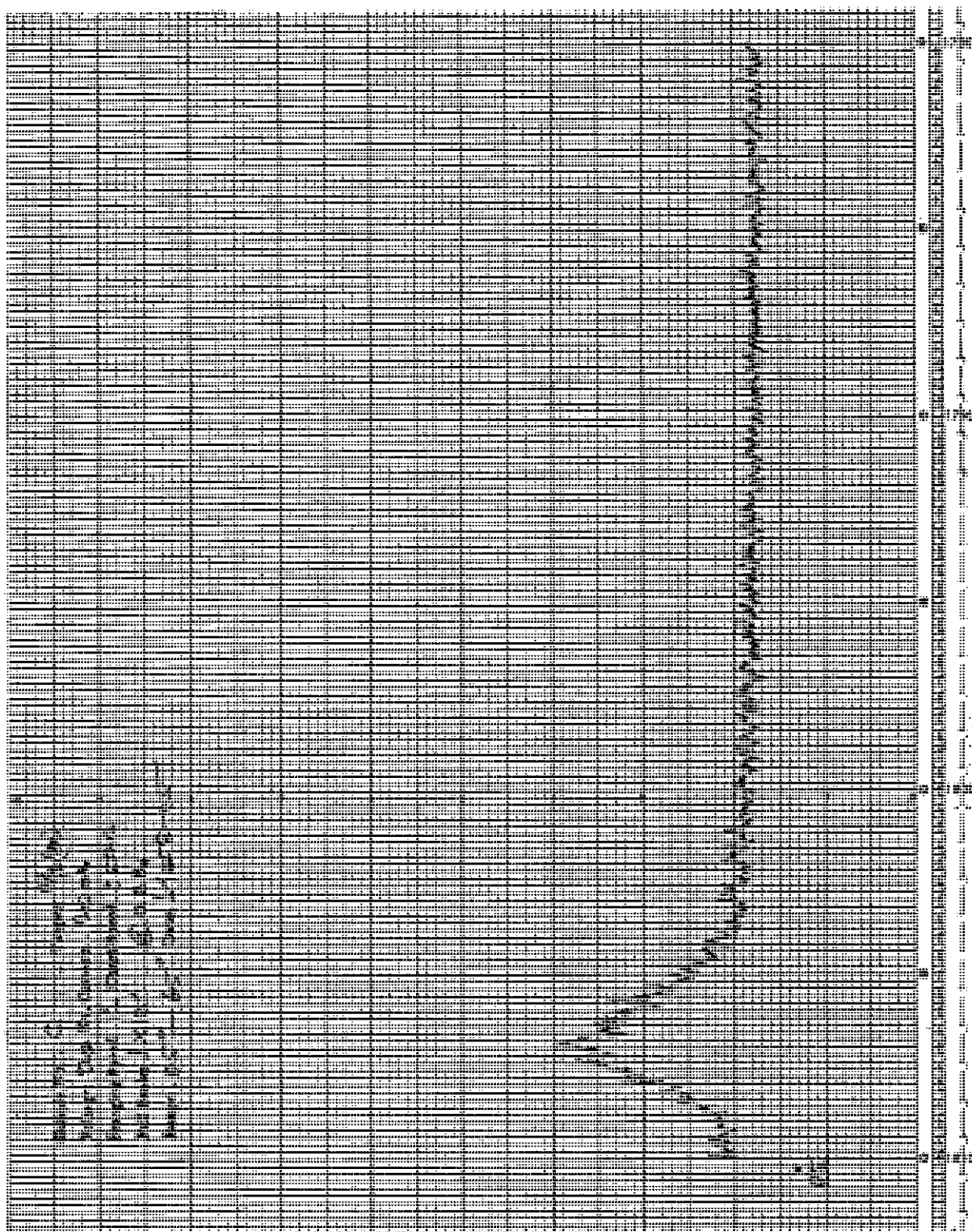
Fig.3.8: XRD pattern of basic-PANI.
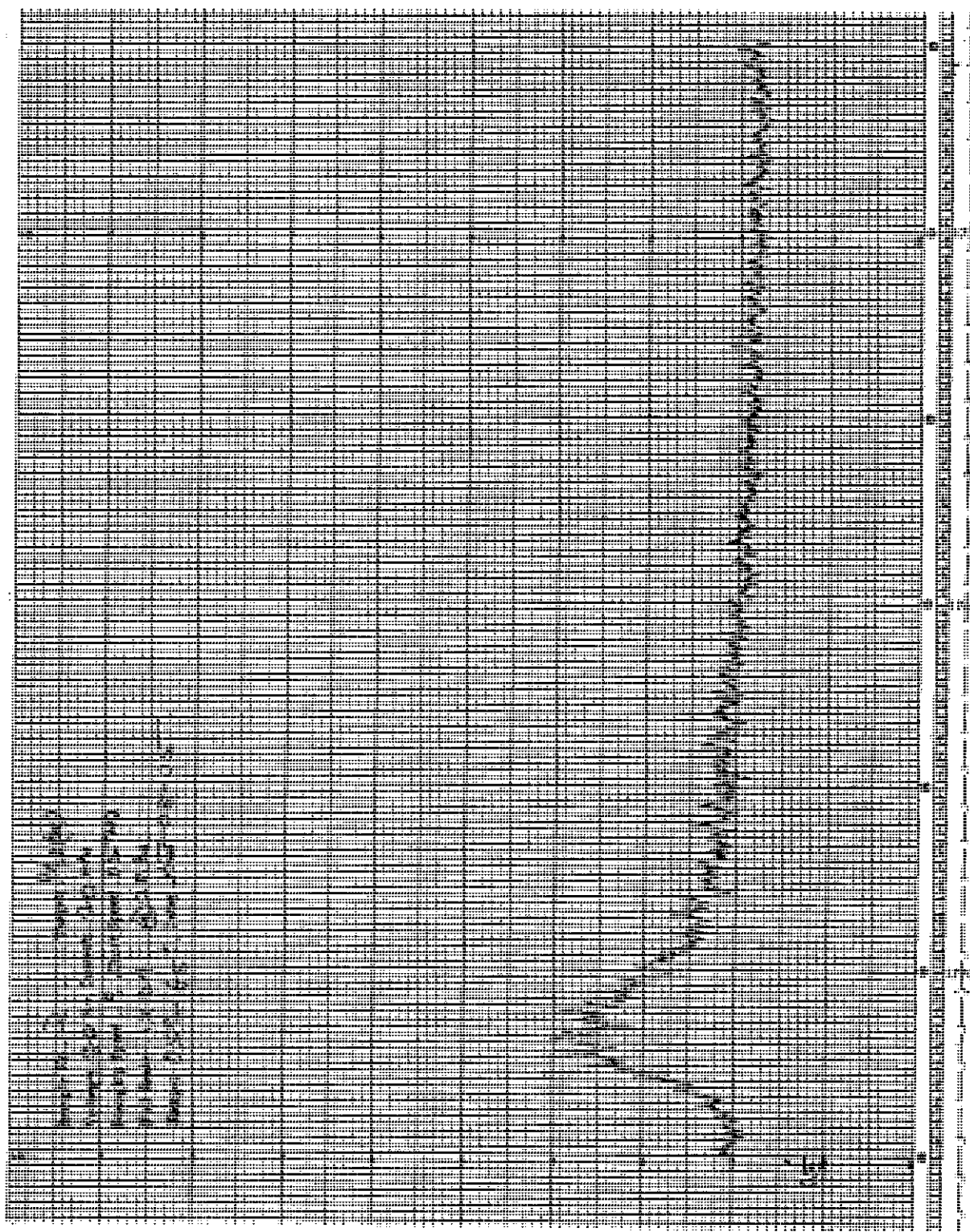
Fig.3.9: XRD pattern of PANI/SiO$_2$.

3.3.3 Surface morphology

Chemical composition and morphological structure of a material strongly depends on the mode of synthesis, be it chemical or electrochemical, on the synthesis conditions such as pH, concentration of reactants and products, chemical nature of oxidant, oxidation potential etc. Thus, there is a variety of possible chemical structure and morphology of a material may possible. Instead of varying the conditions of synthesis, in this study, PANI samples were synthesized under the same condition but a post-treatment of the PANI was made under different condition to examine if any change occurs in its physico- chemical and morphological properties. In order to examine the surface morphology, scanning electron microscopy appears to be the best choice because of its potential for precise analysis of a solid surface. Chemical composition and morphological structure of a material strongly depends on the mode of synthesis, be it chemical or electrochemical, on the synthetic conditions such as pH, concentration of reactants and products, chemical nature of oxidant, oxidation potential etc. Thus, a variety of chemical structure and morphology of a material is possible. Figure 3.10 shows the SEM images of a PANI samples after treated with (1) aqueous HCl (pH = 1.09), (2) distilled water (pH = 6.95), (3) aqueous NH_3 (pH = 10.15), and $PANI/SiO_2$. It can be seen that on treatment, the morphology of the PANI affected considerably. In (1), acid treatment of PANI results in a hierarchy of agglomerates and piled up over the substrate. When the PANI is treated with double distilled water, the aggregates seem to exhibit granular morphology that assembled in a stone like body and distributed non-uniformly over the substrate. On treatment of the PANI with a basic solution, granular morphology of the PANI also results but the grains were collected to a body like coral with sharp edges. The deposit in the stack is tightly packed and seems to form rigid structure and distributed non-uniformly over the substrate. Thus, the present result clearly demonstrates that surface morphology can be controlled by post-synthesis treatment of the PANI with the solution of different pH. When SiO_2 was incorporated in the PANI structure, the resulting $PANI/SiO_2$ matrix shows a body like a broken brick showing, at least few of them, regular size with sharp edges but the most of the portions are powdery. The present SEM observation clearly suggests that the PANI surface is modified; SiO_2 are incorporated in it. Modification of the PANI surfaces is also reported by the various workers[90-91] by varying synthesis condition. From the observed dissimilar morphological features of the

PANI/SiO$_2$ studied in this work, it may be expected that their surface behaviors toward adsorption and specific surface area could be different. The determination of surface area of these substrates will be discussed in the following sections.
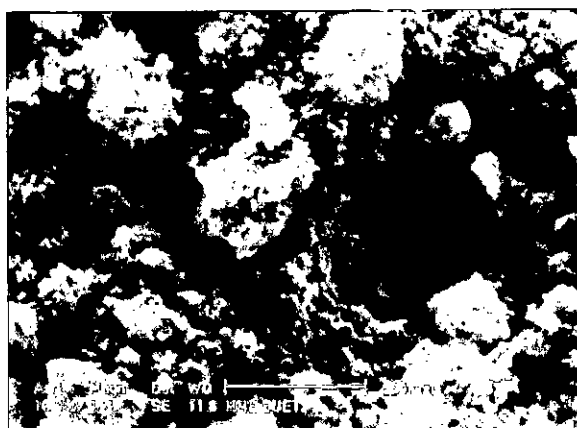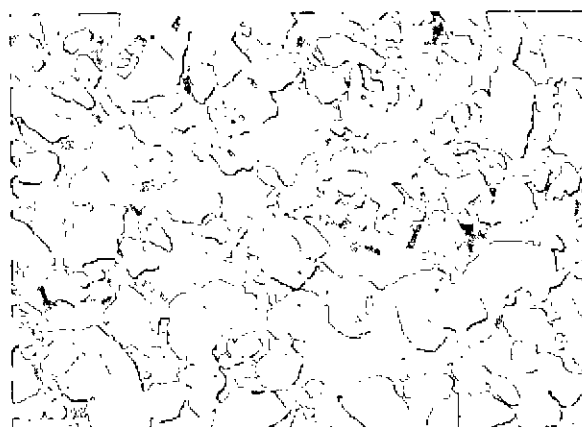
(1)   (2)
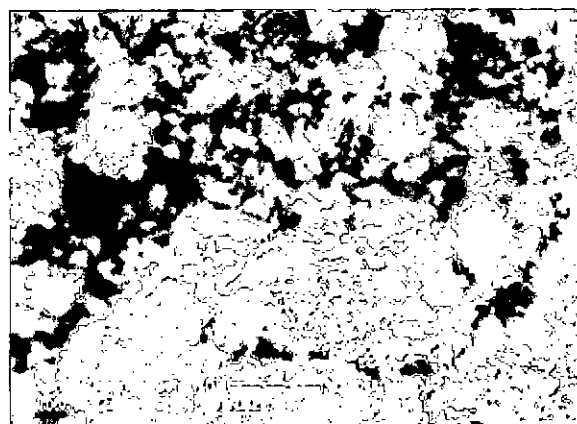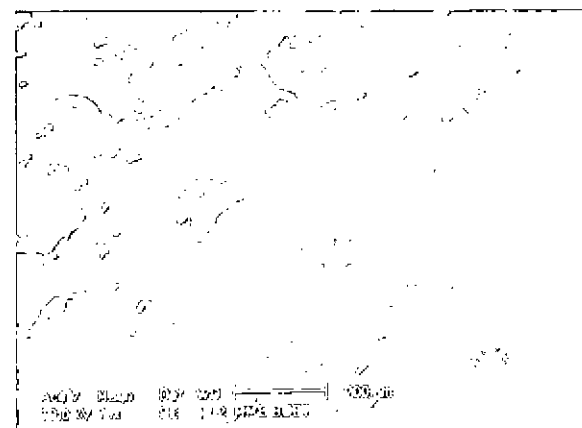
(3)   (4)

Fig. 3.10: SEM micrographs of (1) acidic-PANI, (2) neutral-PANI, (3) basic-PANI and (4) PANI/SiO$_2$.

3.4 Calculation of Monolayer Capacity for Determining Specific Surface Area

For the calculation of monolayer capacity, six different methylene blue (MB) solutions such as 1×10^{-5} M, 2×10^{-5} M, 3×10^{-5} M, 4×10^{-5} M, 5×10^{-5} M, 6×10^{-5} M were used. Each concentration of methylene blue gave equilibrium time at which portion of MB adsorbed become saturated. Then the amount adsorbed (mg g^{-1}) at equilibrium time was calculated from the absorbance data of the original MB solution and that of the remaining MB solution. Finally, the amount adsorbed vs equilibrium concentration curve gave the monolayer coverage. In the determination of specific surface area for the various substrates such as (a) acidic-PANI, (b) neutral-PANI, (c) basic-PANI, and (d) PANI-SiO$_2$, the monolayer coverage thus obtained was used.

Determination of monolayer capacity (χ_m) for acidic-PANI

Table 3.3: The amount of solute adsorbed at equilibrium time and equilibrium concentration from the corresponding absorbance

Initial concentration (M/10^{-5})	Equilibrium time (min.)	Absorbance of the remaining solution at equilibrium time	Amount adsorbed at equilibrium time (mg g^{-1})	Equilibrium concentration (M/10^{-5})
1		0.043	1.80	0.4
2		0.103	3.21	0.9
3	120	0.160	4.51	1.4
4		0.232	5.75	2.0
5		0.290	6.68	2.6
6		0.381	6.95	3.4

Fig.3.11: Determination of monolayer capacity from the adsorption of MB from aqueous solution at equilibrium concentration and equilibrium time

Calculation of specific surface area of acidic-PANI substrate

The specific surface area of acidic-PANI substrate can be calculated using the following equation,

$$S = (\chi_m / M) \times N \times A_m \times 10^{-20}$$

Here,

Monolayer capacity $(\chi_m) = 6.95$ mg g^{-1} $= 6.95 \times 10^{-3}$ g g^{-1}

Molecular mass of MB $(M) = 355.89$ g mol^{-1}

Avogadro constant $(N) = 6.023 \times 10^{23}$ mol^{-1}

(i)   Cross-sectional area of MB $(A_m) = 130$ Å^2 BET with N$_2$

(ii)   Cross-sectional area of MB $(A_m) = 78$ Å^2 BET with Ar

Specific surface area $= S$ (m^2 g^{-1}) $= ?$

(i) $S = (6.95 \times 10^{-3} / 355.89) \times 6.023 \times 10^{23} \times 130 \times 10^{-20}$

$= 15.29 \approx 15$ m^2 g^{-1}

(ii) $S = (6.95 \times 10^{-3} / 355.89) \times 6.023 \times 10^{23} \times 78 \times 10^{-20}$

$= 9.17 \approx 9$ m^2 g^{-1}

Determination of monolayer capacity (χ_m) for neutral-PANI

Table 3.4: The amount of solute adsorbed at equilibrium time and equilibrium concentration from the corresponding absorbance

Initial concentration $(M/10^{-5})$	Equilibrium time (min.)	Absorbance of the remaining solution at equilibrium time	Amount adsorbed at equilibrium time $(mg\ g^{-1})$	Equilibrium concentration $(M/10^{-5})$
1		0.041	1.80	0.4
2		0.113	2.67	1.1
3	120	0.169	3.47	1.8
4		0.232	4.14	2.5
5		0.302	4.80	3.2
6		0.392	4.95	4.1

Fig.3.12: Determination of monolayer capacity from the adsorption of MB from aqueous solution at equilibrium concentration and equilibrium time

Calculation of specific surface area of neutral-PANI substrate

The specific surface area of neutral-PANI substrate can be calculated using the following equation,

$$S = (\chi_m / M) \times N \times A_m \times 10^{-20}$$

Here,

Monolayer capacity (χ_m) = 4.95 mg g^{-1} = 4.95 × 10^{-3} g g^{-1}

Molecular mass of MB (M) = 355.89 g mol^{-1}

Avogadro constant (N) = 6.023 × 10^{23} mol^{-1}

(iii)   Cross-sectional area of MB (A_m) = 130 Å^2 BET with N$_2$

(iv)   Cross-sectional area of MB (A_m) = 78 Å^2 BET with Ar

Specific surface area = S (m^2 g^{-1}) = ?

(i)   S = (4.95 × 10^{-3} / 355.89) × 6.023 × 10^{23} × 130 × 10^{-20}

       = 10.89 ≈ 11 m^2 g^{-1}

(ii)   S = (4.95 × 10^{-3} / 355.89) × 6.023 × 10^{23} × 78 × 10^{-20}

       = 6.53 ≈ 7 m^2 g^{-1}

Determination of monolayer capacity (χ_m) for basic-PANI

Table 3.5: The amount of solute adsorbed at equilibrium time and equilibrium
concentration from the corresponding absorbance

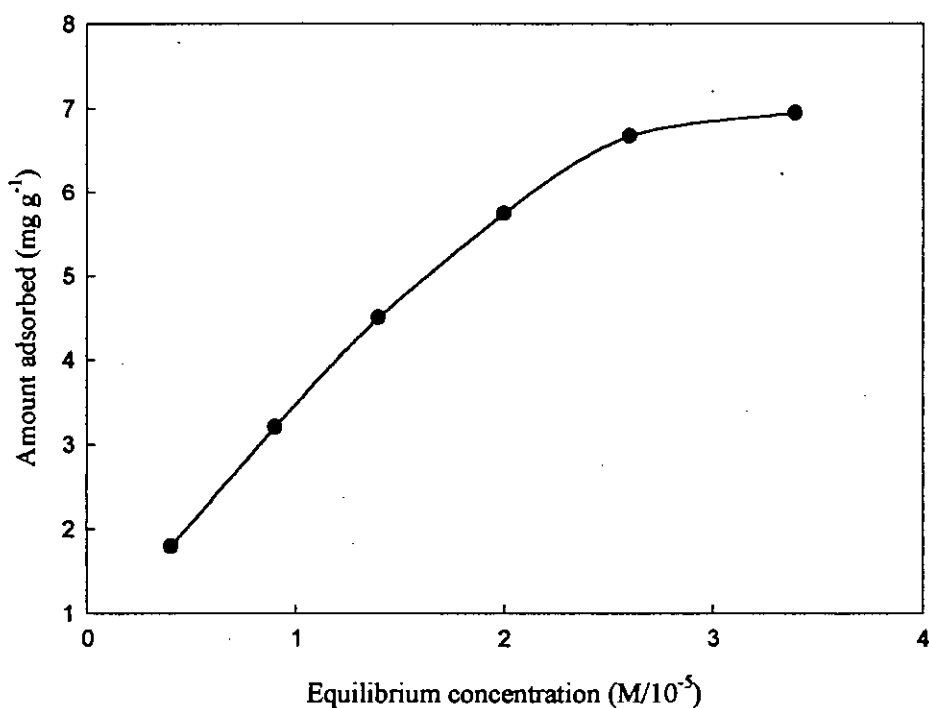| Initial concentration $(M/10^{-5})$	Equilibrium time (min.)	Absorbance of the remaining solution at equilibrium time	Amount adsorbed at equilibrium time $(mg\ g^{-1})$	Equilibrium concentration $(M/10^{-5})$
1		0.020	2.67	0.10
2		0.025	5.08	0.20
3	120	0.048	7.22	0.40
4		0.061	9.50	0.55
5		0.103	11.80	0.85
6		0.140	12.90	1.25

Fig.3.13: Determination of monolayer capacity from the adsorption of MB from aqueous
solution at equilibrium concentration and equilibrium time

Calculation of specific surface area of basic-PANI substrate

The specific surface area of basic-PANI substrate can be calculated using the following equation,

$$S = (\chi_m / M) \times N \times A_m \times 10^{-20}$$

Here,

Monolayer capacity $(\chi_m) = 13.0$ mg g^{-1} $= 13.0 \times 10^{-3}$ g g^{-1}

Molecular mass of MB $(M) = 355.89$ g mol^{-1}

Avogadro constant $(N) = 6.023 \times 10^{23}$ mol^{-1}

(v)　　Cross-sectional area of MB $(A_m) = 130$ Å^2 BET with N_2

(vi)　　Cross-sectional area of MB $(A_m) = 78$ Å^2 BET with Ar

Specific surface area $= S$ (m^2 g^{-1}) $= ?$

(i)　　S $= (13.0 \times 10^{-3} / 355.89) \times 6.023 \times 10^{23} \times 130 \times 10^{-20}$

$= 28.6 \approx 29$ m^2 g^{-1}

(ii)　　S $= (13.0 \times 10^{-3} / 355.89) \times 6.023 \times 10^{23} \times 78 \times 10^{-20}$

$= 17.16 \approx 17$ m^2 g^{-1}

Determination of monolayer capacity (χ_m) for acidic-PANI/SiO$_2$

Table 3.6: The amount of solute adsorbed at equilibrium time and equilibrium concentration from the corresponding absorbance

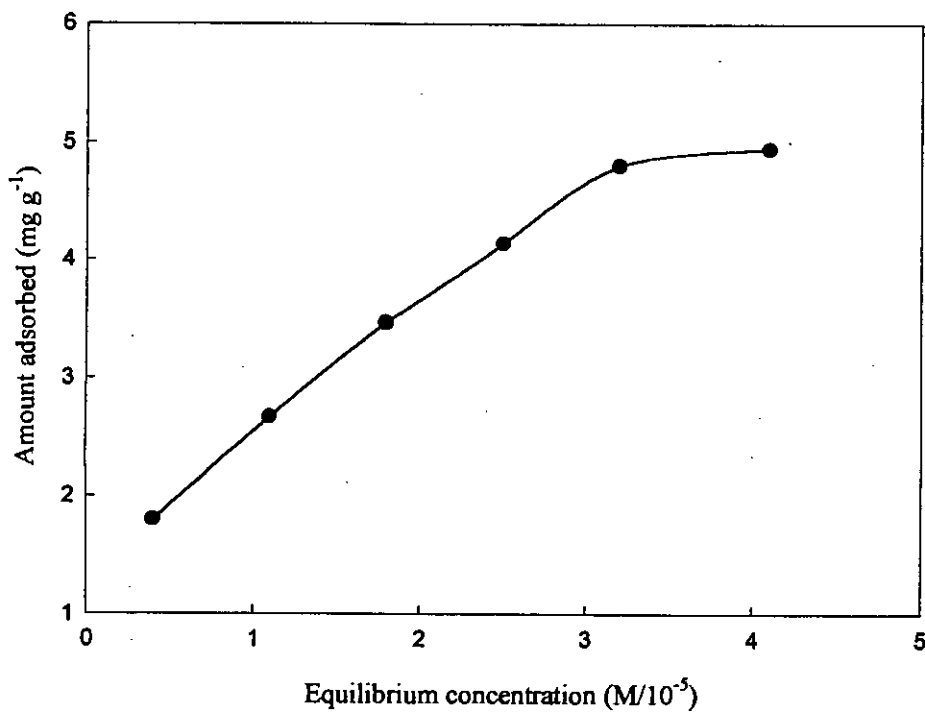| Initial concentration (M/10^{-5})	Equilibrium time (min.)	Absorbance of the remaining solution at equilibrium time	Amount adsorbed at equilibrium time (mg g^{-1})	Equilibrium concentration (M/10^{-5})
1		0.021	2.40	0.20
2		0.053	4.28	0.50
3	120	0.095	6.02	0.85
4		0.149	7.60	1.30
5		0.204	8.83	1.80
6		0.293	9.09	2.60

Fig.3.14: Determination of monolayer capacity from the adsorption of MB from aqueous solution at equilibrium concentration and equilibrium time

Calculation of specific surface area of acidic-PANI/SiO$_2$ substrate

The specific surface area of acidic-PANI/SiO$_2$ substrate can be calculated using the following equation,

$$S = (\chi_m \,/\, M\,) \times N \times A_m \times 10^{-20}$$

Here,

Monolayer capacity (χ_m) $= 9.0$ mg g^{-1} $= 9.0 \times 10^{-3}$ g g^{-1}

Molecular mass of M MB (**M**) $= 355.89$ g mol^{-1}

Avogadro constant (**N**) $= 6.023 \times 10^{23}$ mol^{-1}

(vii)   Cross-sectional area of MB (**A$_m$**) $= 130$ Å^2 BET with N$_2$

(viii)   Cross-sectional area of MB (**A$_m$**) $= 78$ Å^2 BET with Ar

Specific surface area $= S$ (m^2 g^{-1}) $= ?$

(i) $S = (9.5 \times 10^{-3} \,/\, 355.89\,) \times 6.023 \times 10^{23} \times 130 \times 10^{-20}$

$= 20.9 \approx 21$ m^2 g^{-1}

(ii) $S = (9.5 \times 10^{-3} \,/\, 355.89\,) \times 6.023 \times 10^{23} \times 78 \times 10^{-20}$

$= 12.54 \approx 13$ m^2 g^{-1}

Determination of monolayer capacity (χ_m) for neutral-PANI/SiO$_2$

Table 3.7: The amount of solute adsorbed at equilibrium time and equilibrium
concentration from the corresponding absorbance

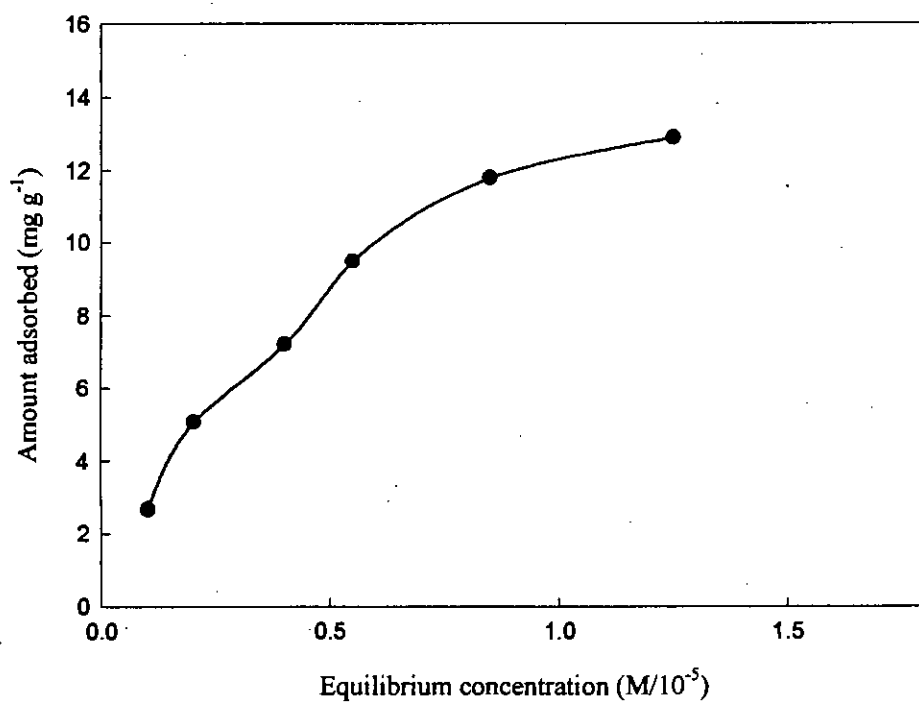| Initial concentration (M/10^{-5})	Equilibrium time (min.)	Absorbance of the remaining solution at equilibrium time	Amount adsorbed at equilibrium time (mg g^{-1})	Equilibrium concentration (M/10^{-5})
1		0.022	2.27	0.25
2		0.058	4.01	0.60
3	120	0.089	5.75	0.95
4		0.143	6.95	1.45
5		0.198	7.76	2.10
6		0.280	8.02	3.00
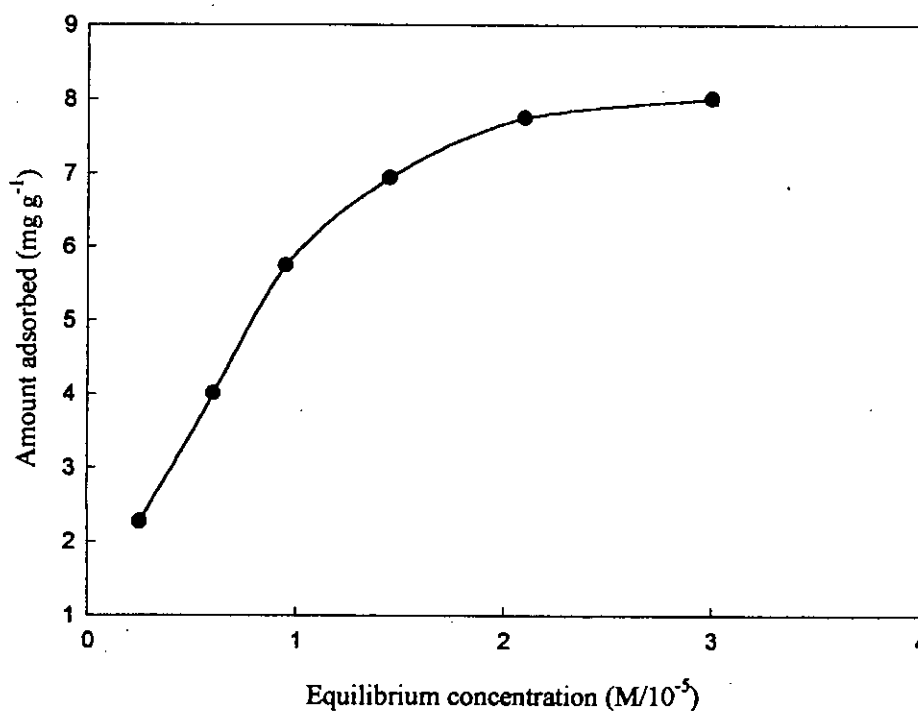
Fig.3.15: Determination of monolayer capacity from the adsorption of MB from aqueous
solution at equilibrium concentration and equilibrium time

Calculation of specific surface area of neutral-PANI/SiO₂ substrate

The specific surface area of neutral-PANI/SiO$_2$ substrate can be calculated using the following equation,

$$S = (\chi_m / M) \times N \times A_m \times 10^{-20}$$

Here,

Monolayer capacity $(\chi_m) = 8.0$ mg g^{-1} $= 8.0 \times 10^{-3}$ g g^{-1}

Molecular mass of MB $(M) = 355.89$ g mol^{-1}

Avogadro constant $(N) = 6.023 \times 10^{23}$ mol^{-1}

(ix)   Cross-sectional area of MB $(A_m) = 130$ Å^2 BET with N$_2$

(x)   Cross-sectional area of MB $(A_m) = 78$ Å^2 BET with Ar

Specific surface area $= S$ (m^2 g^{-1}) $= ?$

(i) $S = (8.0 \times 10^{-3} / 355.89) \times 6.023 \times 10^{23} \times 130 \times 10^{-20}$

   $= 17.6 \approx 18$ m^2 g^{-1}

(ii) $S = (8.0 \times 10^{-3} / 355.89) \times 6.023 \times 10^{23} \times 78 \times 10^{-20}$

   $= 10.56 \approx 11$ m^2 g^{-1}

Determination of monolayer capacity (χ_m) for basic-PANI/SiO$_2$

Table 3.8: The amount of solute adsorbed at equilibrium time and equilibrium concentration from the corresponding absorbance

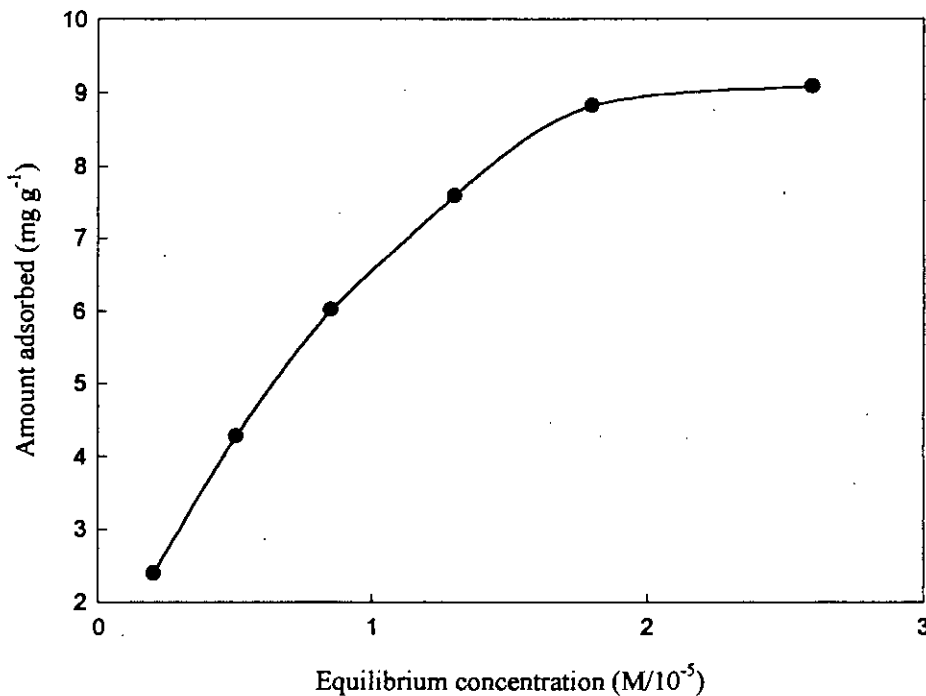| Initial concentration (M/10^{-5})	Equilibrium time (min.)	Absorbance of the remaining solution at equilibrium time	Amount adsorbed at equilibrium time (mg g^{-1})	Equilibrium concentration (M/10^{-5})
1		0.002	2.60	0.02
2		0.010	5.22	0.05
3	120	0.018	7.79	0.09
4		0.020	10.30	0.15
5		0.031	12.80	0.21
6		0.058	14.70	0.50
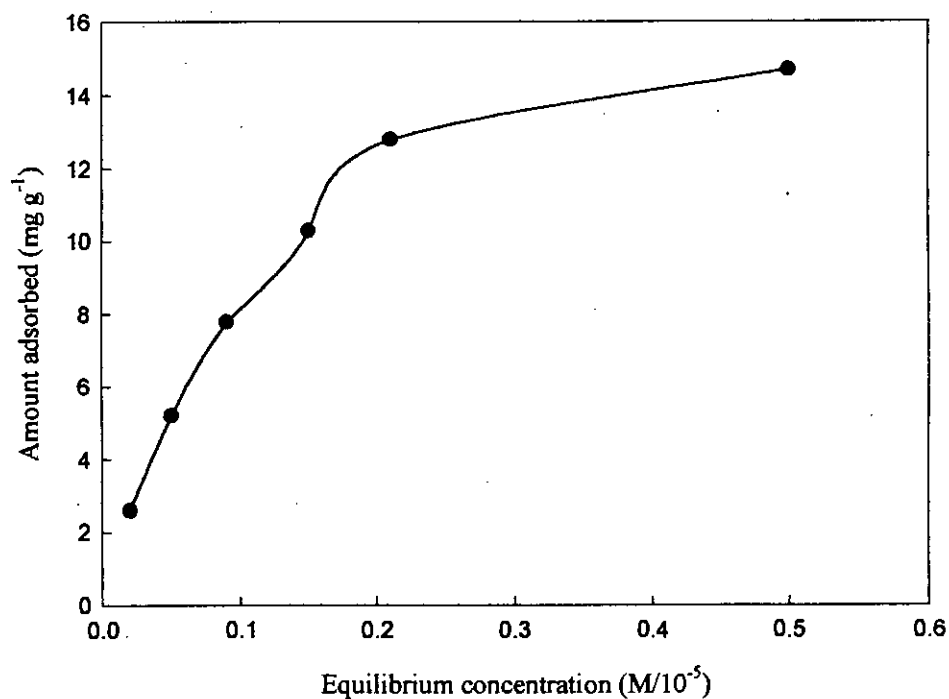
Fig.3.16: Determination of monolayer capacity from the adsorption of MB from aqueous solution at equilibrium concentration and equilibrium time

Calculation of specific surface area of acidic-PANI substrate

The specific surface area of acidic-PANI substrate can be calculated using the following equation,

$$S = (\chi_m / M) \times N \times A_m \times 10^{-20}$$

Here,

Monolayer capacity $(\chi_m) = 15.0$ mg g^{-1} $= 15.0 \times 10^{-3}$ g g^{-1}

Molecular mass of MB (M) $= 355.89$ g mol^{-1}

Avogadro constant (N) $= 6.023 \times 10^{23}$ mol^{-1}

(xi) Cross-sectional area of MB $(A_m) = 130$ Å^2 BET with N$_2$

(xii) Cross-sectional area of MB $(A_m) = 78$ Å^2 BET with Ar

Specific surface area $= S$ (m^2 g^{-1}) $= ?$

(i) $S = (15.0 \times 10^{-3} / 355.89) \times 6.023 \times 10^{23} \times 130 \times 10^{-20}$

$= 33.0$ m^2 g^{-1}

(ii) $S = (15.0 \times 10^{-3} / 355.89) \times 6.023 \times 10^{23} \times 78 \times 10^{-20}$

$= 19.8 \approx 20$ m^2 g^{-1}

3.5 Comparison of Specific Surface Area of Substrates

The variation in surface area of different substrates is listed in table 3.9 using the two different A_m values.

Table 3.9: Comparison of specific surface area of PANI and PANI/SiO$_2$ at different pH values

Substrate	Calculated values of monolayer coverage, χ_m (mg g^{-1})	Calculated surface area (m^2 g^{-1})	
		$A_m = 130\ \text{Å}^2$	$A_m = 78\ \text{Å}^2$
Acidic-PANI	6.95	15	9
Neutral-PANI	4.95	11	7
Basic-PANI	13.0	29	17
Acidic-PANI/SiO$_2$	9.5	21	13
Neutral-PANI/SiO$_2$	8.0	18	11
Basic-PANI/SiO$_2$	15.0	33	20

3.6 Adsorption Capacity: Calculation of Adsorption Coefficient, K_L

To investigate the adsorption capacities of the ionic dye onto the PANI and PANI/SiO$_2$ matrices, the isotherms for the adsorption processes were studied. The adsorption data were analyzed using the following linearized equation for the Langmuir adsorption isotherms:

$$\frac{C_e}{(x/m)} = \frac{1}{K_L k_L} + \frac{C_e}{k_L}$$

where, C_e is the concentration of the dye (MB) after attaining the adsorption equilibrium on the PANI and PANI/SiO$_2$ matrices, x is the mass (in grams) of dye adsorbed onto m g of substrate, k_L is the proportionality constant and K_L is the adsorption coefficient that should indicate the affinity of the dye to the adsorbents[97].

The adsorption coefficient, K_L can be evaluated from the plot of $C_e/(x/m)$ vs C_e using the slope and the intercepts of the plots. The plots are shown in Fig.3.17-3.22 for different substrates.

3.6.1 Calculation of Adsorption Coefficient, K_L for the acidic-PANI Substrate

Table 3.10: Data for the evaluation of adsorption coefficient, K_L for acidic-PANI

Initial concentration (M)/10^{-5}	Equilibrium concentration, C_e (M)/10^{-5}	Amount adsorbed at equilibrium time, (x/m) (g g^{-1})/10^{-3}	C_e / (x/m) (M)/10^{-2}	Adsorption Coefficient, K_L (L mol^{-1})
1	0.4	1.80	0.22	
2	0.9	3.21	0.28	
3	1.4	4.51	0.31	0.502×10^5
4	2.0	5.75	0.35	
5	2.6	6.68	0.39	
6	3.4	6.95	0.49	
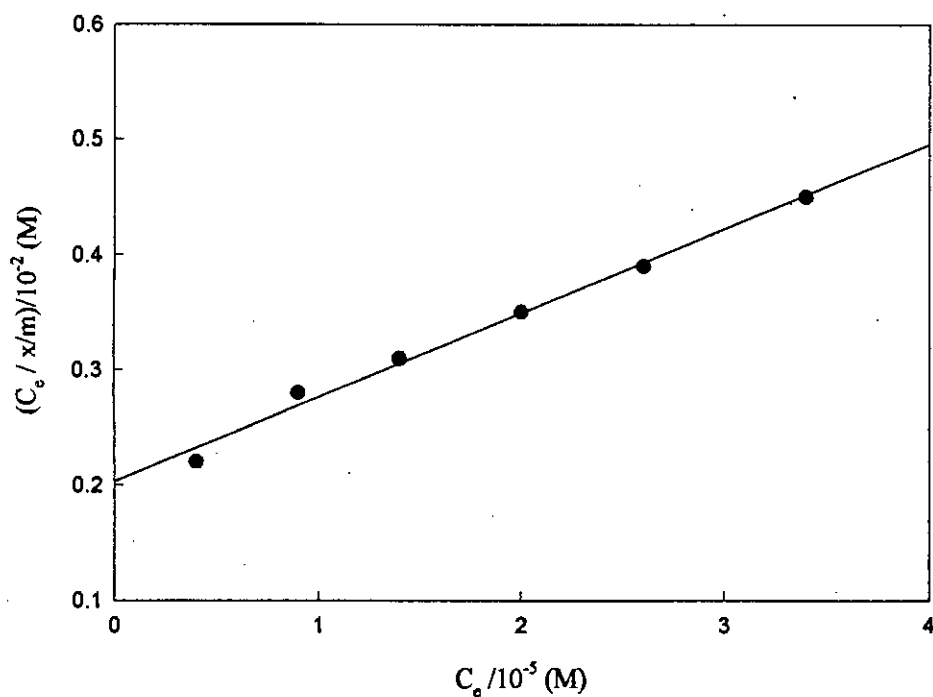
Fig. 3.17: Langmuir plot for acidic-PANI to calculate the adsorption coefficient, K_L

3.6.2 Calculation of Adsorption Coefficient, K_L for the neutral-PANI Substrate

Table 3.11: Data for the evaluation of adsorption coefficient, K_L for neutral-PANI

Initial concentration (M)/10^{-5}	Equilibrium concentration, C_e (M)/10^{-5}	Amount adsorbed at equilibrium time, (x/m) (g g^{-1})/10^{-3}	C_e / (x/m) (M)/10^{-2}	Adsorption Coefficient, K_L (L mol^{-1})
1	0.4	1.80	0.22	
2	1.1	2.67	0.41	
3	1.8	3.47	0.52	0.49×10^5
4	2.5	4.14	0.60	
5	3.2	4.80	0.67	
6	4.1	4.95	0.83	

Fig. 3.18: Langmuir plot for neutral-PANI to calculate the adsorption coefficient, K_L

3.6.3 Calculation of Adsorption Coefficient, K_L for the basic-PANI Substrate

Table 3.12: Data for the evaluation of adsorption coefficient, K_L for basic-PANI

Initial concentration (M)/10^{-5}	Equilibrium concentration, C_e (M)/10^{-5}	Amount adsorbed at equilibrium time, (x/m) $(g\ g^{-1})/10^{-3}$	C_e / (x/m) (M)/10^{-2}	Adsorption Coefficient, K_L (L mol^{-1})
1	0.10	2.67	0.037	
2	0.20	5.08	0.040	
3	0.40	7.22	0.055	1.39×10^5
4	0.55	9.50	0.058	
5	0.85	11.80	0.072	
6	1.25	12.90	0.097	

Fig. 3.19: Langmuir plot for basic-PANI to calculate the adsorption coefficient, K_L

3.6.4 Calculation of Adsorption Coefficient, K_L for the acidic-PANI/SiO$_2$ Substrate

Table 3.13: Data for the evaluation of adsorption coefficient, K_L for acidic-PANI/SiO$_2$

Initial concentration (M)/10^{-5}	Equilibrium concentration, C_e (M)/10^{-5}	Amount adsorbed at equilibrium time, (x/m) (g g^{-1})/10^{-3}	C_e / (x/m) (M)/10^{-2}	Adsorption Coefficient, K_L (L mol^{-1})
1	0.20	2.40	0.08	
2	0.50	4.28	0.12	
3	0.85	6.02	0.14	1.07×10^5
4	1.30	7.60	0.17	
5	1.80	8.83	0.20	
6	2.60	9.09	0.29	
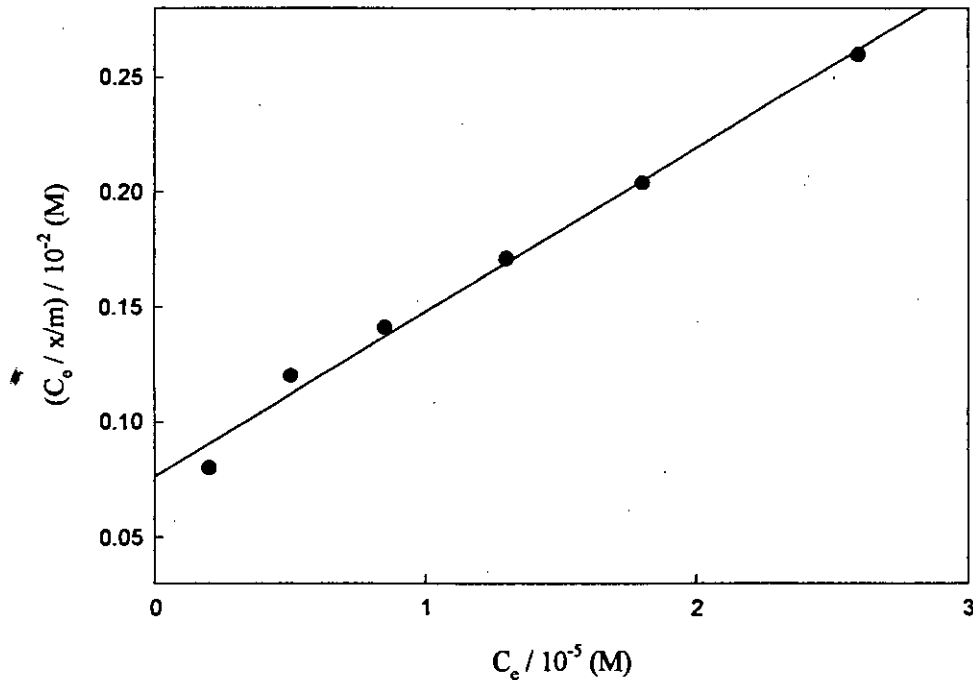
Fig. 3.20: Langmuir plot for acidic-PANI/SiO$_2$ to calculate the adsorption coefficient, K_L

3.6.5 Calculation of Adsorption Coefficient, K_L for the neutral-PANI/SiO$_2$ Substrate

Table 3.14: Data for the evaluation of adsorption coefficient, K_L for neutral-PANI/SiO$_2$

Initial concentration (M)/10^{-5}	Equilibrium concentration, C_e (M)/10^{-5}	Amount adsorbed at equilibrium time, (x/m) (g g^{-1})/10^{-3}	C_e / (x/m) (M)/10^{-2}	Adsorption Coefficient, K_L (L mol^{-1})
1	0.25	2.27	0.11	
2	0.60	4.01	0.15	
3	0.95	5.75	0.17	0.98×10^5
4	1.45	6.95	0.21	
5	2.10	7.76	0.27	
6	3.00	8.02	0.37	
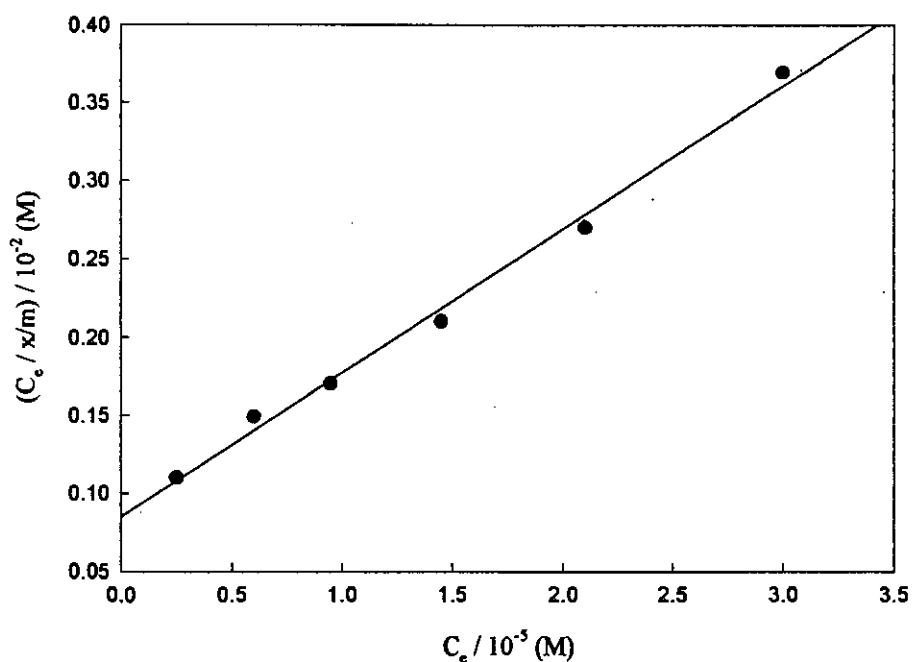
Fig. 3.21: Langmuir plot for neutral-PANI/SiO$_2$ to calculate the adsorption coefficient, K_L
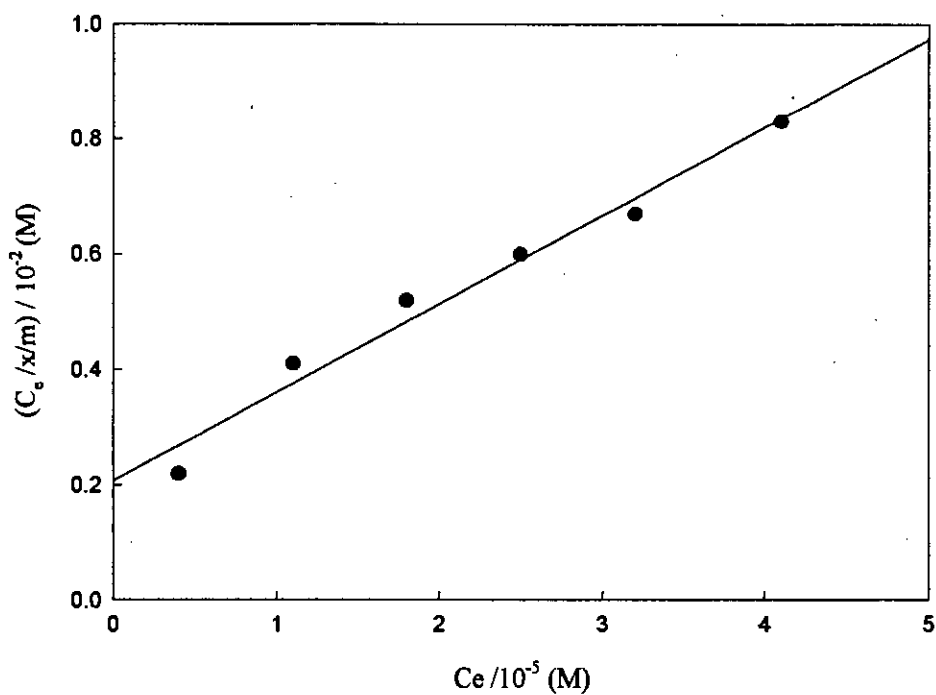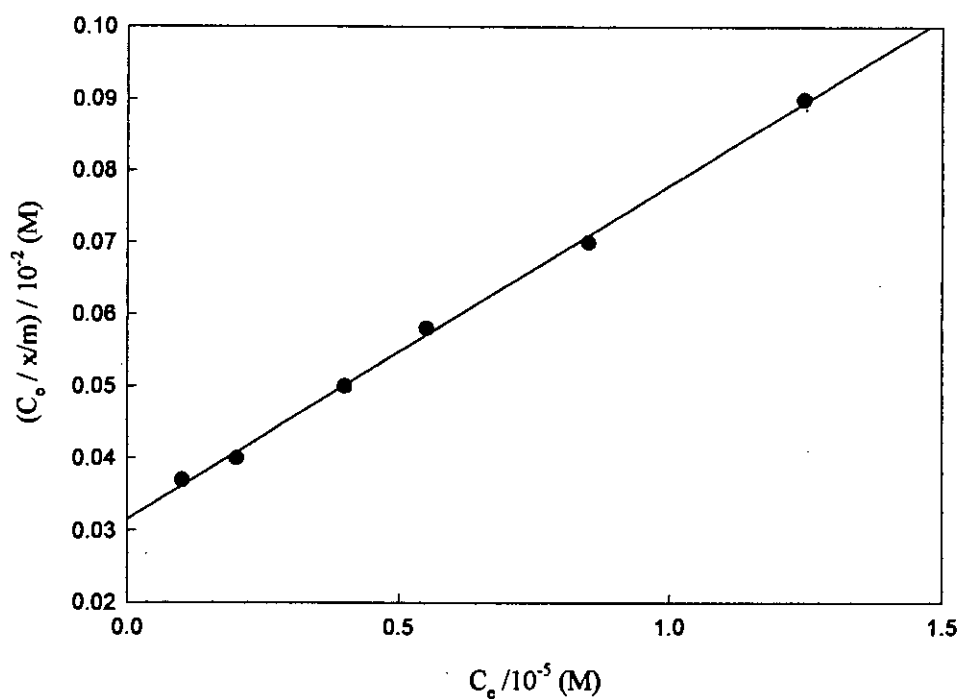
3.6.6 Calculation of Adsorption Coefficient, K_L for the basic-PANI/SiO₂ Substrate

Table 3.15: Data for the evaluation of adsorption coefficient, K_L for basic-PANI/SiO₂

Initial concentration (M)/10^{-5}	Equilibrium concentration, C_e (M)/10^{-5}	Amount adsorbed at equilibrium time, (x/m) (g g^{-1})/10^{-3}	C_e / (x/m) (M)/10^{-2}	Adsorption Coefficient, K_L (L mol^{-1})
1	0.02	2.60	0.76	
2	0.05	5.22	0.96	
3	0.09	7.79	1.15	5.3×10^5
4	0.15	10.3	1.45	
5	0.21	12.8	1.64	
6	0.50	14.7	3.40	
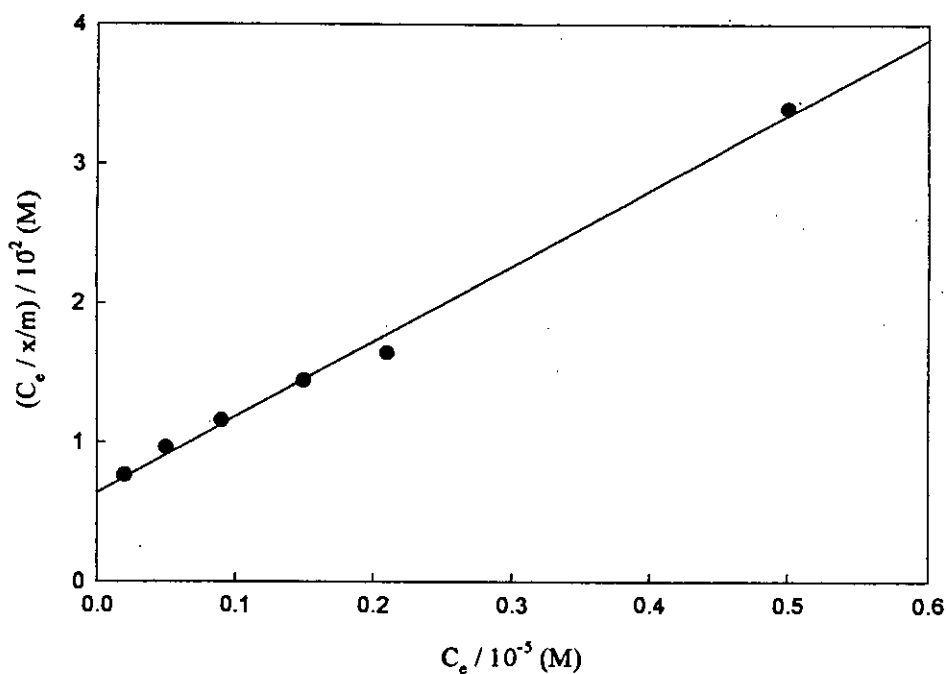
Fig. 3.22: Langmuir plot for basic-PANI/SiO₂ to calculate the adsorption coefficient, K_L

3.7 Concluding Remarks

The adsorption mode of PANI and PANI/SiO$_2$ substrates were studied to investigate the effect of protonation level on the specific surface area of these materials. The surface area of the treated PANI and PANI/SiO$_2$ substrates were determined using MB dyestuff from an aqueous solution allowed the dye to adsorb onto the surface of the matrices.

The post-synthesis treatment of chemically prepared PANI and the polymerization of aniline in the presence of colloidal silica represent a novel and an alternative route for modifying physico-chemical properties of the organic polymer. On the other hand, commercially available small silica particles successfully utilized for the preparation of the PANI/SiO$_2$ composite. Morphology and surface properties of conducting PANI and PANI/SiO$_2$ can be modified by controlling the pH of the solution medium with which the substrates are treated.

On treatment with double distilled water (pH = 6.95), aqueous hydrochloric acid (pH = 1.09) and aqueous ammonia (pH = 10.15), the PANI matrices appear to be neutral and charged. The acid and the base treatments make the PANI matrices charged positively and negatively, respectively while it is neutral if treated with double distilled water.

IR spectra confirmed the conducting and insulating structures for the acid and base treated PANI, respectively. However, the XRD studies of the treated polymers indicate that, on treatment, the molecular arrangement, i.e. crystallinity of the PANI matrices remains unaffected and exists in the amorphous state. As evidenced from the XRD studies, the structure of the bulk PANI and the PANI/SiO$_2$ seem to be indifferent i.e. silica cannot modify the structure of the bulk, which is mostly amorphous in nature.

Surface morphology of the PANI is significantly affected by the post-synthesized acid and base treatments. On acid treatment, a deposit of PANI agglomerates forms while treating it with distilled water or aqueous ammonium hydroxide solution, a granular morphology of the matrices results. For PANI/SiO$_2$ both powdery and stone-like morphology are observed.

The adsorption study indicates that the modified basic-PANI and PANI/SiO$_2$ possess relatively high surface area in comparison to acidic and neutral substrates. The surface area as a consequence of adsorption of the MB dye appears to be significant due to the electrostatic interaction between the ionic dye adsorbate and the charged PANI as well as PANI/SiO$_2$ adsorbents. This variation in specific surface area is also supported by the investigation of the adsorption capacities of the MB dye onto the PANI and PANI/SiO$_2$ matrices. The values of adsorption coefficient, K_L show the similar trend like the surface areas of the substrates. For basic- PANI and PANI/SiO$_2$, the K_L values are 1.39×10^5 L mol^{-1} and 5.3×10^5 L mol^{-1}, respectively, which are higher than the corresponding substrates.

Thus, it may be concluded that PANI exhibits very prominent variation of surface area depending on the protonation levels of the media used and also by incorporating inorganic silica particles to the bulk conducting PANI, that shows significant characteristics for the surface processes.

REFERENCES

1. V. V. Walatka, M. M. Labes and J. H. Perlstein, *J. Phys.Rev. Lett.*, **31** (1973) 1139.

2. A. J. Heeger, G. B. Street and G. Tourillon, *Hand Book of Conducting Polymers* (T. A. Skotheim, ed.), Marcel Dekker, Inc., New York, vol. **1** (1986) 265, 293.

3. R. B. Seymour, *Conducting Polymers*, Plenum Press, New York, (1981) 23.

4. E. K. Sickel, *Carbon Black Polymer Composites*, Marcel Dekker, New York, (1982).

5. A. Malliaris and D. T. Turner, *J. Appl. Phys.*, **42** (1971) 614.

6. H. Inokushi and H. Akamatu, *Solid State Physics*, (F. Seitz and D. Turnbull, ed.), **12** (1955) 93.

7. W. A. Little, *Phys. Rev.* **134A** (1964) 1416.

8. C. K. Chiang, A. J. Hegger and MacDarmid, *Ber. Bunsenges. Phys. Chem.*, **83** (1979) 407.

9. R. de Surville, M. Jozefowicz, L. T. Yu, J. Perichon and R. Buvet, *Electrochim. Acta.*, **13** (1968) 1451.

10. A. G. MacDiarmid, J. -C. Chiang, M. Halpen, W. -S. Huang, S. -L. Mu, N. L. D. Somasiri, W. Wu and S. I. Yaniger, *Mol. Cryst. Liq. Crys*, **121** (1985) 173.

11. E. M. Genies, A. A. Syed and C. Tsintavis, *Mol. Cryst. Liq. Cryst.*, **121** (1985) 181.

12. E. W. Paul, A. J. Ricco and M. S. Wrington, *J. Phys. Chem.*, **89** (1985) 1441.

13. P. M. McManus, S. C. Yang and R. J. Cushman, *J. Chem. Soc., Chem Commun.*, (1985) 1556.

14. D. McInnes, M. A. Druy, P. J. Nigrey, D. P. Nairns, A. G. McDiarmid and A. J. Hegger, *J. Chem. Soc., Chem. Commun.*, **317** (1981).

15. A. G. Hegger, G. B. Street and G. Tourillon, in *Hand Book of Conducting Polymers* (T. A. Skotheim, ed.), Marcel Dekker, Inc., New York, vol **1** (1986) 46, 51.

16. M. G. Kanatzldls, *Chemical Engineering News*, Dec. 03 (1990) 38-42.

17. J. L. Bredas, G. B. Street, *Acc. Chem. Res.*, **18** (1985) 309.

18. R. Noufi and A. J. Nozic, *J. Electrochem. Soc.*, **129**, (1982) 2261.

19. A. J. Epstein, J. M. Ginder, F. Zuo, H.-S. Woo, D. B. Tanner, A. F. Richter, M. Angelopoulos, W. S. Hung and A. G. MacDiarmid, *Synth. Met.*, **21**, (1987) 63.

20. A. G. MacDiarmid, J.-C. Chiang, A. F. Richter, N. L. D. Somasiri and A. J. Epstein, (L. Alcacer, ed.), *Couducting Polymers*, D. Redel Publishing Co., Dordrecht, The Netherlands (1987).

21. A. G. MacDiarmid, J. C. Chiang, A. F. Richter and A. J. Epstein, *Synth. Met.*, **18** (1987) 285.

22. E. M. Genies and C. Tsintavis and A. A. Syed, *Mol. Cryst. Liq.Cryst.*, **121** (1985) 181.

23. J. P. Travers, J. Chroboczek, F. Devreux, F. Genoud, M. Nechtschein, A. A. Syed, E. M. Genies and Tsintavis, *Mol. Cryst. Liq. Cryst.*, **121** (1985) 195.

24. A. G. MacDiarmid, N. L. D. Somasiri, W. R. Salaneck, I. Lundstrom, B. Liedberg, M. A. Hasan, R. Erlandsson and P. Konrasson, *Springer Series in Solid State Sciences*, Vol. **63**, Springer, Berlin, (1985) p-218.

25. R. L. Hand and R. F. Nelson, *J. Electrochem. Soc.*, **125** (1978) 1059.

26. R. L. Hand and R. F. Nelson, *J. Am. Chem. Soc.*, **96** (1974) 850.

27. *Fr. Patent No. EN* 8307958 (1983); *U.S. Patent No.* **698** (1985) 183.

28. L. T. Yu, M. S. Borredon, M. Jozefowicz, G. Belorgey and R. Buvet., *J. Polym. Sci.*, **10** (1987) 2931.

29. D. M. Mohilner, R. N. Adams and W. J. Argersinger, *J. Am. Chem. Soc.*, **84** (1962) 3618.

30. J. Bacon and R. N. Adams, *J. Am. Chem. Soc.*, **90** (1968) 6596.

31. G. Mengoli, M. T. Munari, P. Bianco and M. M. Musiani, *J. Appl. Polym. Sci.*, **26** (1981) 4247.

32. G. Mengoli, M. T. Munari and C. Folonari, *J. Electroanal. Chem.*, **124** (1981) 237.

33. E. M. Genies and C. Tsintavis, unpublished work.

34. E. W. Paul, A. J. Ricco and M. S. Wrighton, *J. Phys. Chem.*, **89** (1981) 1441.

35. B. Pfeiffer, A. Thyssen, M. Wolff and J. W. Schultze, *Int. Workshop – Electrochemistry of Polymer Layers, Dutsburg, F. R. G.*, Sept. 15-17, 1986.

36. C. M. Carlin, L. J. Kepley and A. J. Bard, *J. Electrochem. Soc.*, **132** (1985) 353.

37. R. Noufi, A. J. Nozik, J. White and L. F. Warren, *J. Electrochem. Soc.*, **129** (1982) 226.

38. B. Aurian-Blajeni, I. Taniguchi and J. O'M. Bockris, *J. Electroanal. Chem.*, **149** (1983) 291.

39. A. F. Diaz and J. A. Logan, *J. Electroanal. Chem.*, **111** (1980) 111.

40. A. Kitani, J. Yano and K. Sasaki, *Chem. Lett.*, (1984) 1565.

41. A. Thyssen, A. Hochfeld, R. Kessel, A. Meyer and J. W. Schulzte. *Synth., Met.*, **29** (1989) E357; T. A. Borgerding and J. W. Schulzte, *Makromol. Chem., Macromol. Symp.*, **8** (1987) 143.

42. E. M. Genies, M. Lapkowski, C. Santier and E. Vieil, *Synth. Met.*, **18** (1987) 631.

43. T. Kobayashi, H. Yoneyama and H. Tamura, *J. Electroanal. Chem.*, **161** (1984) 419.

44. F. Cristofini, R. De Surville, M. Josefowicz, L. T. Yu and R. Buvet, *C. R. Acad. Sci., Ser. C.* **268** (1969) 1346.

45. (a) E. P. Lofton, J. W. Thackeray and M. S. Wrighton, *J. Phys. Chem.*, **90** (1986) 6080; (b) S. Chao and M. S. Wrighton, *J. Am. Chem. Soc.*, **109** (1987) 6627.

46. H. Eisazadeh, H. Spinks, and G. G. Wallace, *J. Polym. Int.* **37** (1995) 87.

47. A. G. MacDiarmid, J. C. Chiang, and M. Halpern, *Mol. Crys. Liq. Crys.* **121** (1985) 173.

48. A. G. MacDiarmid, and N. L. D. Sowasiri, Springer series in solid state Sciences, **63** (1985) 218.

49. K. E. Barrett, J(Ed) Dispersion Polymerization in Organic Media, Wiley, New York, (1975).

50. M. J. Buerger and L. V. Azraf, the powder method in X-ray crystallography, McGraw. Hill, New York, (1958).

51. B. D. Cullity, Elements of X-ray diffraction, Weseley publishing Inc., Phillipines, (1978).

52. E. W. Paul, A. J. Ricco, and M. S. Wrighton, *J. Phys. Chem.* **89** (1985) 1441; A. N. Chowdhury, S. R. Jesmeen and M. M. Hossain, *Polym. Adv. Technol.* **15** (2004) 633.

53. F. N. Cogswell, New Materials. And their Applications, ed. Inst. Phys. Conf., Middle Brough, (1987) P-79.

54. H. Eisazadeh, H. Spinks, and G. G. Wallace, *J. Polym. Int.* **37** (1995) 87.

55. K. E. Barrett, J(Ed) Dispersion Polymerization in Organic Media, Wiley, New York, (1975).

56. M. Gill, J. Mykytiuk, S. P. Armes, J. L. Edwards, T. Yeates, P. J. Moreland and C. Mollett., *J. Chem. Soc. Chem Commun*, (1992) 108.

57. M. Gill, S. P. Armes, D. Fairhurst, S. N. Emmett, G. C. Idzorek and T. Pigott, *Langmuir*, **8** (1992) 2178.

58. N. J. Terrill, T. Crowley, M. Gill and S. P. Armes, *Langmuir*, **9** (1993) 2093.

59. D. M. Mohilner, R. N. Adams and W. J. Argersinger, *J. Am. Chem. Soc.*, **84** (1962) 3618.

60. J. Bacon and R. N. Adams, *J. Am. Chem. Soc.*, **90** (1968) 6596.

61. M. Doriomedoff, F. H. Cristofini, R. De Surville, M. Josefowicz, L. T. Yu and R. Buvet, *J. Chim. Phys.*, **68** (1971) 1055.

62. E. M. Genies and C. Tsintavis, *J. Electroanal. Chem.*, **195** (1985) 109.

63. L. T. Yu, M. S. Borredon, M. Jozefowicz, G. Belorgey and R. Buvet, *J. Polym. Sci.*, **10** (1987) 2931.

64. R. L. Hand and R. F. Nelson, *J. Electrochem. Soc.*, **125** (1978) 1059.

65. R. L. Hand and R. F. Nelson, *J. Am. Chem. Soc.*, **96** (1974) 850.

66. T. Ohsaka, Y. Ohnuki, N. Oyama, G. Katagiri and K. Kamisako, *J. Electroanal, Chem.*, **161** (1964) 399.

67. A. Kitani and K. Sasaki, *Stud. Org. Chem.*, **30** (1987) 377.

68. E. M. Genies, J. F. Penneau, M. Lapkowski and A. Boyle, *J. Electroanal. Chem.*, **269** (1989) 63.

69. E. M. Genies, M. Lapkowski and J. F. Penneau, *J. Electroanal. Chem.*, **249** (1988) 97.

70. F. Lux, *Polymer*, **35**(14) (1994) 2915.

71. R. B. Bjorklund, and B. Leidberg, *J. Chem. Soc. Chem. Commun*, (1986) 1293.

72. S. P. Armes, and M. Aldissi, *Polymer*, **31** (1990) 569.

73. F. Epron, F. Henrg, and O. Sagnes, *Makromol. Chem., Macromol.*, **35/36** (1990) 527.

74. R. Olegard, T. A. Skotheim, and H. S. Lee, *J. Electrochem. Soc.* **138** (1991) 2930.

75. S. P. Armes, M. Aldissi, S. F. Agnew, and S. Gottesfeld, *Langmuir*, **6** (1990) 1745.

76. V. Bocchi, L. Chierici, and G. P. Gardini, *Tetrahedron*, **26** (1970) 4073.

77. S. Machida, S. Miyata, and A. Techagumpuch, *Synth. Met.*, **31** (1989).

78. N. J. Terrill, T. Crowley, M. Gill, and S. P. Armes, *Langmuir*, **9** (1993) 2093.

79. W. S. Huang, B. D. Humphrey and A. G. MacDiarmid, *J. Chem. Soc., Faraday Trans. 1*, **82** (1986) 2385.

80. J. Stejskal, P. Kratochvil, and A. D. Jenkins, *Polymer*, **37** (1996) 367.

81. (a) D. Dolphine and A. Wick, *Tabulation of Infrared Spectral Data*, John Wiley & Sons, New York, London, Sydney, Toronto, (1977); (b) A. D. Cross and R. A. Jones, *An Introduction to Practical Infrared Spectroscopy, 3rd edn.*, *Butterworth*, London, (1969).

82. Y. Ohnuki, T. Ohsaka, H. Matsuda and N. Oyama, *J. Electroanal. Chem.*, **158** (1983) 55.

83. A. Volkov, G. Tourillon, P. C. Lacaze and J. E. Dubois, *J. Electroanal. Chem.*, **115** (1980) 279.

84. Y. Cao, S. Li, Z. Xue and D. Guo, *Synth. Met.*, **16** (1986) 305.

85. F. Wang, J. Tang, X. Jing, S. Ni and B. Wang, *Acta Polym. Sinica.*, **5** (1987) 384.

86. G. Socrates, *Infrared Characteristic Group Frequecies*, Wiley, Chichester, (1980) p-53.

87. F. R. Dollish, W. G. Fateley and F. F. Bentley, *Characteristic Raman Frequencies of Organic Compounds*, Wiley, New York, (1974).

88. L. J. Bellamy, *The Infrared Spectra of Complex Molecules*, Chapman and Hall, London, (1975), p. 82, p. 277.

89. L. Wang, X. Jing and F. Wang, *Acta Chem. Sinica*, in press.

90. S. Ni, J. Tang and F. Wang, *Preprints of Symposium on Polymers*, Chinese Chemical Society Polymer Division, Wuhan, China, (1987), p. 638.

91. M. Angelopoulos, G. E. Asturias, S. P. Ermer, A. Roy, E. M. Scherr, A. G. MacDiarmid, A. Akhter and Z. Kiss, *Mol. Liq. Cryst.*, **160** (1988) 151.

92. Y. Roichman, G. I. Titelman, M. S. Silverstein, A. Siegman and M Narkis, *Synth. Met.*, **98** (1999) 201.

93. S-A. Chen and W-G Fang, *Macromolecules*, **24** (1991) 1242.

94. J. P. Pouget, M. E. Jozefowicz, A. J. Epstein, X. Tang and A.G. MacDiarmid, *Macromolecules*, **24** (1991) 779.

95. J. P. Pouget, M. Laridjani, M. E. Jozefowicz, A. J. Esptein, E. M. Scherr and A. G. MacDiarmid, *Synth. Met.*, **51** (1992) 95.

96. J. E. Fischer, X. Tang, E. M. Scherr, V. B. Cajipe and A. G. MacDiarmid, *Synth. Met.*, **41- 43** (1991) 661.

97. A. W. Adamson, *Physical Chemistry of Surfaces*, 3rd Edn., John Wiley & Sons, Inc., (1976), p. 550.